Technische Universität München
TUM School of Medicine and Health

The cannabidiol-induced cross-talk of apoptosis and macroautophagy in colorectal cancer cells involves p53 and Hsp70

Fei Wang

Vollständiger Abdruck der von der TUM School of Medicine and Health der Technischen Universität München zur Erlangung des akademischen Grades einer

Doktorin der Medizin

genehmigten Dissertation.

Vorsitz: apl. Prof. Dr. Stefan Thorban

Prüfer*innen der Dissertation:

1. Prof. Dr. Gabriele Multhoff
2. Prof. Dr. Agnes Görlach
3. Prof. Dr. Udo Gaipl

Die Dissertation wurde am 17.03.2023 bei der Technischen Universität München eingereicht und durch die TUM School of Medicine and Health am 20.12.2023 angenommen.

Table of Contents

List of Figures and Tables

List of abbreviations

BCRP	breast cancer resistance protein
BCL2	B-cell lymphoma 2
CB1/2	cannabinoid receptors type 1/2
CBD	cannabidiol
COX-2	cyclooxygenase 2
CCL	chemokine (C-C motif) ligand 3
CXCL16	chemokine ligand 16
EGFR/AKT	epidermal growth factor receptor signaling pathway
ET-1	endothelin-1
Fluo3	substrate of MRP1
GM-CSF	granulocyte-macrophage colony-stimulating factor
GPR55	G-protein-coupled re-ceptor 55
IFN-γ	interferon-γ
IL	interleukin
Id1	inhibitor of differentiation/DNA binding
ICAM-1	intercellular adhesion molecule 1
LPI	lysophospholipid lysophosphatidylinositol
Mito	mitochondrial

MRP1	multidrug resistance-related protein 1
MAPK	mitogen-activated protein kinase pathway
MMP	matrix metalloproteinase
MRP	multidrug resistance-related protein
NF‐κB	nuclear factor kappa-light-chain-enhancer of activated B cells
NK	natural killer
NFAT	nuclear factor of activated T-cells
NOX4	NADPH Oxidase 4
PPARγ	peroxisome proliferator-activated receptor gamma
P-gp	P-glycoprotein
p22 Phox	human neutrophil cytochrome b light chain
PAI-1	plasminogen activator inhibitor type 1
PDGF-AA	platelet-derived growth factor-AA
Rh123	P-gp substrate Rhodamine 123
ROS	reactive oxygen species
ssDNA	single stranded DNA

TRPV1/2	transient receptor potential vanilloid type 1/2
TRPA1	TRP ankyrin type-1
TRPM8	TRP melastatin type-8
TNF	tumor necrosis factor
TIMP-1	metallopeptidase inhibitor 1
uPA	urokinase-type plasminogen activator
VEGF-2/VEGFA-2	vascular endothelial growth factor 2 and angiopoietin 2
CRC	Colorectal cancer

Abstract

Although it has been established that cannabidiol (CBD), the major non-psychoactive constituent of cannabis, exerts antitumoral activities, the exact mechanism(s) via which tumor cells are killed by CBD are not well understood. This study provides new insights into the potential mechanisms of CBD-induced mutual antagonism of apoptosis and macroautophagy using wild type (HCT116 p53wt, LS174T p53wt), knock-out (HCT116 p53-/-) and mutant (SW480 p53mut) human colorectal cancer cells (CRC). CBD causes a more pronounced loss in the viability of p53wt cells than p53-/- and p53mut cells, and a 5-week treatment with CBD reduced the volume of HCT116 p53wt xenografts in mice but had no effect on the volume of HCT116 p53-/- tumors. Mechanistically, we demonstrate that CBD only significantly elevates ROS production in cells harboring wild type p53 (HCT116, LS174T) and that this is associated with an accumulation of PARP1. CBD-induced elevated ROS levels trigger G0/G1 cell cycle arrest, a reduction in CDK2, a p53-dependent caspase-8/9/3 activation and macroautophagy in p53wt cells. The ROS-induced macroautophagy which promotes the activation of keap1/Nrf2 pathway might be positively regulated by p53wt, since inhibition of p53 by pifithrin-α further attenuates autophagy after CBD treatment. Interestingly, an inhibition of heat shock protein 70 (Hsp70) expression significantly enhances caspase-3 mediated programmed cell death in p53wt cells, whereas autophagy - which is associated with a nuclear translocation of Nrf2 - was blocked. Taken together, our results demonstrate an intricate interplay between apoptosis and macroautophagy in CBD-treated

colorectal cancer cells, which is regulated by the complex interactions of p53wt and Hsp70.

1. Introduction

In the past few decades cannabinoids that can be classified into endogenous cannabinoids, synthetic cannabinoids and phytocannabinoids derived from the plant *Cannabis sativa L.* have attracted great interest in medicine with respect to their broad medical applicability[1]. *Cannabis sativa L*. has been used for the treatment of glaucoma, anxiety, nausea, depression, and neuralgia[2-5]. The therapeutic value of phytocannabinoids has been demonstrated in the management of HIV/AIDS symptoms and multiple sclerosis[6, 7]. Terpenoid compounds are found in the bulbous glands, capitate-sessile glands, and capitate-stalked glands of the pistillate flowers[8]. The capitate-stalked type glands contain the highest amount of non-psychoactive cannabinoids, whereas the well-known psychoactive compound tetrahydrocannabinolic acid (THCA) is predominantly found in the glandular cells of the plant.

Cannabis has been used for the first time for medical purposes in 16th century in Asia for the treatment of analgesic, anticonvulsant, hypnotic, anti-inflammatory, antitussive and expectorant[9]. In 1840, William O'Shaughnessy noticed the medical properties of Indian cannabis for the treatment of different diseases including asthma, insomnia, and opium-use withdrawal[10]. Due to an association of the psychoactive potential of cannabis with crime and mental deterioration the drug was prohibited at the end of 19th century, and other non-psychoactive synthetic derivatives of cannabis have been produced[11, 12]. More than 560 different compounds have been identified in cannabis with

different biological and chemical activities that might qualify as potential drug candidates[12]. Phytocannabinoids that interact with the endocannabinoid system have been analyzed extensively[13]. Phytocannabinoids contain high-amounts of non-psychoactive compounds such as cannabichromene (CBC), cannabigerol (CBG) and cannabidiol (CBD)[14], and lower amounts of psychoactive cannabinoids [15] such as Δ9-tetrahydrocannabinol (Δ9-THC)[16, 17]. The chemical structures of the compounds are shown in Figure 1. Δ9-THC and CBD are the two best-studied active components of Cannabis sativa L. which can either be directly extracted from the plant or synthesized chemically for medical applications[17, 18]. Clinical and preclinical trials have shown that CBD[19-21], unlike Δ9-THC, does not induce hallucinogenic effects[22]. Presently, maceration (ME), ultrasound-assisted extraction (UAE) and reflux heat extraction (RHE) are used to isolate phytocannabinoids such as CBD. UAE is superior above the other methods with respect to time, energy consumption and costs[23]. Due to its suitable polarity ethanol (96%) works best as an extraction solvent[24, 25].

1.1 Molecular targets of cannabidiol (CBD)

CBD, one of the phytocannabinoids of Cannabis sativa L., was firstly identified by Raphael Mechoulam in the 1960s[26]. CBD with a molecular weight of 314.464 g/mol, consists of a cyclohexene ring, a phenolic ring and a pentyl side chain. In addition, methyl, n-propyl, n-butyl, and n-pentyl side chain homologs are present in CBD[27, 28]. The metabolism of CBD starts with a hydroxylation

on position C-7, which results in (−)-7-hydroxy-CBD, followed by (−)-7-carboxy-CBD after a further oxidation step[29].

Cannabinoid receptors and other constituents of the endocannabinoid system also have been identified and characterized. The cannabinoid receptor interaction influences different physiological processes such as appetite, pain, and inflammation[30, 31]. Based on their molecular structure, cannabinoid receptors belong to the guanine nucleotide binding protein (G protein)-coupled receptor superfamily[32], that stimulates guanosine 5′-O-(3-[35S]thio)-triphosphate ([35S]GTPγS) and thereby decreases the affinity of the GDP binding[33, 34]. The cannabinoid receptor CB1 contains seven-transmembrane domains which initiate the mitogen-activated protein kinase via G proteins for cell signaling. The cannabinoid receptor CB2 shares a sequence homology of 48% with CB1. Cannabinoid-specific receptors are expressed on a large variety of different mammalian tissues. In contrast to CB1, CB2 is not expressed on cells of the central nervous system, but on some peripheral neuronal tissues. CB1 and CB2 are both ex-pressed on many primary immune cells[35, 36]. Δ9-THC specifically binds to both cannabinoid receptors, CB1 and CB2. In the CB1 receptor-containing endocannabinoid system Δ9-THC acts as an agonist, but its agonistic potency is significantly lower than that of other cannabinoids receptor agonists (e.g. CP55940, WIN55212) with a high intrinsic activity[37]. The binding of Δ9-THC to the CB2 receptor is weaker than that to the CB1 receptor[38]. Unlike Δ9-THC, CBD acts as a cannabinoid receptor antagonist with low affinity to both receptors [39-41] whereas, the isomers (+)-CBD exhibits a high affinity to CB1 and CB2[41]. A study has shown that CBD antagonizes both cannabinoid receptors in whole-brain membrane tissues of mice and

Chinese hamster ovary cells which were transfected with the human CB2 receptor [42]. A few reports have shown that CBD might act as a negative allosteric modulator of the CB1 and CB2 receptors [43, 44](Table 1).

Transient receptor potential vanilloid (TRPV) channels are members of the TRP superfamily that modulate the transmission of iron and calcium in cells and thereby mediate a variety of neuronal signaling processes such as the sensing of temperature, pressure, pH, smell, etc. The occurrence of some common diseases, inflammatory and chronic pain for instance, are associated with dysfunctional TRPV1 and TRPV2 receptors[41, 45]. It is well accepted that CBD has a weak affinity to the CB1 and CB2 receptors, but predominantly interacts with TRPV1 and TRPV2 receptors and the mustard oil receptor[45-47], that acts as a negative allosteric modulator of the CB1 receptor[48]. TRPV1 interacts with phosphatidylinositol-3-kinase (PI3K) signaling [49] and thereby supports cell survival. In contrast to TRPV1, TRPV2 predominantly gets activated by different phytocannabinoids [50] including CBD[51].The efficacy of CBD to activate TRPV3/4 is weaker compared to that of TRPV1/2 (~54,~15 vs. ~78, ~67%, respectively) [52](Table 1). CBD displays a high potency to agonistically support the TRP ankyrin type-1 (TRPA1) channel activity (efficacy ~ 108%)[52], whereas it antagonizes the TRP melastatin type-8 (TRPM8) channel activity[53]. Other molecular targets of CBD that are mediated through CB1/CB2 receptors include the fatty acid neurotransmitter[54-56], G-protein coupled receptors (GPR55/ GPR18) [57-60], serotonin receptor 5-HT1[61], peroxisome proliferator-activated receptor γ (PPARγ)[62, 63], cyclooxygenase-2 (COX-2) enzymes, and glycine-receptor [64]. Furthermore, CBD mediates neuroprotection by influencing the cytosolic Ca2+ and K+ homeostasis via blocking low-voltage-

activated (T-type) Ca2+ channels[65, 66], reducing Ca2+ levels, preventing Ca2+ oscillations under high-excitability, and altered K+ levels[45].

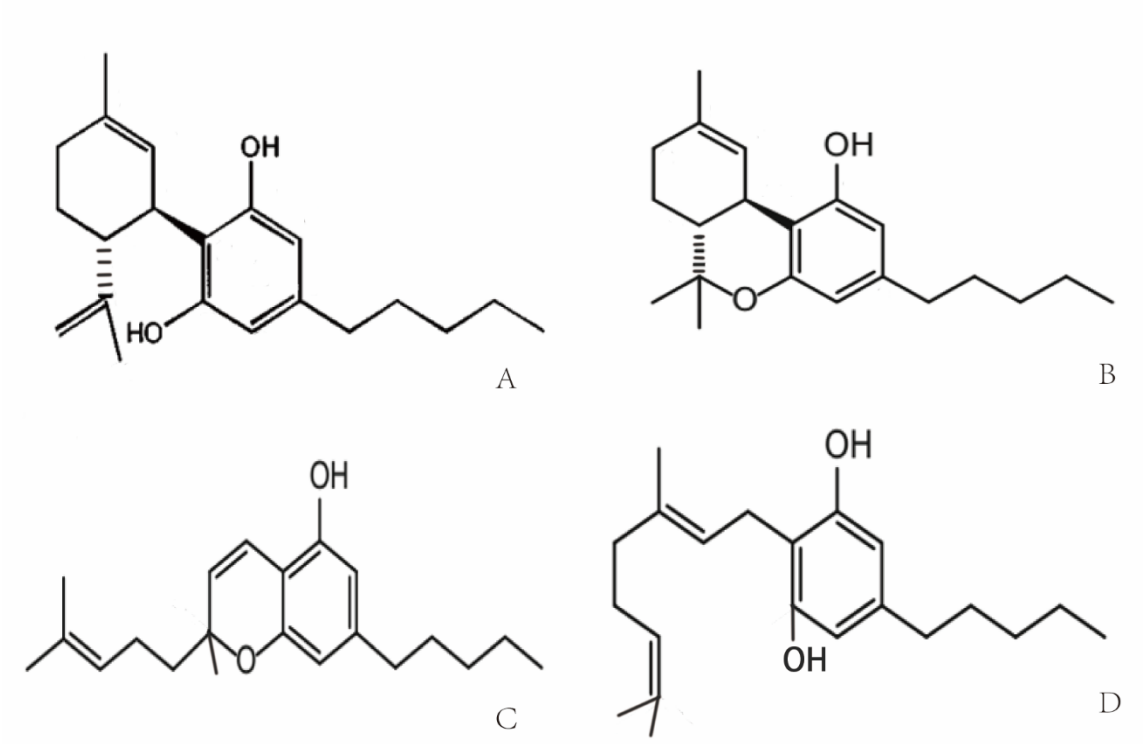

Figure 1. Molecular structures of cannabidiol (CBD; A)[26], Δ9-tetrahydrocannabinol (Δ9-THC; B), cannabichromene (CBC; C), and cannabigerol (CBG; D) [16]. (Repurposing Cannabidiol as a Potential Drug Candidate for Anti-Tumor Therapies,Fei Wang, Gabriele Multhoff, Biomolecules. 2021 Apr 15;11(4):582. doi: 10.3390/biom11040582)

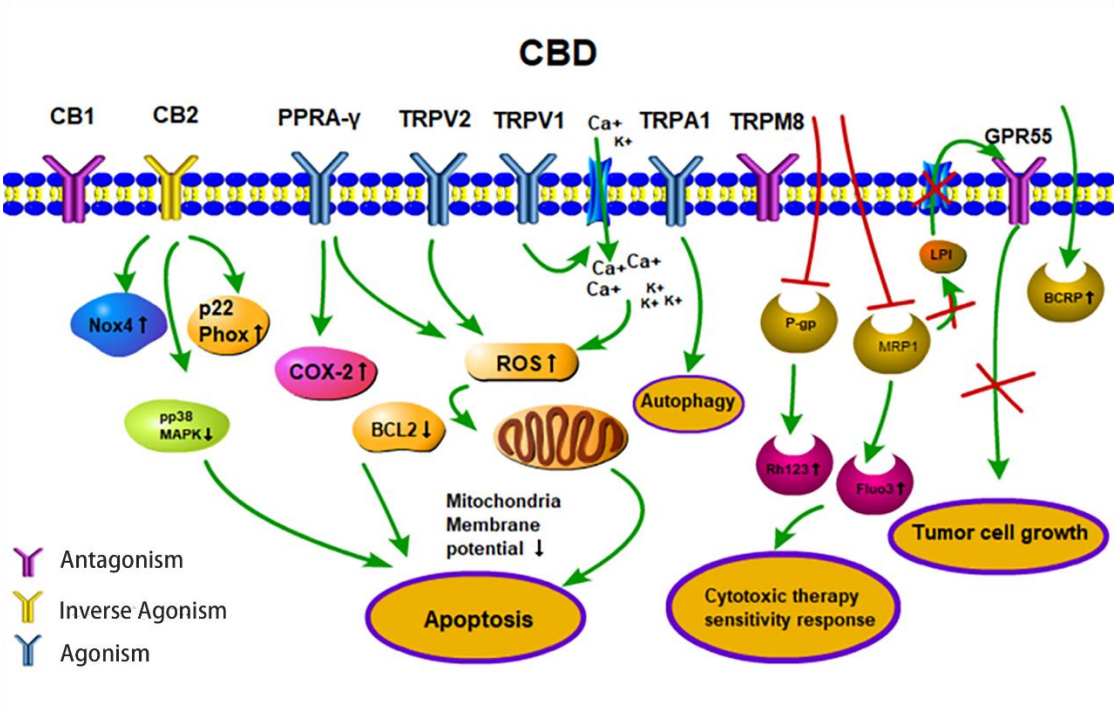

Figure 2. Anti-tumor activities (apoptosis, therapy sensitivity, autophagy, tumor cell growth) of CBD. CBD acts as an agonist for the receptors TRPV1/2, TRPA1 and PPARγ. CBD acts as an inverse agonist of the receptors CB1/CB2 and as an antagonist of the receptors GPR55 and TRPM8. CBD inhibits the efflux transporters P-gp and MRP1 and thereby reverses multi-drug resistance. CBD inhibits the MRP1 pump LPI out and the autocrine loop with GPR55 thereby reduces cell proliferation. (Repurposing Cannabidiol as a Potential Drug Candidate for Anti-Tumor Therapies,Fei Wang, Gabriele Multhoff, Biomolecules. 2021 Apr 15;11(4):582. doi: 10.3390/biom11040582)

1.2 CBD and cancer

Cancer has become the second cause of disease-related deaths worldwide in the past few decades[67]. The major treatment strategies of cancer are based on surgery, chemotherapy and/or radiotherapy. However, normal tissue toxicity and therapy resistance of the tumor cells often limit the efficacy of these three major treatment pillars. Therefore, there is a high medical need for anti-cancer drugs which are well tolerated and highly effective against cancer cells. CBD could serve as a potential anti-cancer drug candidate that fulfills these criteria. In vitro studies with fetal rat telencephalon cells revealed that highly lipophilic cannabinoids can easily cross the blood-brain-barrier and thereby get access to tumor target cells within in the nervous system[68]. Since CB2 receptors mediate neuronal cell survival and proliferation, a treatment with the antagonist CBD could inhibit the formation and propagation of malignant glial tumor cells[36]. Lipophilic CBD influences mitochondrial calcium stores, glycine receptors and fatty amide hydrolases[69]. Due to its non-psychoactive characteristics, lipophilic CBD has the potential to become an important drug in the treatment of glioblastoma[70]. Preclinical studies demonstrated that CBD

impedes tumor cell proliferation, metastatic spread, and induces autophagy and/or apoptosis in tumor cells[71]. CBD induces tumor cell apoptosis through activating the pro-caspases-3/8/9 and increases the pro-duction of reactive oxygen species (ROS) in human glioma cells. In addition, CBD disturbs the redox homeostasis by depletion of intracellular glutathione stores via stimulating the activity of glutathione reductase and glutathione peroxidase. Interestingly, CBD does not influence the viability of normal primary glia cells[72]. An incubation of human glioblastoma cell lines U87 and U373 with CBD reduces their proliferative capacity in a concentration-dependent manner[73]. The partial activation of the CB2 receptor activity by CBD is not impaired by the antagonistic activity of the CB1 receptor, and in the absence of the ROS scavenger alpha-tocopherol/vitamin E the induction of apoptosis by CBD is not inhibited[72, 73]. The treatment of leukemia cells with CBD resulted in a CB2 receptor mediated cell death. CBD treatment results in a disruption of the mitochondrial membrane potential which is accompanied by a release of the pro-apoptotic factor cytochrome c[74]. Other studies have demonstrated that CBD affects the regulation of CB2, NAD(P)H oxidases Nox4 and p22 (Phox)[75]. In non-small cell lung cancer (NSCLC) cell lines (A549, H460, H358) the inhibition of the invasive capacity of the tumor cells by CBD was related to a reduction in the plasminogen activator inhibitor-1 (PAI-1)[76]. COX-2 inhibitor (NS-298) and PPAR-γ antagonist (GW9662) studies in lung cancer cell lines (A549, H460) and primary lung cancer cells demonstrated that the CBD-induced apoptosis is associated with an upregulation of the pro-apoptotic markers COX-2 and PPAR-γ[77]. An activation of the cannabinoid receptors by CBD induces apoptotic cell death in epidermal tumor cells in vitro and results in a significant growth

inhibition in an epidermal tumor mouse model. Interestingly, the viability of non-transformed normal epidermal cells remained unaffected by CBD [78] (Figure 2).

Depending on the applied concentration, CBD mediates different pharmacological effects. Low CBD concentrations in the range of 0.01 µM up to 9 µM do not impair tumor cell viability but result in an increased migratory capacity of U87 glioblastoma cells. In this low concentration range the biological activities of CBD are neither related to the CB1/CB2 receptors nor to the TRPV1 receptor[79], whereas the effects of higher CBD concentrations clearly depend on these receptors [41]. Furthermore, CBD acts as a TRPV2-selective activator by intensifying Ca2+ influx and thereby inducing apoptosis in U87 glioblastoma cells [80]. Other studies suggest that CBD may promote doxorubicin-mediated cell death in hepatocellular carcinoma (BNL1 ME) and triple negative breast cancer (TNBC) cells by facilitating the uptake of doxorubicin via the activation of TRPV2 channels[81, 82]. An overexpression of TRPV3 in human lung cancer cells correlates with a poor overall survival of lung cancer patients but a blocking of TRPV3 efficiently inhibits the proliferation of lung cancer cells[83]. The low binding capacity of CBD to TRPV3 might be another explanation for its anti-tumoral effects. A treatment of the triple negative breast carcinoma cell line MDA-MB-231 with CBD induces both, autophagy and apoptosis as demonstrated by a ROS accumulation, Beclin1 activation and Bcl-2 inhibition[84]. TRPA1 /TRPM8 receptors which have been shown to promote autophagy and the metabolic transformation of UCP2 (uncoupling protein 2), respectively, in Lewis lung cancer (LLC) cells [84] might be responsible for CBD-induced autophagy and modulated ROS levels (Figure 2).

In combination with temozolomide (TMZ, the benchmark drug for the management of GBM) cannabinoids enhance autophagy in U87MG glioblastoma cells in vitro, and in a xenograft glioblastomas mouse models, and a subsequent reduction in tumor size is associated with an increase in active cleaved caspases[85]. A treatment of U251 and SF126 glioblastoma cell lines with both Δ9-THC plus CBD is superior to a mono-therapy with Δ9-THC with respect to the ERK signaling, G0-G1 arrest and repression of tumor cell survival[86]. Additionally, a combined treatment resulted in a modulation of the oxidative stress response and the lipoxygenase pathway[79, 85, 86]. Ligresti et al. re-ported an accumulation of intracellular Ca2+ and reactive oxygen species (ROS) upon CBD treatment, followed by an induction of apoptosis in MDA-MB-231 cells through either a direct or indirect activation of CB2 and/or TRPV1 receptors[87]. Another study in MDA-MB-231 cells shows the induction of autophagy and apoptosis, and an increase in the ER stress response, AKT/mTOR pathway and cell cycle arrest by CBD[84]. Moreover, CBD significantly inhibits EGFR/AKT, MAPK/ERK as well as NF-kB signal-ing that mediate proliferation and chemotaxis[88]. CBD also inhibits some efflux transporters, such as P-glycoprotein (P-gp), multidrug resistance-related protein 1 (MRP1) by reversing multiple drug resistance (MDR) in anti-cancer therapies. A de-creased P-gp expression correlated with an accumulation of the P-gp substrate Rhodamine 123 (Rh123) and promotes the sensitivity of human T lymphoblastoid leukemia cell line (CEM/VLB(100)) and a mouse fibroblast MDR1 transfected cell line (77.1) to-wards the P-gp substrate vinblastine[89]. Moreover, CBD increases the uptake of intracellular MRP1 substrates, Fluo3 and vincristine in ovarian carcinoma cells[90]. An-other study has shown P-gp

efflux function is down-regulated after a long-term (72h) CBD exposure, while the breast cancer resistance protein (BCRP), one of the efflux transporters, is up-regulated in a choriocarcinoma cell line[91]. The MRP1 (ATP-binding cassette transporter) pump LPI (lysophospholipid lysophosphatidylinositol) initializes cascades downstream of GPR55 to induce proliferation and migration in prostate and ovarian cancer cells[92]. CBD has also been shown to inhibit the GPR55-mediated mi-gratory and proliferative capacity in breast cancer cells[93]. CBD strongly inhibits the anti-invasive capacity of tumor cells by reducing Id-1 (an inhibitor of basic he-lix-loop-helix transcription factors), as shown by in vitro and in vivo experiments[94, 95]. The intercellular adhesion molecule-1 (ICAM-1) and tissue inhibitor of matrix metal-loproteinases-1 (TIMP-1) which are frequently decreased in tumor cells upon treatment are up-regulated by CBD, whereas an opposite trend is detected for matrix metallo-proteinases (MMPs) in lung cancer cells, which obstruct the capabilities of tumor cells to pass through complex extracellular matrices [96].

Due to their small size, targeted nanoparticles loaded with drugs show an advantageous biodistribution and dissemination in the body and have the capacity to release the drug in close proximity to the tumor[97, 98]. Although CBD is a potentially effective anti-cancer drug poor water-solubility and the requirement for organic solvents such as ethanol or methanol limits its broader application[99, 100]. Due to these limitations, nanoparticles loaded with CBD (CBD-NPs) at a ratio 1:5 or 3% (w/w) were firstly tested to treat ovarian cancer cells in vitro and in in vivo models. Compared to free CBD in organic solvents, CBD-NPs induced apoptosis and tumor growth inhibition at lower IC50

values[101]. CBD in lipid nanocarriers exhibits a high brain targeting ability by enhancing the passage across the blood-brain-barrier in vitro and in vivo, and therefore might provide a novel strategy to treat CNS tumors[102].

1.3 Aim of study

Colorectal cancer (CRC) is one of the most common malignant tumors in the gastrointestinal tract and the third leading cause of cancer-related deaths worldwide. Adenocarcinoma is the most common pathohistological type and accounts for more than 90% of all CRC cases[103]. Although advanced chemotherapeutic concepts such as FOLFOX or FOLFIRI in combination with molecular targeted drugs have achieved better clinical outcomes, the 5-year survival rate remains at only 12.5%[104], and acquired resistance to therapy occurs in 90% of CRC patients with metastatic disease.

Genomic instability, including microsatellite instability (MSI), chromosomal instability (CIN), and chromosome translocations play crucial roles in the etiology of CRC[105]. Mutations in tumor suppressor genes such as APC (Adenomatous Polyposis Coli) and TP53, as well as an inactive epigenetic mismatch repair (MMR) system and a genetic mutation in MLH1 (MutL Homolog 1) [105, 106]are also involved in tumorigenesis. The TP53 gene encodes for the p53 tumor suppressor protein that regulates a large variety of different cellular processes such as apoptosis, senescence, cell-cycle arrest and metabolism[107]. TP53 is the most frequently mutated gene in multiple human malignancies, including colon adenocarcinoma, and 60% of all colon cancers are associated with mutations in the TP53 gene locus [108, 109] that frequently result in a functional loss of p53 in later stages of cancer

progression[110].Cannabidiol (CBD), one of the phytocannabinoids of Cannabis sativa L., is well-tolerated and has antitumoral properties[87].

Although multiple antitumoral activities have been described for CBD, the interaction of p53 with CBD and its consequences on tumor cell death remain to be elucidated. In this study, we have shown that the antitumoral activity of CBD is dependent on p53wt in different colon carcinoma cells and that Hsp70 plays a key role in the decision of colon cancer cells to undergo apoptosis or autophagy. A better understanding of the anti-tumorigenic mechanisms and pathways induced by CBD will assist the design of more effective, combined therapeutic strategies for CRC.

2.Materials and Methods

2. 1 Materials

The HCT116 (p53wt) and HCT116 p53 double knock out (HCT116 p53-/-) human colon adenocarcinoma cell lines were kindly provided by Prof. Bert Vogelstein (Johns Hopkins University, Baltimore, USA). The SW480 human adenocarcinoma colorectal cancer cell line (ATCC#CCL-228™; ATCC, USA) which carries two-point mutations (R273H/P309S) was cultured in Dulbecco's modified Eagle’s medium (DMEM, Sigma-Aldrich) supplemented with 10% (v/v) fetal bovine serum (FBS) and 1% (v/v) penicillin/streptomycin (Sigma-Aldrich). LS174T (p53wt, ATCC#CL-188™; ATCC, USA) human adenocarcinoma colorectal cancer cells were cultured in DMEM supplemented with 10% (v/v) FBS and 1% (v/v) penicillin/streptomycin (Sigma-Aldrich), 2 mM L-glutamine (Sigma-Aldrich) and 1 mM sodium pyruvate (Sigma-Aldrich) at 37°C in a 5%

CO2 atmosphere. After seeding at the desired density, cells were incubated overnight prior to the experiments. Cells were routinely checked for mycoplasma contamination.

2.1.1 Equipment

ThermoStatPlus, Eppendorf (Z605190). PerkinElmer 2030 multilabel reader (PerkinElmer LAS GmbH, Germany), FACSCalibur™ flow cytometer BD Biosciences (Heidelberg, Germany), BIO-RAD Trans-Blot Turbo(1704150EDU), ChemiDoc™ Touch Imaging System (BIO-RAD). Leica TCS SP8 confocal microscope.

2.1.2 Software

ModFit LT™ software (Scripps Research, La Jolla, CA, USA), BD FACSDiva™ software (version 6.1.3; BD Biosciences), Fiji software (https://imagej.net/software/fiji/, accessed on 22 April 2021), GraphPad Prism (version 8.0, Graphpad Software, USA).

2.1.3 Chemicals

ML385 (keap1-Nrf2 inhibitor, Sigma-Aldrich ,846557-71-9), Bafilomycin A1 (specific inhibitor of vacuolar type H+-ATPase, V-ATPase, Sigma-Aldrich ,19-148) and PES-CI (Hsp70 inhibitor, Sigma-Aldrich ,5310670001) were dissolved in DMSO (D2650, Sigma-Aldrich). The antioxidant NAC (N-Acetyl-L-cysteine, Sigma-Aldrich, A9165) was diluted in sterile H2O. Growth medium was used as the vehicle for test substances, and contained 0.5% (v/v) methanol for

cannabidiol and ⩽0.1% (v/v) DMSO for ML385, PES-CI and Bafilomycin A1. McCoy’s 5A medium(Sigma-Aldrich) , Dulbecco's modified Eagle’s medium(Sigma-Aldrich),Milchpulver(Blottinggrade,ROTH,T145.2),TRIS (ROTH,AE15.2),Glycin (ROTH, 0079.3),Rotiphorese NF-Acrylamid(ROTH,a124.2),Triton X-100(Sigma-Aldrich, T8787),TWEEN80 (Sigma-Aldrich,P4780),D-Glucose(Sigma-Aldrich, G8270), Transfer Buffer (BIO-RAD,10026938,), Pierce ECL western blotting substrate(Thermo scientific,32106),ultra Tablets(Roche,05 892 791 001).

2.1.4 Antibodies and kit

p53 (murine IgG2a clone DO-1, sc-126, Santa Cruz), LC3B – autophagosome marker (rabbit polyclonal, ab48394, Abcam) , Nuclear Factor-Like 2 (Nrf2, murine IgG1 clone A-10, sc-365949, Santa Cruz). IgG (H+L) goat anti-mouse Alexa Fluor™ 488 Superclonal™ recombinant polyclonal secondary antibody (A28175, Invitrogen). 40, 6-diamidino-2-phenylindole (DAPI; 1 µg/ml for 1 min). SQSTM1/p62 (recombinant rabbit monoclonal, ab211324, Abcam), p21 Waf1/Cip1 (rabbit monoclonal, 2947, Cell Signaling Technology), CDK2 (recombinant rabbit monoclonal, ab32147, Abcam), PARP1 (rabbit polyclonal, 9542, Cell Signaling Technology), Hsp70 (murine IgG1 monoclonal clone cmHsp70.1, multimmune GmbH), Nrf2 inhibitor keap1 (keap1, rabbit monoclonal, 8047, Cell Signaling Technology), β-Actin (murine IgG2a monoclonal antibody clone AC-74, A2228, Sigma-Aldrich). anti-caspase 3, cleaved (9661, Cell Signaling Technology) Horseradish peroxidase (HRP)-conjugated rabbit anti-mouse immunoglobulins (P0260, Dako-Agilent) and HRP-conjugated swine anti-rabbit immunoglobulins (P0217, Dako-Agilent)

secondary antibodies. AnnexinV-FITC Apoptosis Detection kit(R&D, 4830-250-K),Pierce BCA Protein Assay Kit(Thermo scientific,23225), DCFDA / H2DCFDA Cellular ROS Assay Kit (ab133851; Abcam), FITC-Caspase-3 antibody (345815; R&D Systems) or FITC-Caspase 8 / PE-Caspase-9 antibodies (ab65615/ab65618; Abcam), TUNEL Assay Kit (ThermoFisher, A23210), JC-I Mitochondrial Membrane Potential Assay Kit (ab113850, Abcam).

2.1.5 Animals

Female SCID mice purchased from the Pasteur Institute, Iran was kept under standard laboratory conditions and all experiments were performed according to the requirements of a project license (EE/1401.2.24.105658/SCU.AC.IR) issued by the Faculty of Veterinary Medicine Animal Ethics Committee of the Shahid Chamran University of Ahvaz, Iran.

2.2 Methods

2.2.1 Screening of potential targets of CBD and enrichment assay

Well-reported pharmacological targets of cannabidiol were identified using the Drugbank[111], Swiss Target Prediction [112]and SuperPred [113] databases. The Genecard [114]database was used to screen for pathogenic targets in CRC. Potential targets for CBD in CRC were analyzed using Venn diagrams and the interactome network, functional processes and molecular pathways visualized using Metascape[115].

2.2.2 Cells and Cell Culture

The HCT116 (p53wt) was purchased from ATCC and HCT116 p53 double knock out (HCT116 p53-/-) human colon adenocarcinoma cell line was kindly provided by Prof. Bert Vogelstein (Johns Hopkins University, Baltimore, USA) and maintained in McCoy's 5A medium (Sigma-Aldrich). The SW480 human adenocarcinoma colorectal cancer cell line (ATCC#CCL-228™; ATCC, USA) which carries two-point mutations (R273H/P309S) was cultured in Dulbecco's modified Eagle's medium (DMEM, Sigma-Aldrich) supplemented with 10% (v/v) fetal bovine serum (FBS) and 1% (v/v) penicillin/streptomycin (Sigma-Aldrich). LS174T (p53wt, ATCC#CL-188™; ATCC, USA) human adenocarcinoma colorectal cancer cells were cultured in DMEM supplemented with 10% (v/v) FBS and 1% (v/v) penicillin/streptomycin (Sigma-Aldrich), 2 mM L-glutamine (Sigma-Aldrich) and 1 mM sodium pyruvate (Sigma-Aldrich) at 37°C in a 5% CO2 atmosphere. After seeding at the desired density, cells were incubated overnight prior to the experiments. Cells were routinely checked for mycoplasma contamination.

2.2.3 Cell Viability Assay

The effect of CBD and PES-CI on the viability of cells was determined using a CCK-8 (Cell Counting Kit-8,) assay (Sigma-Aldrich). For this, 5000 cells/well were seeded in 96 well plates and incubated with culture medium containing 5, 10, 15, 20 µM of CBD for 24-48 h, after which the 10% CCK-8 reagent was added into each well for 1.5 h at 37 °C under 5 % CO2. Same volume of methanol and DMSO as CBD or PES-CI was added into wells containing media only and serves as a blank. The absorbance at 450 nm was measured using a

PerkinElmer 2030 multilabel reader (PerkinElmer LAS GmbH, Germany). The absorbance of the cells incubated in medium alone was used as a control (survival rate: 100%).

2.2.4 Cell Cycle Analysis

The cell cycle distribution of CBD-treated cells was determined by flow cytometry. Cells were harvested with 1 ml of 0.05 % trypsin-EDTA. 4 milliliters of media were added to the cells to inactivate trypsin and the cell suspension was centrifuged at 500 g for 5 min. The supernatant was discarded and pellet was re-suspended twice in 1 ml PBS. Cell suspension was centrifuged at 500g for 5 min and PBS was discarded. 1 milliliters of pre-chilled absolute ethanol were added to the cell suspension followed by storage at −20 °C overnight, to allow efficient permeabilization and fixing of the cells. After that, cells were centrifuged at 500g for 5 min to remove ethanol. The pellet was washed twice with PBS and centrifuged at 500 g to remove PBS. Five hundred microliters of PI/RNase Staining solution was added to the cells and incubated for 1h. Fluorescence detection of propidium iodide (PI)-DNA complexes was determined by flow cytometry (FACSCalibur™ flow cytometer BD Biosciences, Heidelberg, Germany). The distribution of cells in different stages of the cell cycle was analyzed using ModFit LT™ software (Scripps Research, La Jolla, CA, USA). A minimum of 30,000 cells was analyzed.

2.2.5 Apoptosis Assay

An Annexin V-FITC/PI double staining assay was performed according to the manufacturer’s instructions (TACS® Annexin V Kits, R&D Systems). After 24 h

treatment, cells were harvested with 1 ml of 0.05 % trypsin-EDTA. 4 milliliters of media were added to the cells to inactivate trypsin and the cell suspension was centrifuged at 500 g for 5 min.Cells were collected and incubated with TACS Annexin V-FITC in binding buffer containing propidium iodide (Incubation Reagent) for 15 minutes at room temperature. Fluorescence intensity was measured using a FACSCalibur™ flow cytometer (BD Biosciences), and the apoptotic rates of CBD-treated cells were analyzed using BD FACSDiva™ software (version 6.1.3; BD Biosciences). A minimum of 10,000 cells were analyzed.

2.2.6 Mitochondrial Membrane Potential Assay

Mitochondrial membrane potential was determined using the JC-I Mitochondrial Membrane Potential Assay Kit (ab113850, Abcam), according to the manufacturer's instructions. After 24 h of indicate culture, cells were washed with 1x dilution buffer and incubated with 2.5 μM JC-1 solution for 30min at 37 °C in the dark and were harvested with 1 ml of 0.05 % trypsin-EDTA. 4 ml of FACS buffer (PBS+10%FCS) were added to the cells to inactivate trypsin and the cell suspension was centrifuged at 500 g for 5 min. Cell pellets were resuspended by 500ul FACS buffer. Fluorescence intensity of cells was measured using a FACSCalibur™ flow cytometer (BD Biosciences). A minimum of 30,000 cells were analyzed.

2.2.7 Total Reactive Oxygen Species Measurement

Total intracellular ROS levels were determined using DCFDA / H2DCFDA Cellular ROS Assay Kit (ab133851; Abcam). The DCFDA assay protocol is

based on the diffusion of DCFDA / H2DCFDA / DCFH-DA / DCFH into the cell. It is then deacetylated by cellular esterases to a non-fluorescent compound, which is later oxidized by ROS into highly fluorescent 2',7'–dichlorofluorescein (DCF). After 24 h of indicate culture, cells were incubated with 10 μM DCFH-DA solution for 1h at 37 °C in the dark. The medium was aspirated and the cells were washed once with PBS, following trypsinized process. 500ul of FACS buffer (PBS+10%FCS) were added to the cells at the end to resuspend the pellets. Cellular fluorescence (excitation / emission, ~485 nm / ~535 nm) was quantified by flow cytometry. A minimum of 10,000 cells were analyzed.

2.2.8 Caspase Activity Assay

Measurements of activated caspase-8/9/3 were performed according to the manufacturer's instructions using FITC-Caspase-3 antibody (345815; R&D Systems) or FITC-Caspase 8 / PE-Caspase-9 antibodies (ab65615/ab65618; Abcam). After 24 h of indicate culture, cells were trypsinized and harvested by centrifuged at 500 g for 5 min. Cell pellets were washed twice with PBS and incubated with antibody FITC-Caspase 8 / PE-Caspase-9 at 37 °C in the dark for 1h and antibody FITC-Caspase-3 was been used for incubation at 4°C after cells fixation. Cells were centrifugated at 500 g for 5 minutes and remove supernatant afterward. Resuspended cells by 300ul wash buffer. Samples were analyzed by flow cytometry. A minimum of 10,000 cells were analyzed.

2.2.9 DNA double strand break labeling by flow cytometry (TUNEL assay)

The TUNEL assay was performed using BrdUTP analysis following the instructions of the assay kit (TUNEL Assay Kit, ThermoFisher). Fluorescence

intensity was determined by flow cytometry (FACSCalibur™ flow cytometer BD Biosciences, Heidelberg, Germany). A minimum of 10,000 cells were analyzed per sample.

2.2.10 Immunofluorescence

Cells were fixed with 4% (w/v) formaldehyde in phosphate buffered saline (PBS), and then permeabilized by incubation with 0.15% (v/v) Triton X-100 in PBS, after which cells were incubated overnight at 4°C with monoclonal antibodies to p53 (murine IgG2a clone DO-1, sc-126, Santa Cruz) , LC3B – autophagosome marker (rabbit polyclonal, ab48394, Abcam) or Nuclear Factor-Like 2 (Nrf2, murine IgG1 clone A-10, sc-365949, Santa Cruz). Primary antibody binding was detected using IgG (H+L) goat anti-mouse Alexa Fluor™ 488 Superclonal™ recombinant polyclonal secondary antibody (A28175, Invitrogen). Nuclei of labeled cells were counterstained with 40, 6-diamidino-2-phenylindole (DAPI; 1 µg/ml for 1 min). Fluorescence images were taken using a Leica TCS SP8 confocal microscope. Fiji software (https://imagej.net/software/fiji/, accessed on 22 April 2021) was used for quantification.

2.2.11 Immunoblot Analysis

Cell lysates were prepared, separated by SDS-PAGE and blotting performed as described previously [23]. The protein content was determined using the Pierce™ BCA Protein Assay Kit (Thermo Fisher Scientific). The following antibodies directed against the indicated antigens were used in immunoblotting experiments: p53 (murine IgG2a monoclonal clone DO-1, Santa Cruz), LC3B – autophagosome marker (rabbit polyclonal, ab48394, Abcam), SQSTM1/p62

(recombinant rabbit monoclonal, ab211324, Abcam), p21 Waf1/Cip1 (rabbit monoclonal, 2947, Cell Signaling Technology), CDK2 (recombinant rabbit monoclonal, ab32147, Abcam), PARP1 (rabbit polyclonal, 9542, Cell Signaling Technology), Hsp70 (murine IgG1 monoclonal clone cmHsp70.1, multimmune GmbH), Nrf2 inhibitor keap1 (keap1, rabbit monoclonal, 8047, Cell Signaling Technology), β-Actin (murine IgG2a monoclonal antibody clone AC-74, A2228, Sigma-Aldrich). Primary antibody binding was detected using horseradish peroxidase (HRP)-conjugated rabbit anti-mouse immunoglobulins (P0260, Dako-Agilent) and HRP-conjugated swine anti-rabbit immunoglobulins (P0217, Dako-Agilent) secondary antibodies and a Pierce™ ECL Western Kit (Thermo Fisher Scientific). Blots were digitally imaged using a ChemiDoc™ Touch Imaging System (Bio-Rad). Fiji software (https://imagej.net/software/fiji/, accessed on 22 April 2021) [22] was used for quantifying Western blot signals.

2.2.12 In Vivo Tumor Xenograft Model

Female SCID mice purchased from the Pasteur Institute, Iran was kept under standard laboratory conditions and all experiments were performed according to the requirements of a project license (EE/1401.2.24.105658/SCU.AC.IR) issued by the Faculty of Veterinary Medicine Animal Ethics Committee of the Shahid Chamran University of Ahvaz, Iran. Specifically, animals had ad libitum access to food and water during maintenance under standard conditions (22°C, 50% relative humidity, and 12 h light/dark cycles). Mice were adapted to the standard housing conditions for one week before the start of the experiments. All animal procedures were performed in compliance with the revised Animals Directive 2010/63/EU of the European Union.

Mice were randomly divided into two groups. HCT116 p53wt (2×106) and the slower growing HCT116 p53-/- cells (2.8×106) were subcutaneously injected into 8-week-old female SCID mice in 100 µl McCoy‘s 5A medium 24h after a 3 Gy whole body irradiation. Tumor size, as measured using a caliper and body weight were measured twice per week. CBD (PhytoLab GmbH&Co.KG) was dissolved in a solution (5% DMSO, 5% Tween 80 (P4780, Sigma), 90% stroke-physiological saline solution) injected intraperitoneally (20 mg/kg, i.p.) 5 times a week for 5 weeks in total, from day 5 onwards. Mice were sacrificed on day 40 by isoflurane.4-6 mice were included in each group.

2.2.13 Immunohistochemistry assay

Tissue was fixed in formalin overnight and embedded in paraffin. Blocks were sectioned in 2 µm slices and stained with hematoxylin (Mayer's hematoxylin) and eosin (eosin y-solution 0.5% (v/v) aqueous) to visualize tissue structure according to standard protocols. Caspase-3 staining using the antibody rabbit anti-caspase 3, cleaved (9661, Cell Signaling Technology) was performed to determine the extent of apoptosis. Biotin-conjugated secondary antibodies were incubated for 1 h at room temperature. Nuclear counterstaining was done using hematoxylin.

2.2.14 Statistical analysis

Data from the in vitro experiments are presented from triplicate independent experiments. Statistical analyses were performed using GraphPad Prism (version 8.0, Graphpad Software, USA). Groups of two were analyzed with Student’s t-test, groups greater than two with a single variable were compared

using one-way ANOVA analysis. Groups greater than two with two independent variables were compared using two-way ANOVA analysis. The value of $p<0.05$ were considered statistically significant. Data are presented as mean values with standard deviations (SD) or standard error of mean (SEM).

3.Results

3.1 Screening for potential targets and pathways induced by CBD in CRC

By importing the 2D molecular structure files of CBD (SMILES:CCCCCC1=CC(=C(C(=C1)O)C2C=C(CCC2C(=C)C)C)O) from the PubChem Database (http://pubchem.ncbi.nlm.nih.gov/) [116] into the SwissTargetPrediction (probability score >0.9 as potential targets), Drugbank and SuperPred databases a total of 161 gene products that potentially interact with CBD were identified. The GeneCard (https://www.genecards.org/) database was used to identify CRC-related targets which are associated with the treatment of CRC using a relevance score $\geqslant 10$. The Veeny 2.1 (https://bioinfogp.cnb.csic.es/tools/venny/) intersection program (Figure 3a) identified 124 overlapping target genes that play a role in CRC after treatment with CBD. Metascape were used for pathway and process enrichment analysis (Figure 3b, Table 1), Protein–Protein Interaction (PPI) network map (Figure 3c, Table 2) and Predicted Transcriptional Process Enrichment analysis (Figure 3d, Table 3) of potential target genes involved in the interaction of CBD with CRC. Pathway and process enrichment analysis were performed with the following ontology sources: KEGG Pathway, GO Biological Processes, Reactome Gene Sets, Canonical Pathways, CORUM, WikiPathways and PANTHER Pathway.

Transcriptional process enrichment analysis was undertaken using the TRRUST database[117]. Only terms with a p-value <0.01, a minimum count of 3, and an enrichment factor >1.5 (the enrichment factor is the ratio between the observed counts and the counts expected by chance) were considered and grouped into clusters based on their membership similarities. Based on target gene enrichment assay, the TP53 regulation was identified as one of the most commonly affected transcriptional processes after treatment of CRC with CBD (Log10(P) = -6.5) (Figure 3d, Table 3).

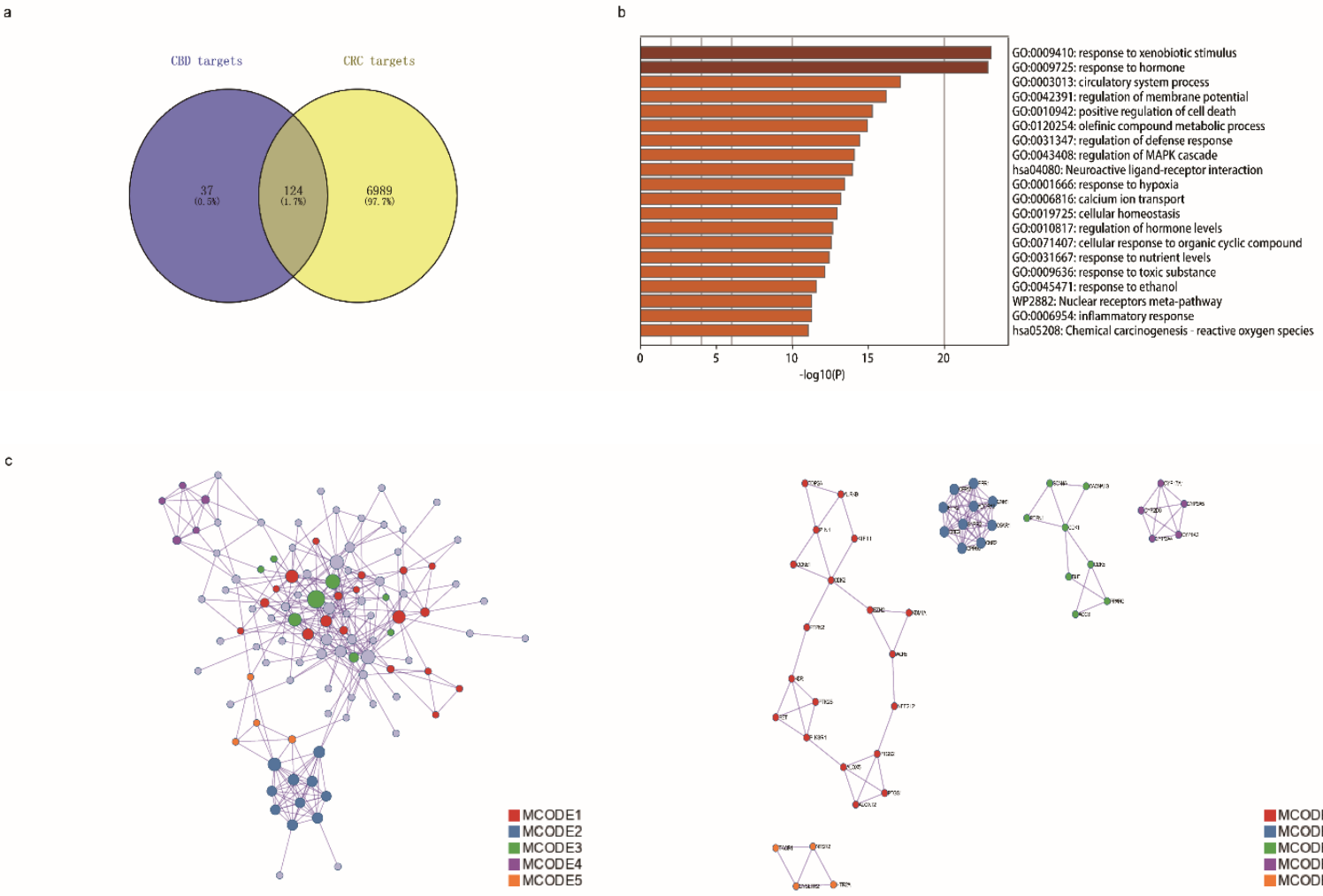

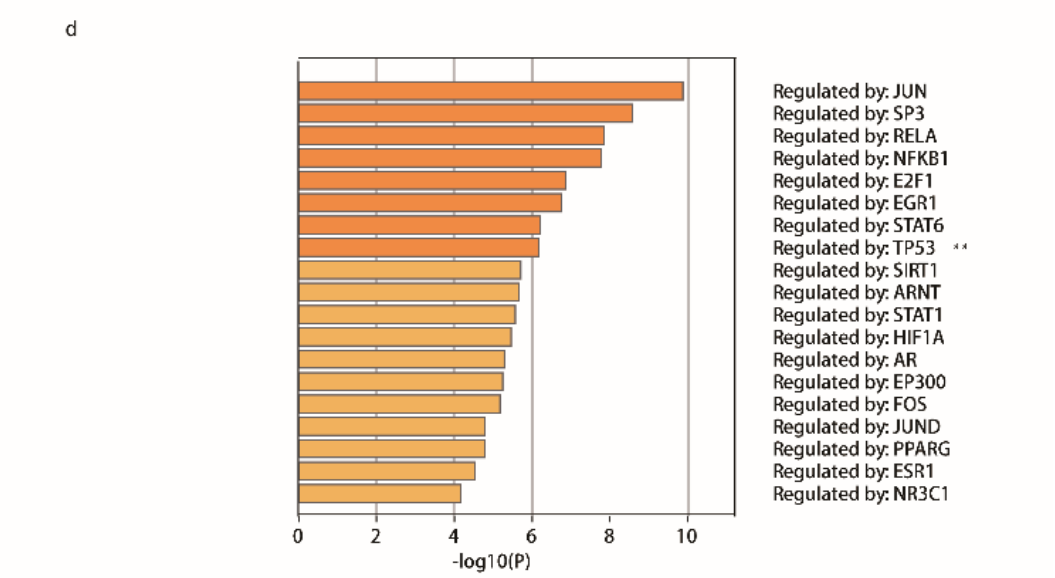

Figure 3. Screening of potential targets of CBD based on the target gene enrichment assay. (a) The Venn diagram identifies overlapping target genes affected in CRC after CBD treatment. (b) Hierarchy of 124 overlapping target genes acquired from the Venn analysis based on the p-values of the Pathway and Process Enrichment Analysis. (c) Protein-protein interaction network and identified MCODE components. (d) List of most affected genes identified by the TRRUST database. (Cannabidiol-induced crosstalk of apoptosis and macroautophagy in colorectal cancer cells involves p53 and Hsp70, Fei Wang, et al. Cell Death Discov. 2023 Aug 5;9(1):286. doi: 10.1038/s41420-023-01578-9)

Table 1. Pathway and Process Enrichment Analysis.

GO	Category	Description	Count	%	Log10(P)	Log10(q)
GO:0009410	GO Biological Processes	response to xenobiotic stimulus	26	20.97	-23.07	-18.81
GO:0009725	GO Biological Processes	response to hormone	32	25.81	-22.86	-18.81
GO:0003013	GO Biological Processes	circulatory system process	23	18.55	-17.12	-13.55
GO:0042391	GO Biological Processes	regulation of membrane potential	21	16.94	-16.18	-12.79
GO:0010942	GO Biological Processes	positive regulation of cell death	23	18.55	-15.27	-11.98
GO:0120254	GO Biological Processes	olefinic compound metabolic process	14	11.29	-14.94	-11.74
GO:0031347	GO Biological Processes	regulation of defense response	23	18.55	-14.43	-11.29

GO:0043408	GO Biological Processes	regulation of MAPK cascade	23	18.55	-14.08	-10.98
hsa04080	KEGG Pathway	Neuroactive ligand-receptor interaction	18	14.52	-13.95	-10.89
GO:0001666	GO Biological Processes	response to hypoxia	16	12.9	-13.44	-10.47
GO:0006816	GO Biological Processes	calcium ion transport	15	12.1	-13.2	-10.28
GO:0019725	GO Biological Processes	cellular homeostasis	21	16.94	-12.95	-10.1
GO:0010817	GO Biological Processes	regulation of hormone levels	19	15.32	-12.65	-9.82
GO:0071407	GO Biological Processes	cellular response to organic cyclic compound	19	15.32	-12.55	-9.76
GO:0031667	GO Biological Processes	response to nutrient levels	18	14.52	-12.41	-9.65
GO:0009636	GO Biological Processes	response to toxic substance	14	11.29	-12.14	-9.42
GO:0045471	GO Biological Processes	response to ethanol	11	8.87	-11.59	-8.97
WP2882	WikiPathways	Nuclear receptors meta-pathway	15	12.10	-11.28	-8.70
GO:0006954	GO Biological Processes	inflammatory response	18	14.52	-11.26	-8.69
hsa05208	KEGG Pathway	Chemical carcinogenesis - reactive oxygen species	13	10.48	-11.04	-8.48

Top 20 clusters with their representative enriched terms (one per cluster). "Count" is the number of genes in the user-provided lists with membership in the given ontology term. "%" is the percentage of all of the user-provided genes that are found in the given ontology term (only input genes with at least one ontology term annotation are included in the calculation). "Log10(P)" is the p-value in log base 10. "Log10(q)" is the multi-test adjusted p-value in log base 10. (Cannabidiol-induced crosstalk of apoptosis and macroautophagy in colorectal cancer cells involves p53 and Hsp70, Fei Wang, et al. Cell Death Discov. 2023 Aug 5;9(1):286. doi: 10.1038/s41420-023-01578-9)

Table 2. Protein-protein Interaction Enrichment Analysis.

MCODE	GO	Description	Log10(P)
MCODE_1	R-HSA-9018683	Biosynthesis of DPA-derived SPMs	-9.1
MCODE_1	R-HSA-9025094	Biosynthesis of DPAn-3 SPMs	-9.1
MCODE_1	WP167	Eicosanoid synthesis	-8.7
MCODE_2	R-HSA-373076	Class A/1 (Rhodopsin-like receptors)	-19.6
MCODE_2	R-HSA-500792	GPCR ligand binding	-18.1
MCODE_2	R-HSA-418594	G alpha (i) signalling events	-16.9
MCODE_3	GO:0051223	regulation of protein transport	-5.3
MCODE_3	GO:0070201	regulation of establishment of protein localization	-5.2
MCODE_3	GO:0033157	regulation of intracellular protein transport	-4.7
MCODE_4	GO:0009820	alkaloid metabolic process	-14
MCODE_4	WP43	Oxidation by cytochrome P450	-13.5
MCODE_4	GO:0070989	oxidative demethylation	-12.3
MCODE_5	R-HSA-416476	G alpha (q) signalling events	-8.6
MCODE_5	R-HSA-373076	Class A/1 (Rhodopsin-like receptors)	-7.8
MCODE_5	hsa04080	Neuroactive ligand-receptor interaction	-7.7

Protein-protein interaction enrichment analysis has been carried out with the STRING [65] (physical score > 0.132), and BioGrid [66] were used. The Molecular Complex Detection (MCODE) algorithm [67] has been applied to identify densely connected network components. "Log10(P)" is the p-value in Log base 10. (Cannabidiol-induced crosstalk of apoptosis and macroautophagy in colorectal cancer cells involves p53 and Hsp70, Fei Wang, et al. Cell Death Discov. 2023 Aug 5;9(1):286. doi: 10.1038/s41420-023-01578-9)

Table 3. Summary of enrichment analysis in TRRUST.

GO	Description	Count	%	Log10(P)	Log10(q)

TRR00645	Regulated by: JUN	11	8.9	-9.9	-7.8
TRR01259	Regulated by: SP3	9	7.3	-8.6	-6.6
TRR01158	Regulated by: RELA	12	9.7	-7.9	-6
TRR00875	Regulated by: NFKB1	12	9.7	-7.8	-5.9
TRR00230	Regulated by: E2F1	8	6.5	-6.9	-5.1
TRR00253	Regulated by: EGR1	7	5.6	-6.7	-5
TRR01282	Regulated by: STAT6	5	4	-6.2	-4.5
TRR01419	Regulated by: TP53	8	6.5	-6.2	-4.5
TRR01225	Regulated by: SIRT1	5	4	-5.7	-4.1
TRR00015	Regulated by: ARNT	4	3.2	-5.6	-4
TRR01275	Regulated by: STAT1	6	4.8	-5.6	-4
TRR00484	Regulated by: HIF1A	6	4.8	-5.5	-3.9
TRR00011	Regulated by: AR	6	4.8	-5.3	-3.7
TRR00270	Regulated by: EP300	5	4	-5.2	-3.7
TRR00342	Regulated by: FOS	5	4	-5.2	-3.6
TRR00647	Regulated by: JUND	4	3.2	-4.8	-3.3
TRR01062	Regulated by: PPARG	5	4	-4.8	-3.3
TRR00275	Regulated by: ESR1	5	4	-4.5	-3
TRR00908	Regulated by: NR3C1	4	3.2	-4.2	-2.7

"Count" is the number of genes with membership in the given ontology term. "%" is the percentage of genes that are found in the given ontology term (only input genes with at least one ontology term annotation are included in the calculation). "Log10(P)" is the p-value in log base 10. "Log10(q)" is the multi-test adjusted p-value in Log base 10. (Cannabidiol-induced crosstalk of apoptosis and macroautophagy in colorectal cancer cells involves p53 and Hsp70, Fei Wang, et al. Cell Death Discov. 2023 Aug 5;9(1):286. doi: 10.1038/s41420-023-01578-9)

3.2 p53-Dependent Reduction in Viability and Tumor growth of CRC Cells In Vitro and In Vivo

The viability of HCT116 p53wt, HCT116 p53-/-, SW480 p53mut, LS174T p53wt cells after treatment with CBD (5 μM to 20 μM), as determined using the

CCK-8 assay, was reduced in all cell lines in a dose dependent manner after a 24h (Figure 4a) and 48h (Figure 4b) incubation. However, the sensitivity of cells to CBD was cell type dependent: HCT116 p53wt (IC50 = 14.67 µM; 95% CI 13.42-15.79), HCT116 p53-/- (IC50 = 24.26 µM; 95% CI 21.33-34.88), LS174T p53wt (IC50 = 7.918 µM; 95% CI 7.039-8.867) and SW480 p53mut (IC50 = 16.58 µM; 95% CI 14.73-19.17) cells. The data revealed that p53 deficient (HCT116 p53-/-) and p53 mutant (SW480 p53mut) cells are less sensitive to a CBD treatment than p53 wild type cells when compared to each other (HCT116 p53wt vs HCT116 p53-/-, LS174T p53wt vs SW480) (Figure 4a). However, a significant difference between HCT116 p53wt and SW480 p53mut was observed only with a CBD concentration of 20 µM and an incubation period of 24h ($p<0.0001$) (Figure 4a, b). Unlike p53 deletion (HCT116 p53-/-), the two-point mutations (R273H/P309S) in p53 (SW480) triggers a diverse sensitivity to CBD which is probably due to a partially retained p53 function[118]. Based on the IC50 values, a concentration of 15 µM was used as the maximum concentration for in vitro experiments with HCT116 p53wt and p53-/- cells, while LS174T and SW480 cells were treated with 20 µM CBD to enable a better pairwise comparison of intercellular responses to CBD.

We further investigated the antitumoral effect of CBD in a xenograft tumor mouse model. For this, HCT116 p53wt and HCT116 p53-/- cells were injected subcutaneously (s.c.) into immunodeficient SCID mice following a whole-body irradiation with 3 Gy. To avoid methanol induced toxicity in mice, DMSO instead of methanol was used as the vehicle for CBD in the mouse experiment. We could demonstrate that irrespective of the vehicle (methanol or DMSO), CBD exerts comparable effects on cell viability of HCT116 p53wt cells, as

demonstrated in a CCK8 assay (Supplementary Figure 1a). Tumor-bearing mice were treated 5 times a week with CBD with the non-toxic dose of 20 mg/kg for 5 weeks as illustrated schematically in Figure 4c. A significant reduction in the volume of HCT116 p53wt tumors was observed in mice after CBD treatment compared to the DMSO vehicle control from day 37 onwards (Figure 4d). In contrast, the volume of HCT116 p53-/- tumors was not significantly reduced by the CBD treatment at any time point (Figure 4e), suggesting that a long-term CBD treatment only decreases the growth of p53wt, but not p53-/- tumors. Preliminary studies demonstrated that the growth of HCT116 p53wt and HCT116 p53-/- cell-derived tumors was comparable when 2.0 x 106 p53wt and 2.8 x 106 p53-/- cells were injected s.c., respectively (Supplementary Figure1b). The treatment with CBD or the vehicle DMSO did not elicit any negative side effects in mice since the body weight of the mice was comparable in all treatment groups over a period of 40 days (Supplementary Figure 1c). Representative examples of tumors treated either with vehicle or CBD are illustrated in Figure 4f. Immunohistochemical analysis revealed a cell vacuolization in H&E sections of HCT116 p53wt tumors following CBD treatment, which was barely seen in HCT116 p53-/- tumors (Figure 4g). Moreover, CBD induced a weak elevation in caspase-3 expression in HCT116 p53wt tumors which is indicative for apoptosis, whereas almost no apoptosis was apparent in HCT116 p53-/- tumors (Figure 4g). With respect to DNA strand breaks, cleaved PARP1 was only accumulated in HCT116 p53wt cells upon a treatment with CBD at a concentration of 15 µM. This finding corresponds to an increase in the proportion of TUNEL positive cells (Figure 4h, i). Similar to HCT116 p53-/- cells, there was no significant difference in cleaved PARP1 expression after CBD treatment in SW480 p53mut cells

(Figure 4h, Supplementary Figure 2a). However, in contrast to HCT116 p53wt cells, in LS174T p53wt cells neither cleaved PARP1 nor cleaved-caspase-3 were found to be upregulated (Supplementary Figure 2a, b).

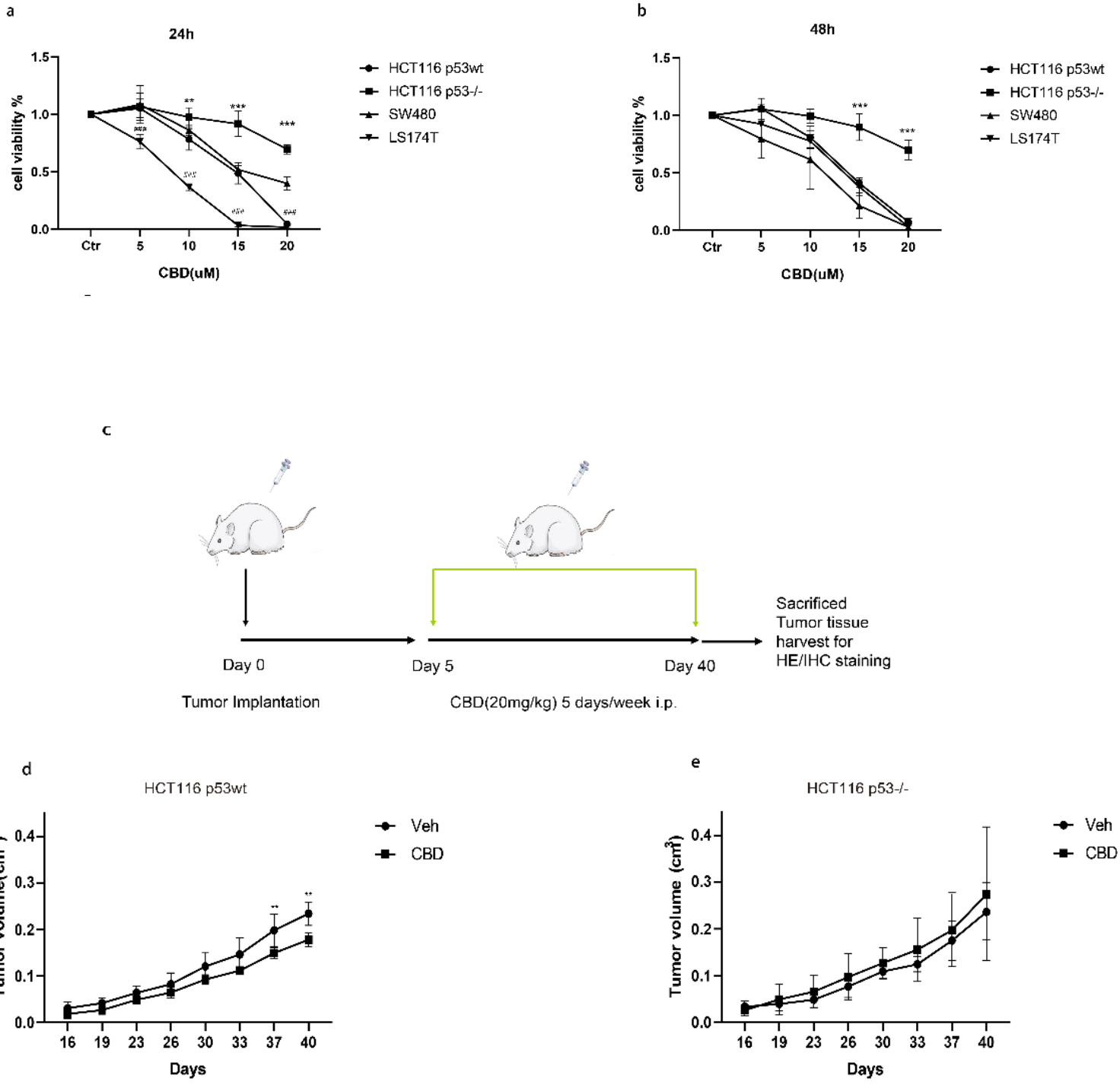

f

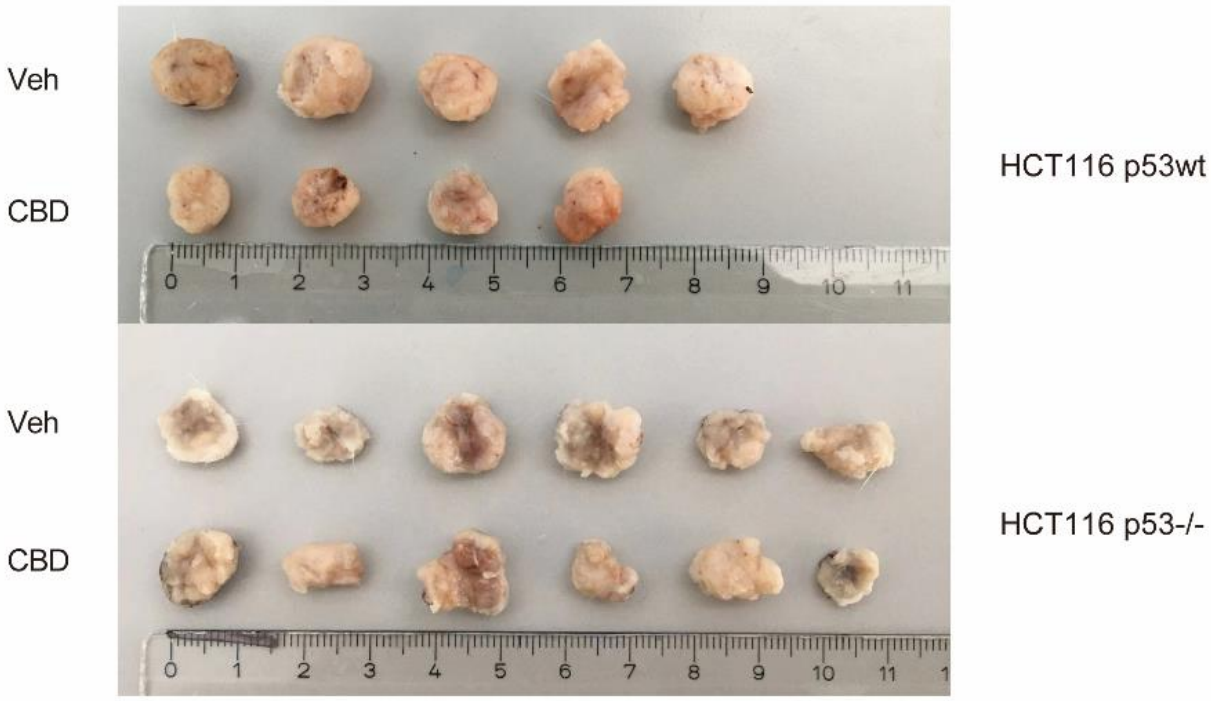
Veh
CBD
HCT116 p53wt
Veh
CBD
HCT116 p53-/-

g

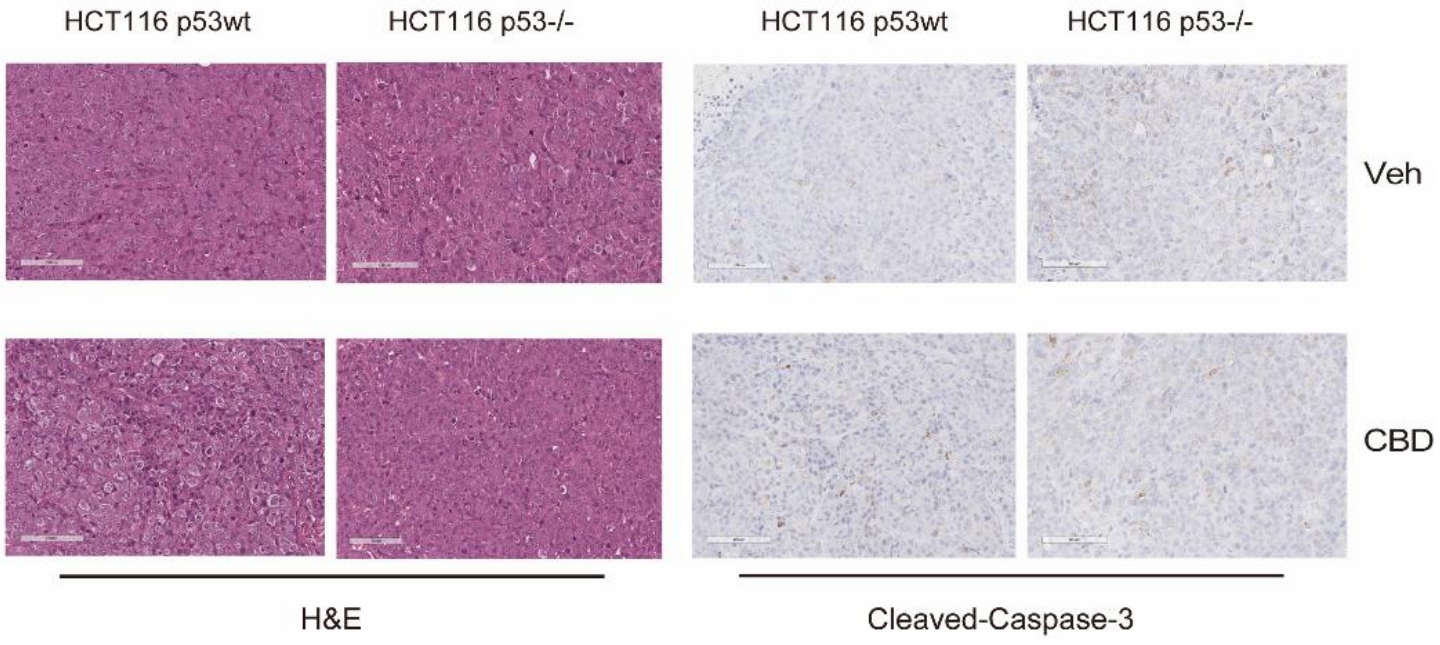
HCT116 p53wt
HCT116 p53-/-
HCT116 p53wt
HCT116 p53-/-
Veh
CBD
H&E
Cleaved-Caspase-3

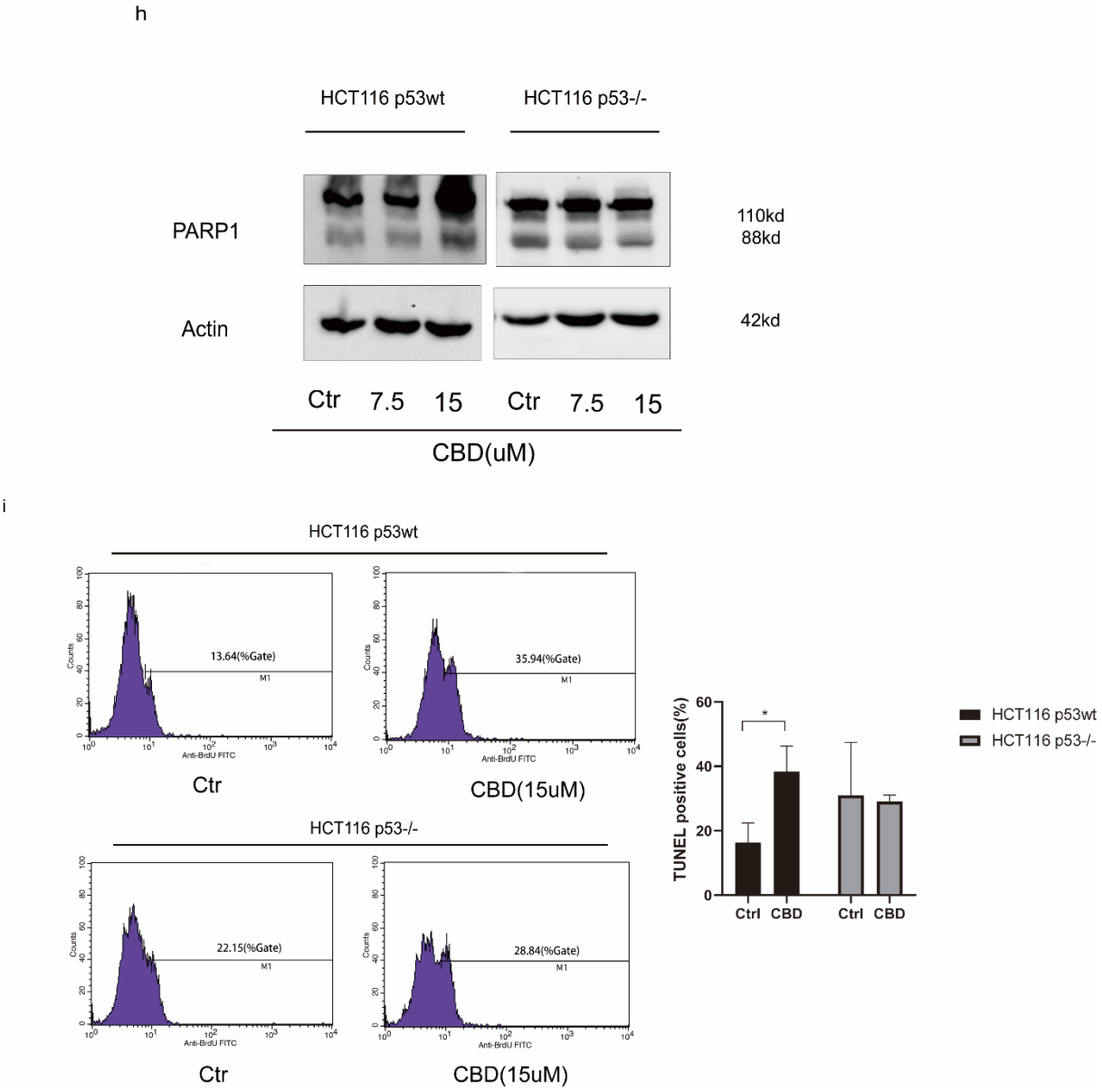

Figure 4. CBD reduces the viability of p53wt CRC cells in vitro and inhibits tumor Growth In Vivo. (a, b) Cell viability was determined using CCK8 assay kit 24h(left) or 48h(right) after CBD treatment. Data are expressed as the percentage of cell viability compared to control. Statistical differences of HCT116 p53-/- was evaluated by compared to HCT116 p53wt (* $p \leq 0.05$, ** $p \leq 0.01$ and *** $p \leq 0.001$) and LS174T compared to SW480 (# $p \leq 0.05$, ## $p \leq 0.01$ and ### $p \leq 0.001$). Two-way ANOVA was used for analysis. Results represent the mean values of 3 independent experiments (n=3). (c) Schematic diagram of workflow for data in vivo. (d–g) HCT116 cells were subcutaneously implanted into SCID mice which received vehicle alone or CBD (20 mg/kg) intraperitoneally 5 times per week over 5 weeks. Tumor size (d, e) were measured twice per week. (f) Representative examples of tumors treated either with vehicle or CBD are illustrated. (g) The hematoxylin and eosin (H&E) stained sections for observation of morphological changes in cells and immunohistochemistry of mice tumor tissue for detection of cleaved-caspase 3 to identify apoptotic cells directly after CBD treatment

(Scale bar: 100 μm). (h） Immunoblot analysis of cytosolic PARP1 and cleaved-PARP1 expression in HCT116 p53wt and HCT116 p53-/- cells 24h after CBD treatment. (i) TUNEL assay has been performed to detect apoptotic cells after CBD treatment using a colorimetric TUNEL system. T test was used. Statistical differences of each group were evaluated by compared to the control (* $p \leq 0.05$, ** $p \leq 0.01$ and *** $p \leq 0.001$) or to the other group (# $p \leq 0.05$, ## $p \leq 0.01$ and ### $p \leq 0.001$). All data are expressed as the mean ± SD of three independent experiments. (Cannabidiol-induced crosstalk of apoptosis and macroautophagy in colorectal cancer cells involves p53 and Hsp70, Fei Wang, et al. Cell Death Discov. 2023 Aug 5;9(1):286. doi: 10.1038/s41420-023-01578-9)

3.3 CBD induces a G0/G1 cell cycle arrest and a p53-dependent ROS over production

CDK2 kinase plays a crucial role in regulating the G1-S transition. Mitotic cell arrest occurs when CDK2 kinase activity is inhibited by the CDK-specific inhibitor p21[119]. We found that CBD in a concentration range of 7.5 and 15 μM induces a significant G0/G1 phase arrest which was more pronounced in p53wt (Figure 5a) cells than p53-/- or p53mut cells, concomitant with a p53-dependent CDK2 downregulation and a p53-independent p21 upregulation (Figure 5b-d). A similar trend was found in another LS174T p53wt cells (Figure 5e). As expected, CBD had no significant impact on the expression of cell cycle proteins in SW480 p53mut cells (Figure 5f). p53 is a transcription factor that acts as an upstream regulator for reactive oxygen species (ROS) in response to stress by activating or repressing several ROS-regulating genes, such as glutathione peroxidase (GPX) and p53-induced genes (PIGs) [120] which act in a pro- or an anti-oxidative environment. Our results indicate that the significant increase in ROS production induced by CBD is proportional to the p53 functional activity, since a nuclear translocation of p53 (Figure 5g, h) together with a ROS

accumulation following CBD treatment only occurs in p53wt cells (Figure 5h), but not in p53 deficient cells (Figure 5h).

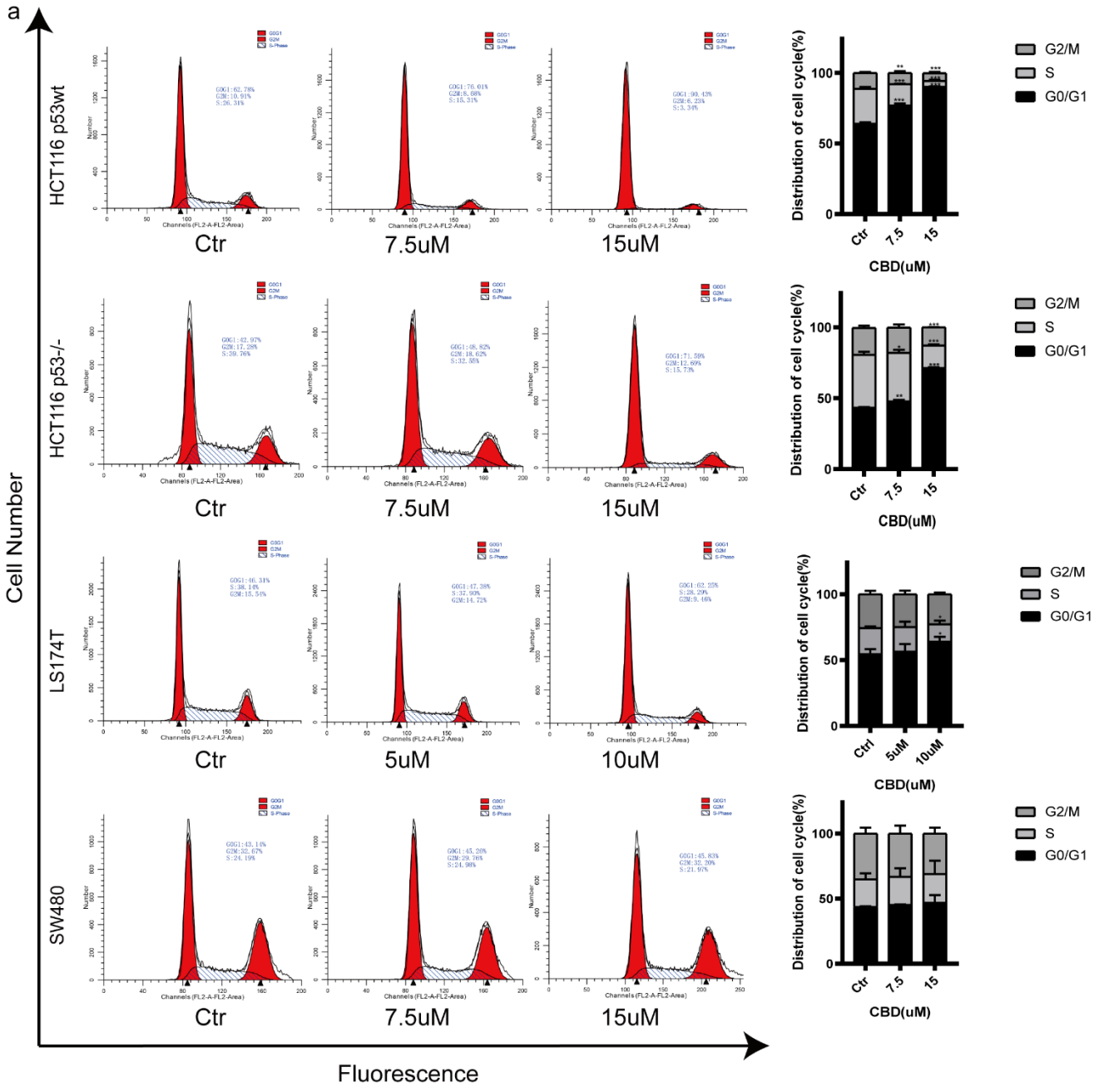

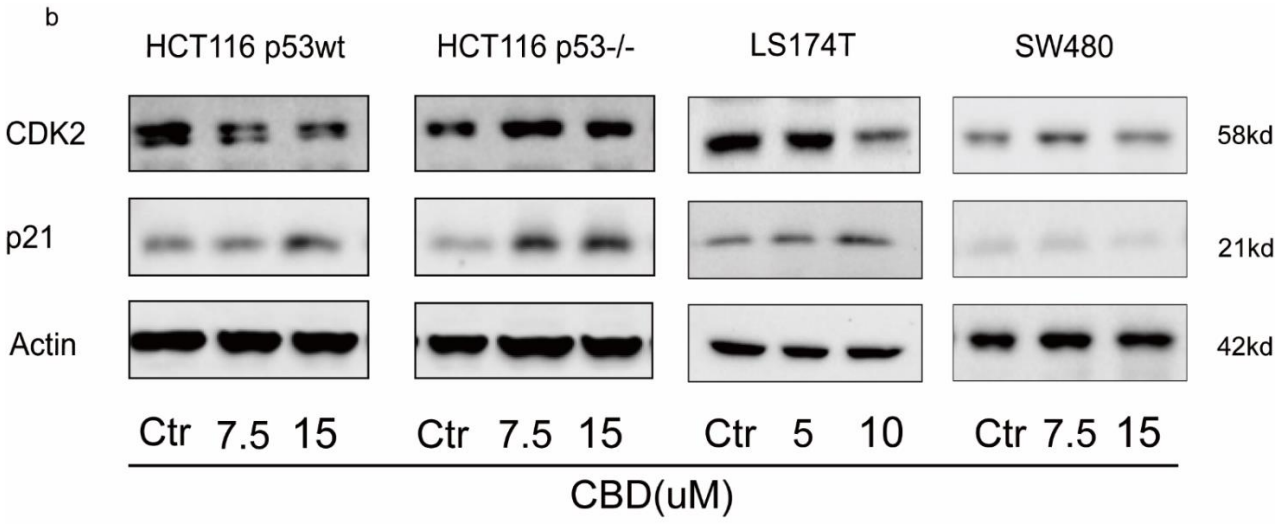
b
HCT116 p53wt
HCT116 p53-/-
LS174T
SW480
CDK2
p21
Actin
58kd
21kd
42kd
Ctr 7.5 15
Ctr 7.5 15
Ctr 5 10
Ctr 7.5 15
CBD(uM)

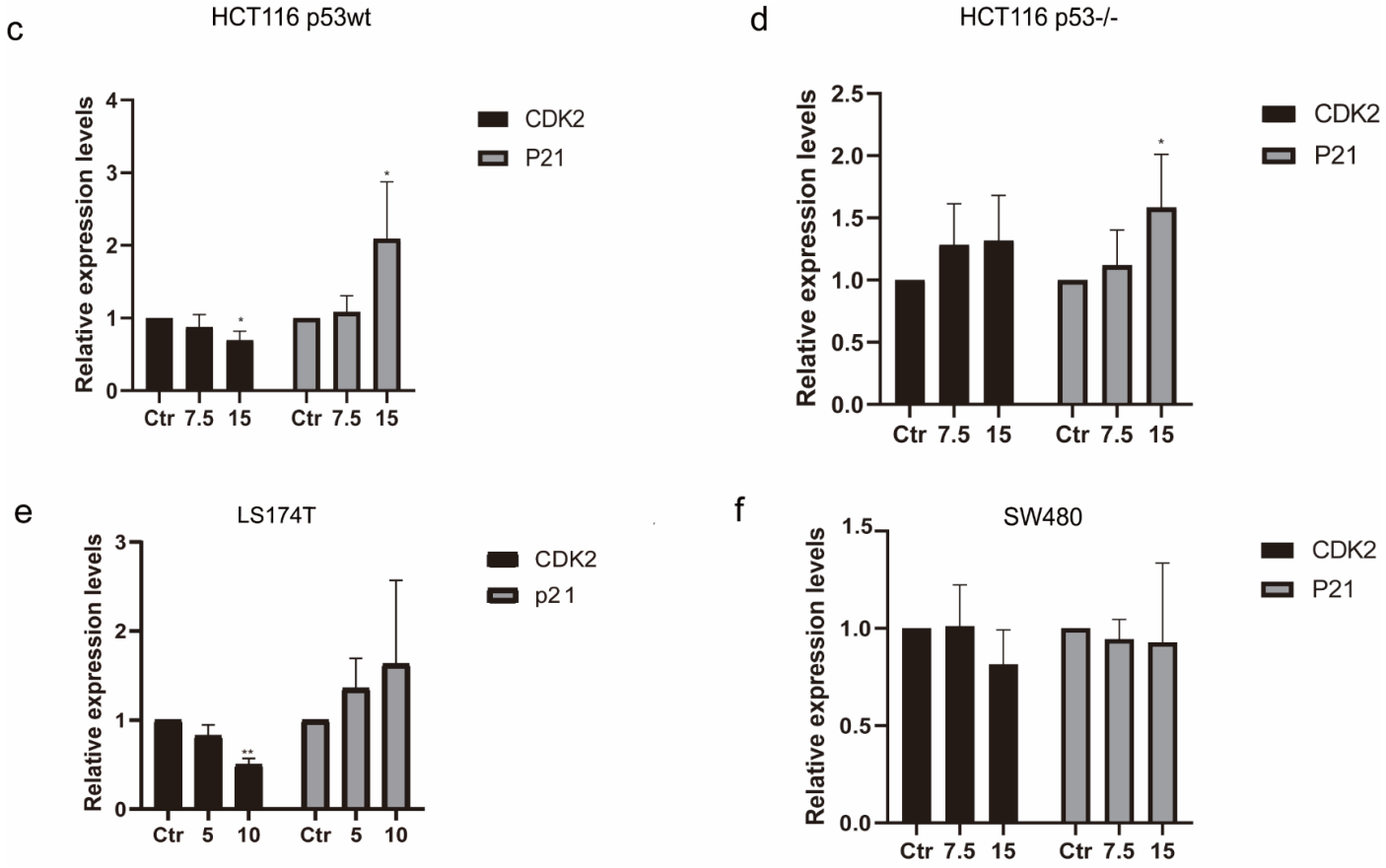
c
HCT116 p53wt
Relative expression levels
CDK2
P21
Ctr 7.5 15 Ctr 7.5 15
d
HCT116 p53-/-
Relative expression levels
CDK2
P21
Ctr 7.5 15 Ctr 7.5 15
e
LS174T
Relative expression levels
CDK2
p21
Ctr 5 10 Ctr 5 10
f
SW480
Relative expression levels
CDK2
P21
Ctr 7.5 15 Ctr 7.5 15

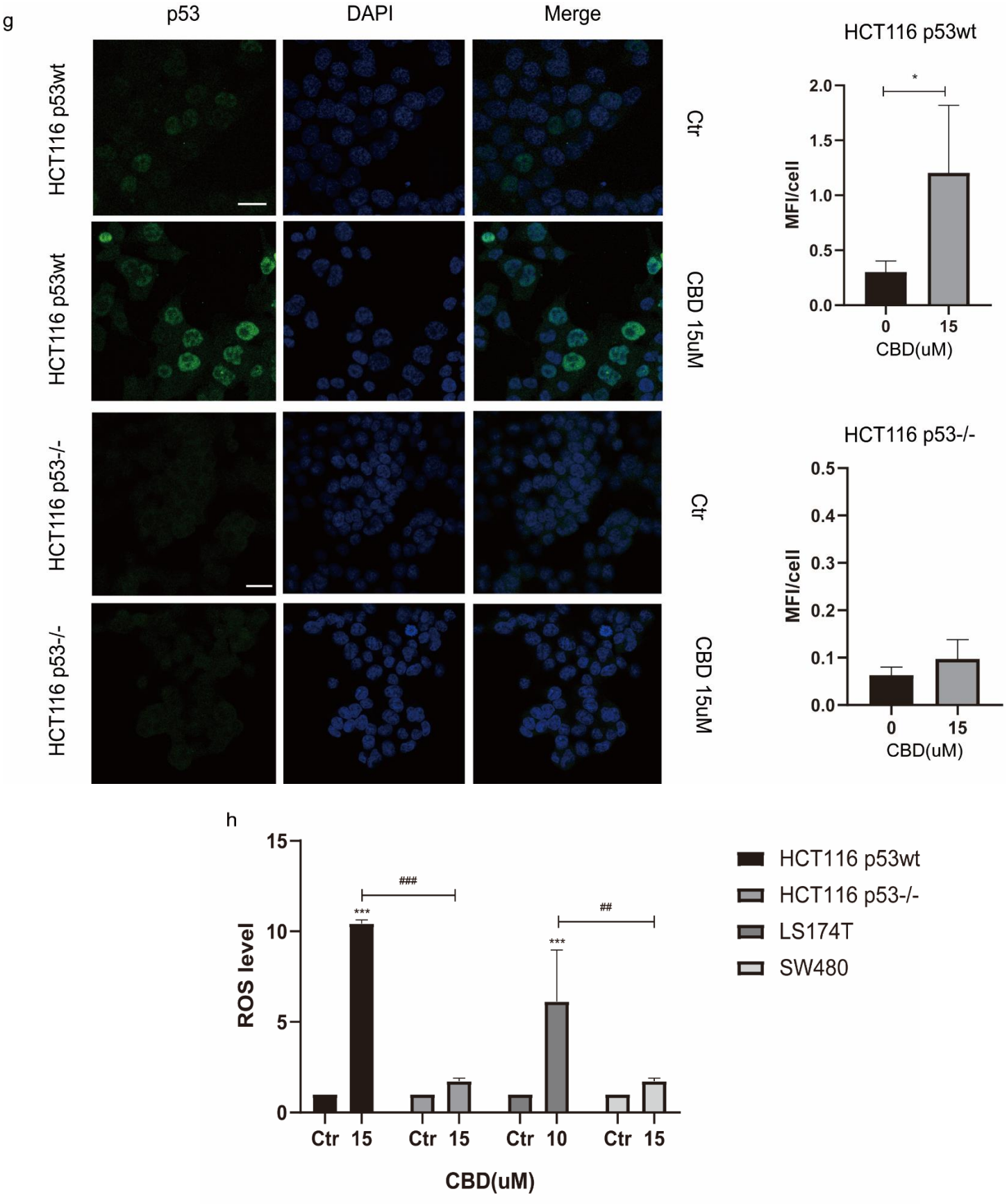

Figure 5. CBD induces G0/G1 cell cycle arrest. (a) Flow cytometry was used to determine the cell cycle distribution in CBD-treated CRC cells. The quantification of each cell cycle phase is shown in the adjacent bar chart. (b) The expression levels of CDK2 and p21 protein in CBD-treated CRC cells were detected by Western blotting. (c-f) The ratio of protein levels was

normalized to the values of the control. (g) HCT116 p53wt and p53-/-cells stained for the expression of p53 were analyzed by confocal microscopy (Scale bar: 25 μm). Quantification of mean fluorescence intensity per cell was presented as adjacent bar charts. p53(green). Nuclei, DAPI (blue). Statistical differences of each group were evaluated by compared to the control group (* $p \leq 0.05$, ** $p \leqslant 0.01$ and *** $p \leqslant 0.001$). T-test was used. Results are shown as mean ± SEM (HCT116 p53wt n =36-43, HCT116 p53-/-n = 53-72). (h) After a 24h CBD treatment, intracellular reactive oxygen species (ROS) levels were determined using the DCFDA assay. One-way ANOVA analysis was used. Statistical differences of each group were evaluated by compared to the control (* $p \leqslant 0.05$, ** $p \leqslant 0.01$ and *** $p \leqslant 0.001$) or to the other group (# $p \leqslant 0.05$, ## $p \leqslant 0.01$ and ### $p \leqslant 0.001$). All data are expressed as the mean ± SD of three independent experiments. (Cannabidiol-induced crosstalk of apoptosis and macroautophagy in colorectal cancer cells involves p53 and Hsp70, Fei Wang, et al. Cell Death Discov. 2023 Aug 5;9(1):286. doi: 10.1038/s41420-023-01578-9)

3.4 Heat shock protein 70 (Hsp70) attenuates apoptosis induced by CBD through inhibiting p53/caspase 8/9/3 pathway

Hsp70, a member of the HSP70 family encoded by HSPA1, is very strongly upregulated by heat stress and a large variety of other stress stimuli including toxic chemicals, particularly heavy metals such as arsenite, cadmium, copper, mercury, etc. Heat shock proteins were originally discovered by Ferruccio Ritossa in the 1960s when a lab worker accidentally boosted the incubation temperature of Drosophila (fruit flies). When examining the chromosomes, Ritossa found a "puffing pattern" that indicated the elevated gene transcription of an unknown protein[108, 109]. This was later described as the "Heat Shock Response" and the corresponding proteins were termed as "Heat Shock Proteins" (HSPs). It is well accepted that many tumor cells overexpress Hsp70 and that this overexpression correlates with resistance to apoptosis-inducing agents, whereas a downregulation of Hsp70 results in an increased sensitivity towards these agents[121]. Hsp70 can interfere with apoptosis pathways by

blocking the aggregation of the functional apoptosome[122]. PES-CI, an Hsp70 inhibitor, binds to the substrate domain of Hsp70 which is important for the binding of client proteins, and thereby represses the enzymatic activity of the anaphase-promoting complex/cyclosome (APC/C)[123]. Previous study showed that PES interacts with the major stress-inducible Hsp70, but not with the consitutively expressed Hsc70[124]. To better understand the potential role of Hsp70 on the antitumoral effects of CBD, we therefore interrogated the potential interaction partners of Hsp70 using the PES-CI inhibitor. As expected, PES-CI reduces the viability of all CRC cells in a dose-dependent manner (Figure 6a), with the sensitivity of HCT116 p53wt (IC50 = 10.33 µM; 95% CI 4.937-13.18), HCT116 p53-/- (IC50 = 14.96 µM; 95% CI 12.59-17.91), LS174T (IC50 = 8.451 µM; (95% CI 5.201-9.902) and SW480 (IC50 = 15.78 µM; 95% CI 13.93-17.86) to PES-IC depending on the p53wt status. A co-treatment of CRC cells with the PES-CI and CBD results in distinct morphological changes which was more pronounced in p53wt cells. In general, the cells became round, detached from the surface of the culture flask and underwent apoptosis (Supplementary Figure 3) which was documented by a disruption of the mitochondrial membrane potential (Figure 6b), concomitant with a substantial increase in the proportion of Annexin V/PI double positive, apoptotic cells (Figure 6c-g). In contrast, the population of Annexin-V single positive cells was only significantly enhanced in p53wt cells, but not in p53-/- or p53mut CRC cells (Figure 6c-g). We further determined cleaved caspase-8/9/3 by flow cytometry to confirm apoptosis induction in wild type p53 CRC cells. We demonstrated that CBD treatment alone considerably increased the levels of reactive oxygen species (ROS), but had only a moderate effect on the percentage of cells

positive for Annexin-V and cleaved caspase-8/9/3 (Figure 7a-d). However, when CBD was used in combination with the Hsp70 inhibitor PES-CI, the expression of cleaved caspase-9/3 was significantly elevated in cells harboring wild type p53 (HCT116 p53wt, LS174T p53wt), but not in p53 deficient or p53 mutant cells (HCT116 p53-/- and SW480 p53mut) (Figure 7d, e). Caspase-8 displays a pivotal role in the p53-independent apoptotic signaling pathway following CBD treatment, and Hsp70 inhibition significantly accelerated caspase-8 dependent apoptosis (Figure 7b). As discussed previously[85], the antioxidant N-acetyl cysteine (NAC) attenuates the antitumoral effect of CBD, as demonstrated by a reduction in the proportion of Annexin-V positive cells and the levels of cleaved caspase-8 ($p = 0.0060$), cleaved caspase-9 ($p = 0.0545$), cleaved caspase-3 ($p = 0.0215$) in HCT116 p53wt cells (Figure 7).

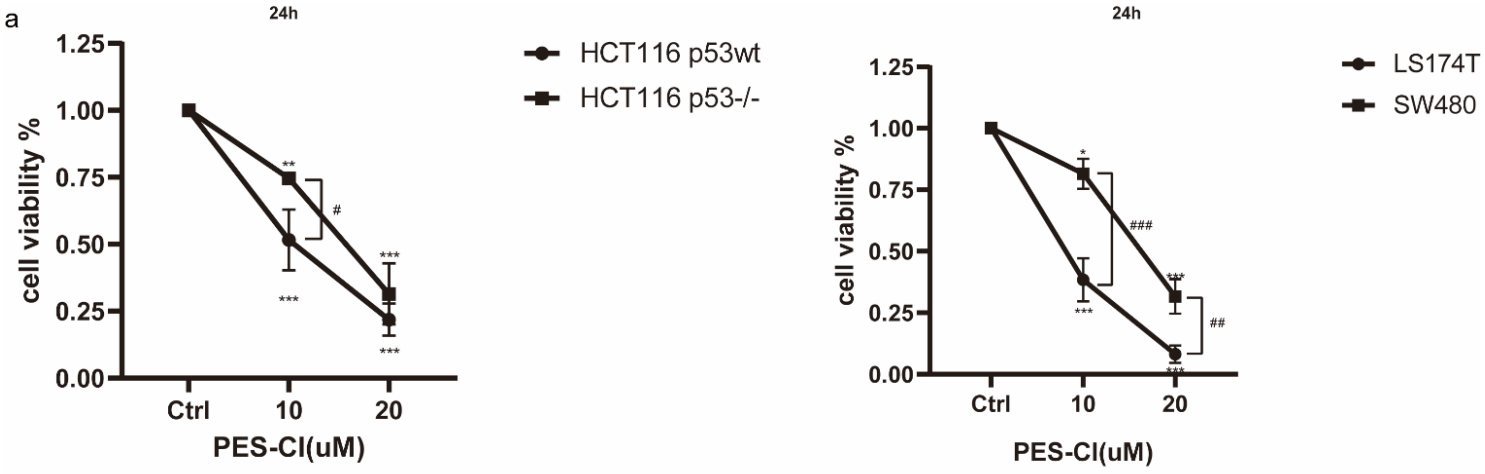

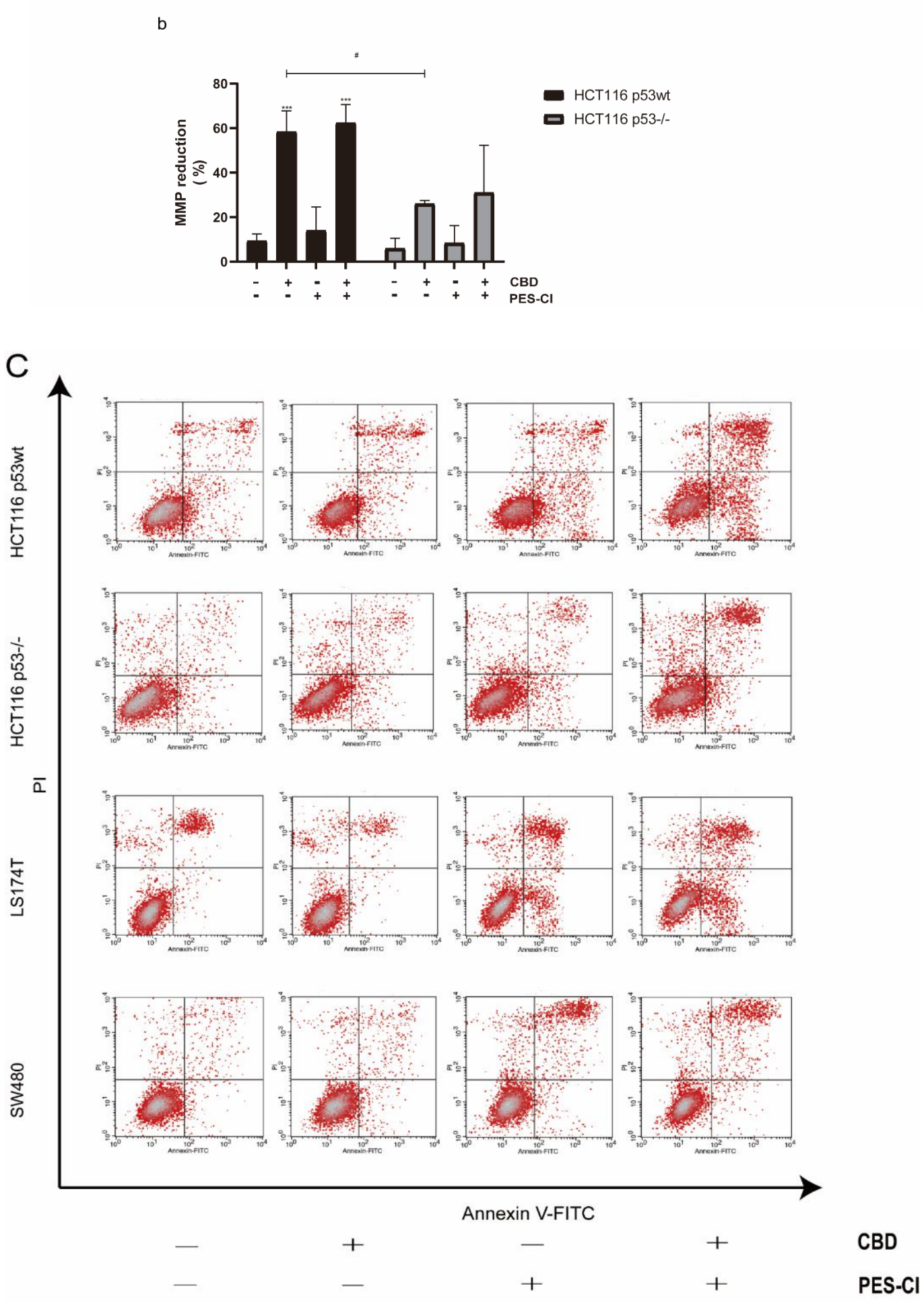
b
#
80
60
40
20
0
MMP reduction (%)
***
***
HCT116 p53wt
HCT116 p53-/-
CBD
PES-CI
C
HCT116 p53wt
HCT116 p53-/-
LS174T
SW480
PI
Annexin-FITC
Annexin V-FITC
CBD
PES-CI

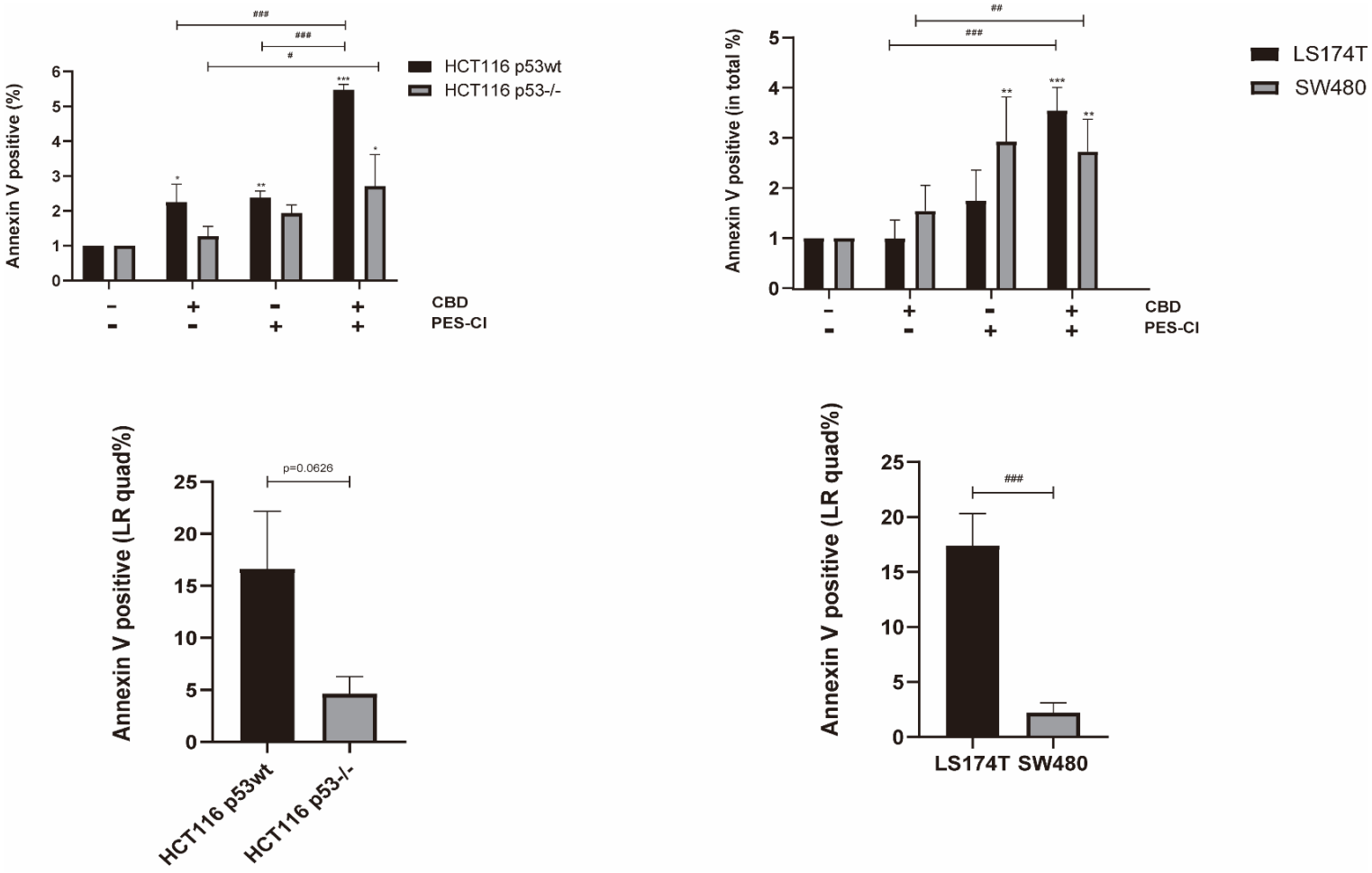

Figure 6. The Hsp70 inhibitor PES-CI potentiates the antitumor effect of CBD. (a) Viability of CRC cells treated with PES-CI. (b) CBD-induced reduction in mitochondrial membrane potential (MMP) (%) in HCT116 cells. (c) Apoptosis determined by Annexin V/PI staining. (d, e) Percentage of apoptotic CRCs (Annexin V positive: UR quad%+LR quad%). (f, g) Percentage of early apoptotic Annexin V positively stained CRCs (LR quad%). Statistical differences of each group were evaluated by compared to the control (* $p \leq 0.05$, ** $p \leq 0.01$ and *** $p \leq 0.001$) or to the other group (# $p \leq 0.05$, ## $p \leq 0.01$ and ### $p \leq 0.001$). One-way ANOVA ,Two-way ANOVA analysis or t-test was used. All data are expressed as the mean ± SD of three independent experiments. (Cannabidiol-induced crosstalk of apoptosis and macroautophagy in colorectal cancer cells involves p53 and Hsp70, Fei Wang, et al. Cell Death Discov. 2023 Aug 5;9(1):286. doi: 10.1038/s41420-023-01578-9)

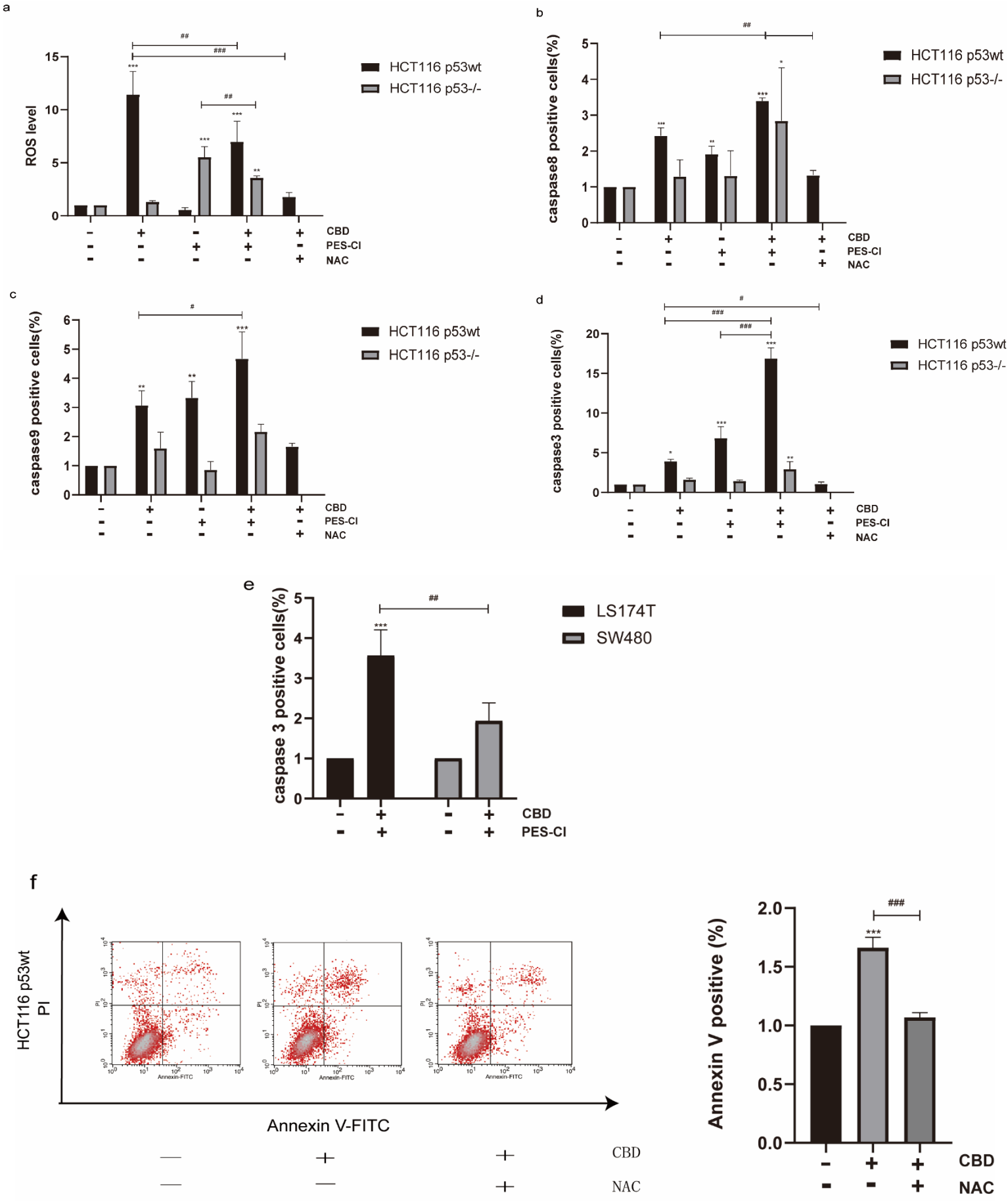

Figure 7. Hsp70 inhibition enhances the p53-dependent cleaved caspase-8/9/3 pathway. (a) Flow cytometry was used to monitor ROS generation in both p53wt and p53-/- HCT116 cells

by staining with DCF-DA after CBD (15 μM) treatment in combination with PES-CI (IC50 value accordingly) or ROS scavenger NAC (2.5 mM). (b-d) Cleaved caspase-8/9/3 levels as measured by flow cytometry. (e). The p53-dependent activation of caspase-3 in LS174T and SW480 cells after treatment with CBD and PES-CI. (f) NAC attenuated apoptosis induced by CBD in HCT116 p53wt cells. Statistical differences of each group were evaluated by compared to the control (* $p \leq 0.05$, ** $p \leq 0.01$ and *** $p \leq 0.001$) or to the other group (# $p \leq 0.05$, ## $p \leq 0.01$ and ### $p \leq 0.001$). One-way ANOVA, Two-way ANOVA or t-test was used. All data are expressed as the mean ± SD of three independent experiments. (Cannabidiol-induced crosstalk of apoptosis and macroautophagy in colorectal cancer cells involves p53 and Hsp70, Fei Wang, et al. Cell Death Discov. 2023 Aug 5;9(1):286. doi: 10.1038/s41420-023-01578-9)

3.5 Protective macroautophagy induced by CBD is related to ROS accumulation and wild type p53 acts as a potential upstream regulator

Associated with the heat shock (stress protein) system, macroautophagy is a regulatory mechanism which maintains cellular protein homeostasis by sequestering and transporting large protein aggregates and damaged or senescent organelles to lysosomes for degradation.

Microtubule-associated protein 1A/1B-light chain 3 (LC3) is a ubiquitously distributed soluble protein which is incorporated into the expanded phagosome upon binding to phosphatidylethanolamine[125]. In this process, phagosome-bound LC3BII acts as a pillar for proteins bound to ubiquitinated substrates[126]. During the macroautophagy flux, autophagosomes fuse with lysosomes, which subsequently hydrolyze and degrade the content inside a cell[125]. The ability of PES-Cl to inhibit macroautophagy has been documented in several different autophagy assays[123, 127]. As shown in Figure 8a, LC3BII appeared to be elevated in HCT116 p53wt cells, but not in HCT116 p53-/- cells. p62 behaves as a linker in the macroautophagy process, and its aberrant aggregation

indicates an impairment of the autophagy degradation pathway. To distinguish whether the accumulation of these proteins is caused by an increased macroautophagy or by a dysregulated auto-lysosomal degradation, we examined the levels of LC3BI and LC3BII in HCT116 p53wt cells 24h after exposure to CBD in the presence and absence of BafA1 (50nM), an autophagy inhibitor which halts the autophagic flux by inhibiting late-stage fusion between autophagosomes and lysosomes [128]. A co-incubation with BafA1 significantly enhances the CBD-induced increase of these proteins in HCT116 p53wt cells (Figure 8b), which means that CBD accelerates the macroautophagy process. Similar results were shown in Figure 6c. The number of LC3B vesicles in p53wt cells were significantly increased after CBD treatment, while they did not significantly alter in p53 deficient cells. In line with a previous report [127], a 24h co-incubation with CBD (15 µM) and PES-CI prevented the autophagy flux in both HCT116p53wt and HCT116 p53-/-cells, whereas p62 overexpression was primarily dependent on the Hsp70 inhibitor in PES-CI in HCT116 p53-/- cells. Additionally, NAC slightly suppressed the CBD-induced macroautophagy, which was induced by ROS in HCT116 p53wt cells, as it attenuated the p62 and LC3BII expression as well as LC3B vesicles without BafA1(p=0.3294 and p=0,3821, respectively; Figure 8a, c) or with BafA1 (p=0.2118 and p=0.1422, respectively; Figure 8b). Autophagy was once known to be triggered by the lack of p53 or mutant p53 mostly during the G1 phase and to a lesser extent in the S phase to avoid that cells enter the G2/M phase [129]. However, our study found that the p53 inhibitor pifithrin-α (20 µM) decelerates the cytosolic expression of p62 (p=0.026) and LC3BII(p=0.2155) which induced by CBD after a 24h cotreatment with BafA1(Figure 8d). Based on the results of the viability

assay, this kind of autophagy displays a cytoprotective effect (Figure 8e). In summary, our data indicates that CBD stimulates protective macroautophagy partially though ROS accumulation and it is likely that wild type p53 displays a role in this process as an upstream regulating factor.

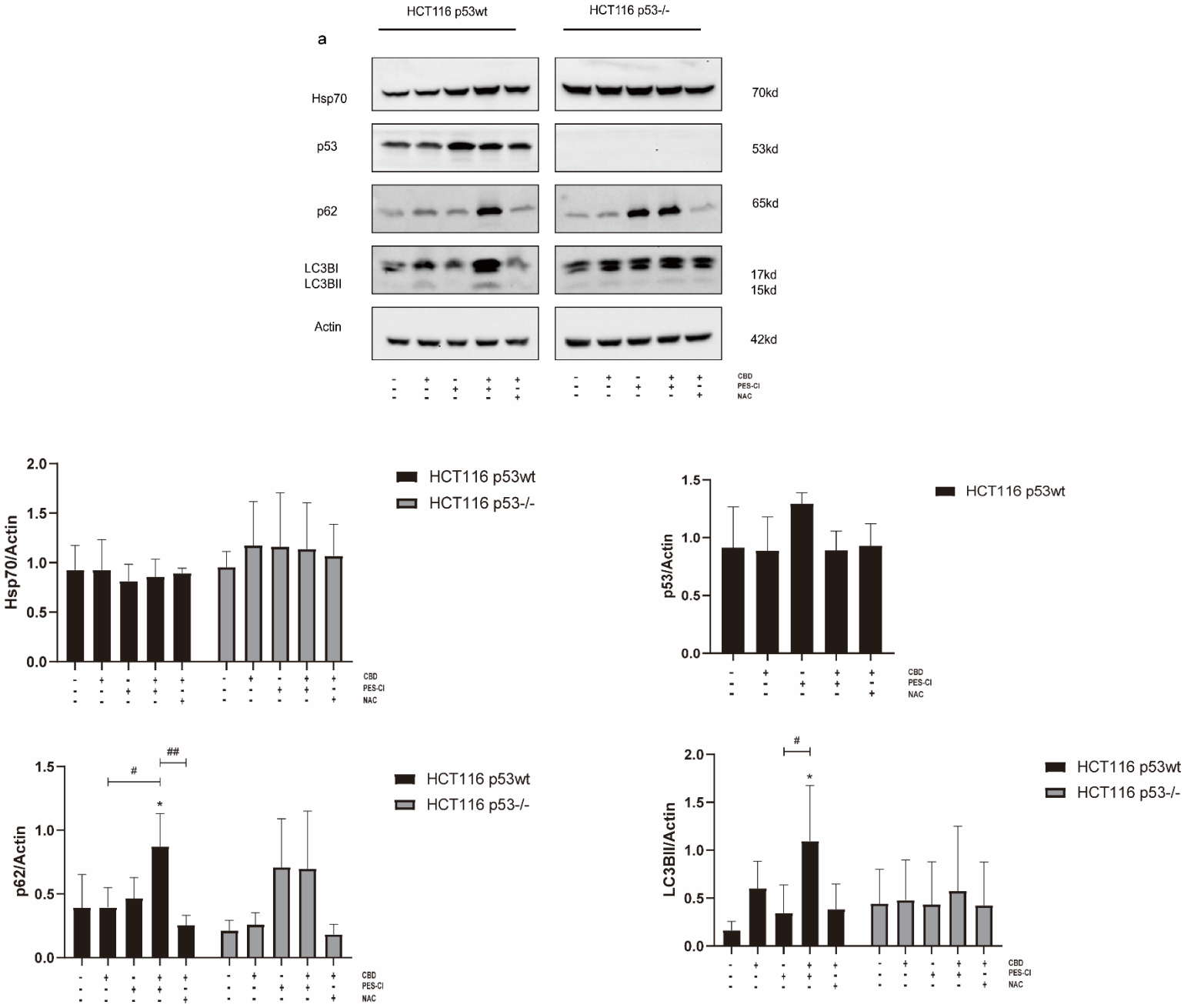

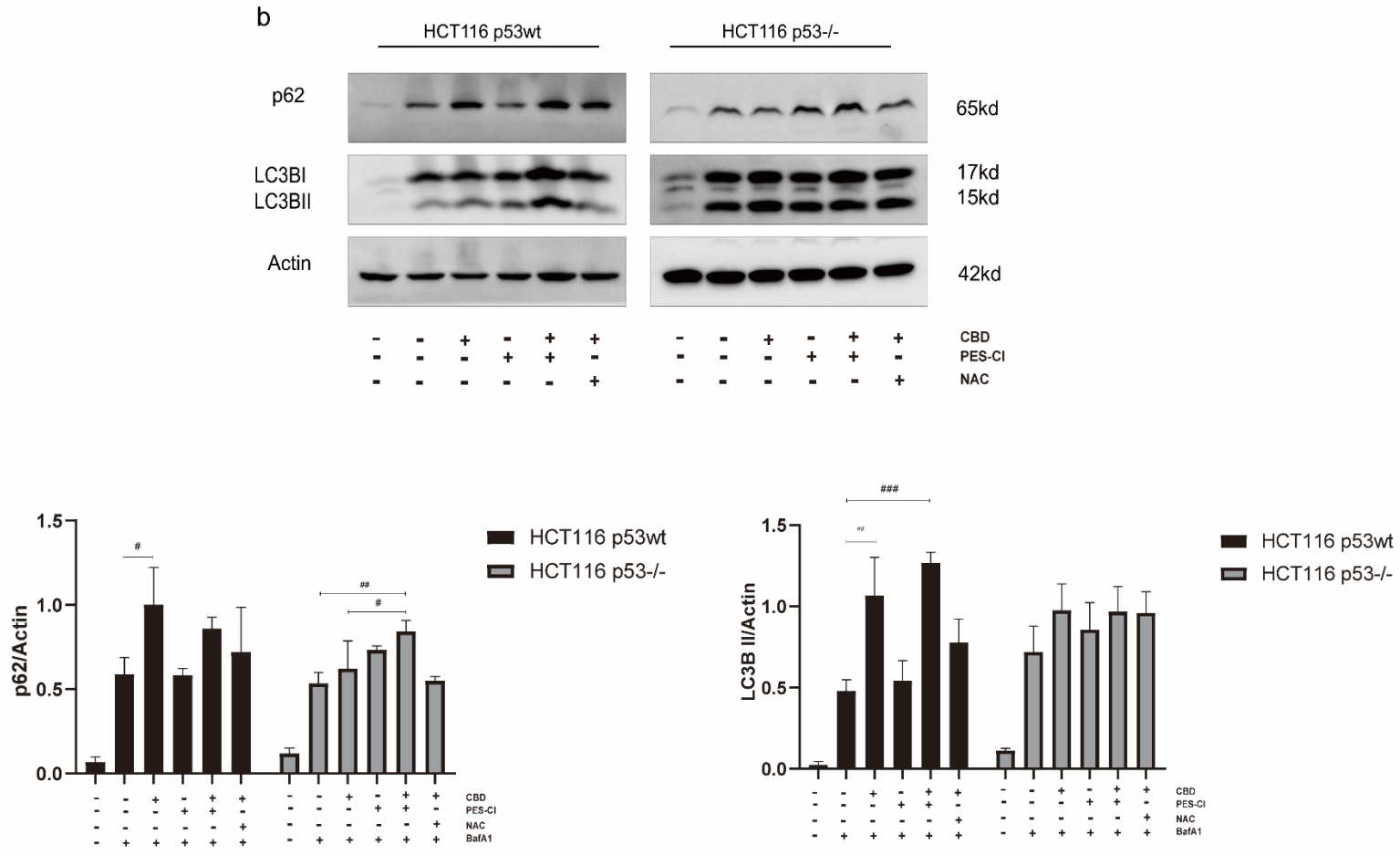
b
HCT116 p53wt
HCT116 p53-/-
p62
LC3BI
LC3BII
Actin
65kd
17kd
15kd
42kd
CBD
PES-CI
NAC
p62/Actin
LC3B II/Actin
HCT116 p53wt
HCT116 p53-/-
BafA1

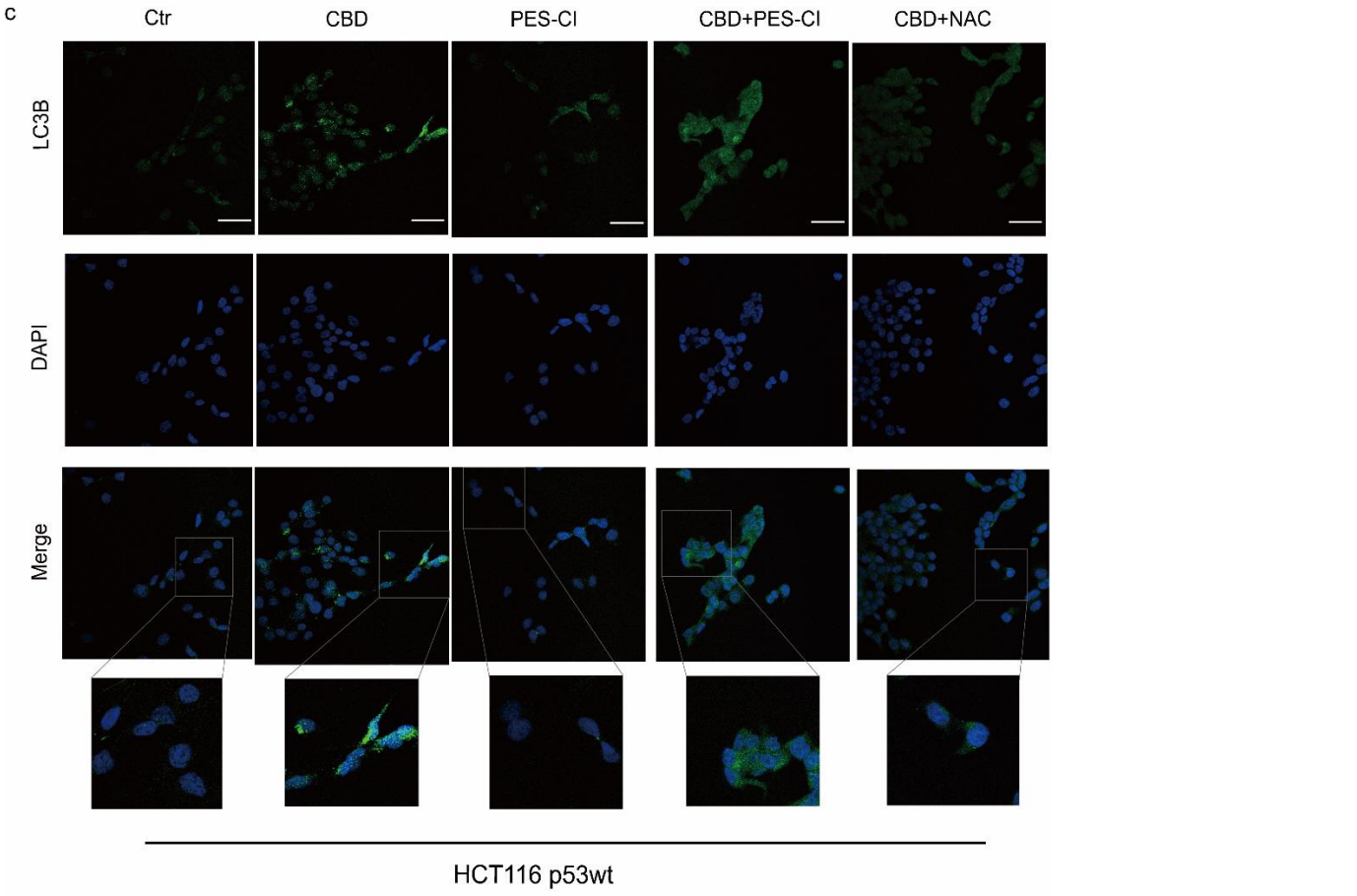
c
Ctr
CBD
PES-CI
CBD+PES-CI
CBD+NAC
LC3B
DAPI
Merge
HCT116 p53wt

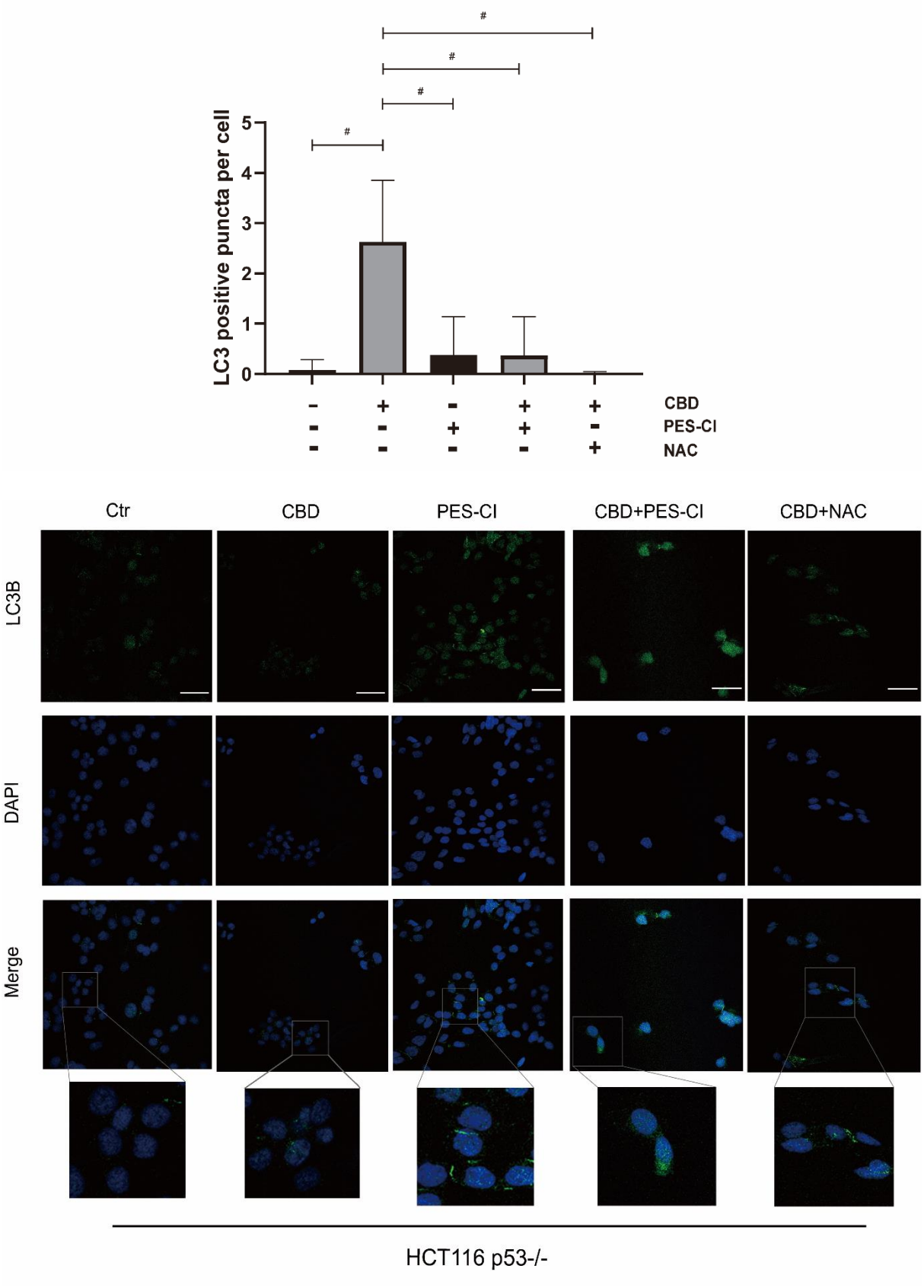
#
#
#
#
LC3 positive puncta per cell
5
4
3
2
1
0
- + - + +
- - + + -
- - - - +
CBD
PES-CI
NAC
Ctr
CBD
PES-CI
CBD+PES-CI
CBD+NAC
LC3B
DAPI
Merge
HCT116 p53-/-

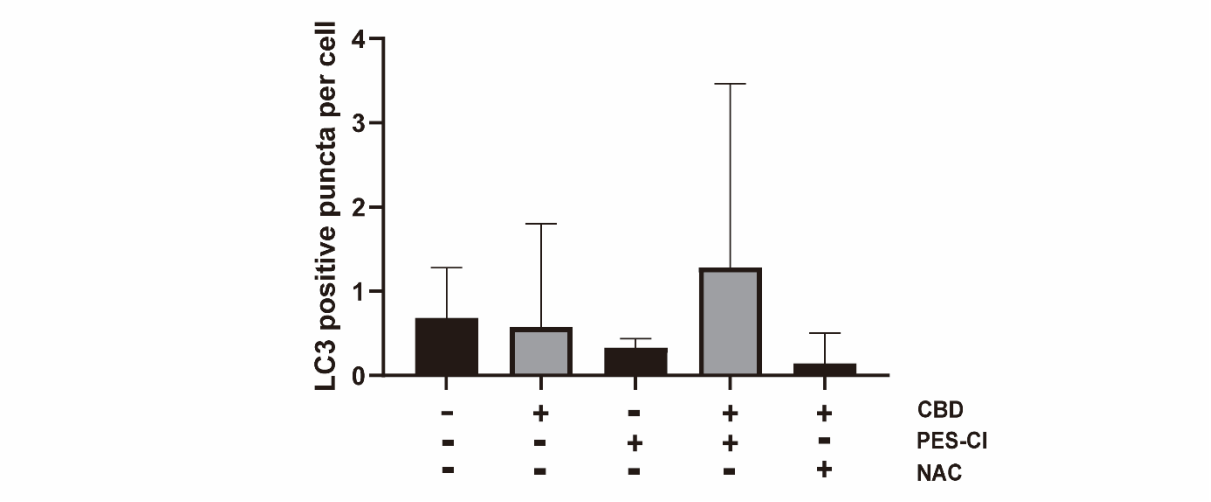
LC3 positive puncta per cell
4
3
2
1
0
CBD
PES-CI
NAC

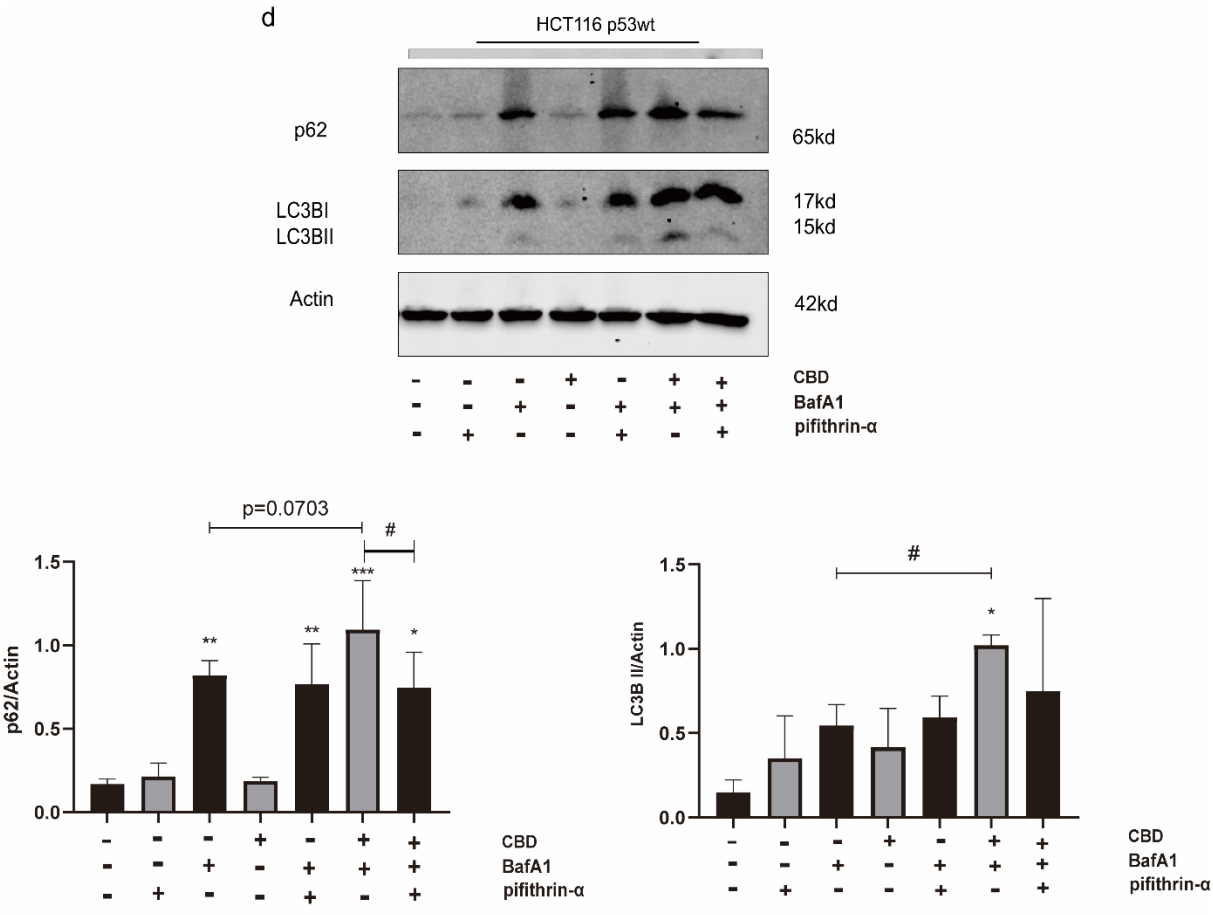
d
HCT116 p53wt
p62
65kd
LC3BI
LC3BII
17kd
15kd
Actin
42kd
CBD
BafA1
pifithrin-α
p=0.0703
#
p62/Actin
1.5
1.0
0.5
0.0
LC3B II/Actin

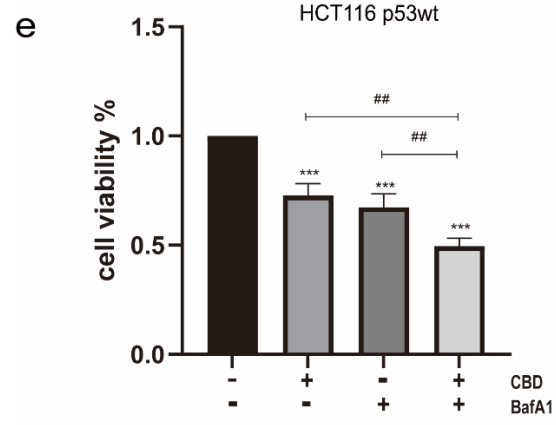
e
HCT116 p53wt
cell viability %
1.5
1.0
0.5
0.0
##
CBD
BafA1

Figure 8. Protective autophagy induced by elevated ROS levels after CBD treatment in HCT116 p53wt cells. (a) Immunoblot of cytosolic Hsp70, p62 and LC3BII expression levels in HCT116 p53wt and HCT116 p53-/- cells after CBD treatment (15 µM) and a co-treatment with the Hsp70 inhibitor PES-CI (IC50 value correspondingly) and/or the ROS scavenger NAC (2.5 mM). Adjacent bar charts show the quantification of Hsp70, p62 and LC3BII expression upon a combined treatment with the different reagents in HCT116 p53wt and p53-/- cells. (b) Representative immunoblot showing the expression of intracellular p62 and LC3B 24h after co-incubation of p53wt cells with treatment above and BafA1 (50nM), a quantification of the p62 and LC3BII expression level are shown in the adjacent bar chart. (c) Quantification of LC3B vesicles using confocal fluorescence microscopy. (Left) Exemplary confocal images of LC3B (green) expressing HCT116 p53wt and HCT116 p53-/- cells. Nuclei, DAPI (blue). Scale bar: 100 µm. (Right) Quantification of the LC3B vesicles per cell of HCT116 cells. Statistical differences of each group were evaluated by compared to the other group (# $p \leq 0.05$, ## $p \leq 0.01$ and ### $p \leq 0.001$). One-way ANOVA was used. Results are shown as mean± SEM (HCT116 p53wt n =20-85, HCT116 p53-/-n = 9-80). (d) The amount of p62 is increased in CBD-treated HCT116 p53wt cells in the presence of p53 inhibitor pifithrin-α (20uM). The relative expression levels of p62 and LC3B are shown in the adjacent bar graph. (e) CBD-induced cytoprotective autophagy is associated with a reduced cell viability following co-treatment with BafA1, as determined with the CCK-8 viability assay in HCT116 p53wt cells. Statistical differences of each group were evaluated by compared to the control (* $p \leq 0.05$, ** $p \leq 0.01$ and *** $p \leq 0.001$) or to the other group (# $p \leq 0.05$, ## $p \leq 0.01$ and ### $p \leq 0.001$). One-way ANOVA was used. All data are expressed as the mean ± SD of three biological replicates. (Cannabidiol-induced crosstalk of apoptosis and macroautophagy in colorectal cancer cells involves p53 and Hsp70, Fei Wang, et al. Cell Death Discov. 2023 Aug 5;9(1):286. doi: 10.1038/s41420-023-01578-9)

3.6 p53-associated ROS accumulation activate Nrf2 pathway

The macroautophagy element p62 is a target gene of the Nrf2 (nuclear factor erythroid-derived 2-like 2-antioxidant response element, ARE) transcriptional pathway and its accumulation has been reported to maintain Nrf2 activation by means of autophagic degradation together with the Nrf2 repressor protein keap1 (kelch-like ECH-associated protein 1)[130]. In our study, overexpression of p62 and macroautophagy activation were associated with a downregulation of keap1 during oxidative stress which results in the nuclear translocation of Nrf2 (Figure

9a, d) in HCT116 p53wt cells. Since this effect can be reversed by NAC (Figure 8a, Figure 9d) it is assumed that p53wt-associated oxidative stress continuously triggers the autophagic degradation of keap1 and thereby contributes to the excessive activation of Nrf2. In addition to the degradation of keap1 which is induced by an activated autophagy, inhibition of autophagy also leads to a cytoplasmic accumulation of p62 and a persistent activation of Nrf2[131]. The inhibition of autophagy by the Hsp70 inhibitor PES-CI results in a decrease in reactive oxygen species (ROS) (Figure 6a) and a corresponding decrease in the keap-1 expression in both p53-/- and p53wt HCT116 cells ($p=0.3415$, $p=0.0276$, respectively) (Figure 9a). However, the nuclear translocation of Nrf2 was attenuated only in HCT116 p53wt cells (Figure 9d). This effect might be associated with a repression of Hsp70-assisted Nrf2 nuclear translocation. However, Nrf2 overexpression occurs only after a 24h treatment with the Hsp70 inhibitor PES-CI in p53 deficient cells and is associated with an increased ROS production (Figure 7a, Figure 9d). Recent studies have also demonstrated that p62 is a potential target of Nrf2[132], and that the induction of the p62 gene by oxidative stress is mediated via Nrf2. As shown in Figure 9d, PES-CI pronounced the Nrf2 expression in HCT116 p53-/-cells, which might be an explanation for the abnormal accumulation of p62 after a treatment with PES-CI (Figure 8a). NAC partially reverses the downregulation of keap1, but almost completely suppresses the expression of Nrf2 (Figure 9a, d) in HCT116 p53wt cells. A Nrf2 inhibitor (ML385, 5 µM) enhances the antitumor effect of CBD by increasing apoptosis in p53wt cells, whereas there is a blunted induction of apoptosis in p53 knockout cells (Figure 9b, c). Activation of the keap1-Nrf2 system is supposed to protect cells from excessive ROS toxicity which is caused

by CBD, as suggested by the oxidative stress hypothesis [133] and thereby inhibits the activation of the apoptotic pathway, mediated by p53.

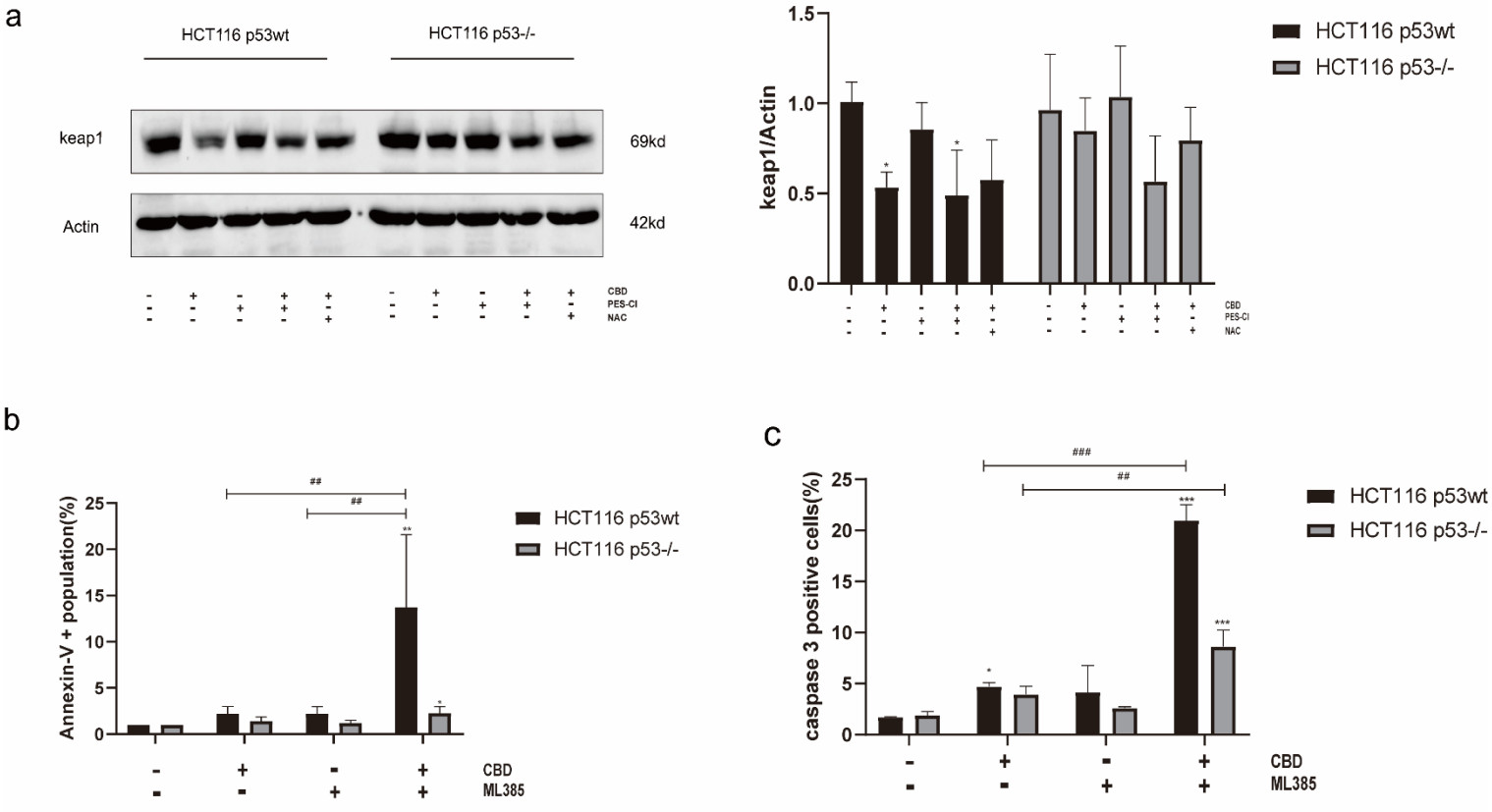

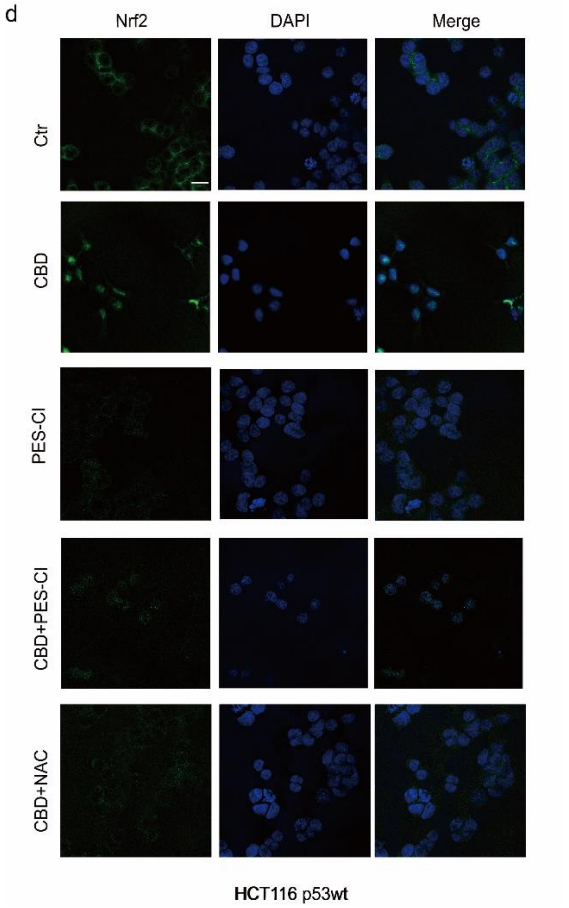

Figure 9. p53-associated oxidative stress activates the keap1-Nrf2 pathway. (a) Immunoblot of keap1 and Actin. A quantification of the keap1: actin ratio is shown in the adjacent bar chart. (b. c) Inhibition of Nrf2 by ML385 (5uM, 24h) enhances the antitumoral effect of CBD via an increase in apoptosis in p53wt cells, whereas only a moderate effect is observed for p53 knockout cells. Statistical differences of each group were evaluated by compared to the control (* $p \leq 0.05$, ** $p \leq 0.01$ and *** $p \leq 0.001$) or to the other group (# $p \leq 0.05$, ## $p \leq 0.01$ and ### $p \leq 0.001$). One-way ANOVA was used. All data are representative of three independent experiments. (d) HCT116 p53wt and p53-/-cells stained for Nrf2 after different treatments as determined by confocal microscopy (Scale bars: 25 μm). (Cannabidiol-induced crosstalk of apoptosis and macroautophagy in colorectal cancer cells involves p53 and Hsp70, Fei Wang, et al. Cell Death Discov. 2023 Aug 5;9(1):286. doi: 10.1038/s41420-023-01578-9)

4. Discussion

In response to a wide range of stimuli that might cause genomic instability, the tumor suppressor protein p53 acts as a redox-active transcription factor that coordinates and controls cellular responses to maintain genomic integrity[134]. Following transcriptional activation of p53, for example, p21 expression is upregulated which results in RB-E2F complex formation and downregulation of a large number of cell cycle genes[135]. Double allelic mutations in the TP53 gene locus result in the loss of wild-type function of p53[106]. We found that the cell cycle arrest induced by CBD is associated with an upregulated p21 expression which is p53 independent. It is known that missense mutations in the DNA-binding domain of p53 partially or completely lose their tumor suppressive capability and enhance invasion, migration and treatment resistance of tumor cells [107, 136]. Reactive oxygen species (ROS) can act as signaling molecules or as cellular toxins. Wild-type p53 organizes the transcription of multiple genes in response to cellular stressors that cause DNA damage, minimize the

dissemination of damaged DNA [137]by inducing cell cycle arrest, senescence, or apoptosis through differential activation of different target genes[138]. Our study suggests that the CBD-induced ROS production depends on a functional activation of p53, since the ROS accumulation and nuclear translocation of p53 only occurs in p53 WT cells upon CBD treatment (Figure 5). Recent studies showed that ROS performs dual activities as an up-stream signal triggering p53 activation and a downstream factor mediating apoptosis. The repression of antioxidant genes and transactivation of pro-oxidant enzymes by a p53 activation at the promoter level have been identified as an additional way to increase oxidative stress[139]. p53 directly regulates glycolysis and apoptosis regulator (TIGAR) and cytochrome c oxidase 2 (sCO2) gene expression, for instance, thereby enhancing oxidative phosphorylation and overexpression in ROS accumulation, which play major roles in programmed cell death[140-142]. As shown in Figure 5 and Figure 6, apoptotic pathways were only moderately activated (cleaved caspase-8/9/3 upregulated) by CBD in the case of a dramatic increase over ROS, and the antioxidative ROS scavenger NAC, further diminished the p53-dependent apoptosis.

It is well accepted that Hsp70, which is abundantly overexpressed in many different cancer types, suppresses both the extrinsic and intrinsic apoptotic pathway and thereby allows cancer progression[143]. Transcription factor Jun is a protein encoded by the JUN gene. c-Jun, in combination with protein c-Fos, forms the AP-1 early response transcription factor, which mediates cell cycle progression and anti-apoptotic activity[144, 145]. JNK (c-Jun-N-terminal Kinase) activity was shown to play an important role in the induction of the intrinsic apoptotic pathway through mitochondrial dysfunction [146]that can be inhibited

by the Hsp70-CHIP complex[147], and wild-type p53 mediates JNK-dependent apoptosis[148]. The results of our study revealed that the Hsp70 inhibitor PES-CI enhances the intrinsic apoptotic pathway triggered by CBD in HCT116 p53wt cells, as illustrated in Figure 6, which is associated with a considerable overproduction of cleaved caspases-9/3[149]. In addition, the cysteine protease caspase-8, which represents the extrinsic apoptotic pathway[150], was activated by CBD in a p53-independent manner (Figure 6). Based on our transcriptional process enrichment analysis (Figure 3), the transcription factor JUN signaling pathway is one of a series of CBD-CRC-relative transcriptional processes, which might provide an up-stream signal of p53 mediated cell death upon CBD treatment.

ROS-induced DNA damage activates the PARP1 signaling pathway which further initiates autophagy[151]. A specialized autophagy response, resulting in the removal of damaged organelles and protecting cells, can be triggered by organellar stress[152]. We found an increased production of reactive oxygen species induced by CBD and subsequently an activated protective macroautophagy, which might hinder the programmed cell death mediated by p53. This protective macro-autophagy can be reversed by an Hsp70 inhibition that blocks autophagy. A previous study showed that PES interacts with Hsp70, but not with Hsc70[124]. However, it was later proven that PES inhibited both Hsp70 and Hsc70 in vitro[153]. PES-CI, which is derived from PES containing 2-(3-chlorophenyl) ethynesulfonamide, has superior ability to inhibit macroautophagy compared to PES[123]. At present, the available evidence is insufficient to rule out the possibility that the ability of PES-Cl to inhibit autophagy is partially due to a suppression in Hsc70-mediated CMA

(chaperone-mediated autophagy)[154]. This possibility and the potential function of CMA regarding the antitumor effect of CBD remains to be explored. A mildly decelerated p62 induced by a p53 inhibitor suggests a potential mutual constraint relationship between these two signaling pathways. Similar results were obtained by in vitro and in vivo analysis, showing a weak upregulation of cleaved caspase-3 upon CBD treatment in wild-type cells despite an intense ROS generation (Figure 4-6). The protective role of Hsp70 was partially dependent on macro-autophagy activation, indicating a crosstalk between Hsp70 and macro-autophagy in the oxidative stress response induced by CBD.

Autophagy is one of the main routes to eliminate damaged material induced by oxidative stress. Oxidative stress is associated with elevated levels of intracellular reactive oxygen species (ROS) that trigger the activation of transcription factors, such as Nrf2, to maintain redox homeostasis by inducing the antioxidative pathways[155]. In this study we could show that CBD causes the production of ROS which in turn activates the keap1-Nrf2-antioxidant system to attenuate ROS toxicity (Figure 9). In addition, the enhanced macroautophagy induced by keap1 ablation can be suppressed by an Hsp70 inhibition which results in an downregulation of keap1 but a weaker translocation of Nrf2 into the nucleus (Figure 9), thereby eliminating the anti-apoptotic effect This attenuated nuclear translocation of Nrf2 may be related to the chaperone role of Hsp70[156], which maintains intracellular environmental homeostasis after stressor damage by assisting Nrf2 nuclear transport.

5. Summary

Pharmacological effects, as well as complex mechanisms of CBD on activated biological targets, which belong to up- and/or down-stream targets of CBD were studied with respect to their anti-tumor capacities. It has been shown that CBD either alone or in combination with other therapies has the potential of a novel anti-tumor, anti-inflammatory and anti-pain drug in preclinical studies and first clinical trials. Few clinical trials demonstrated beneficial pharmacokinetic and pharmacodynamic characteristics of the drug, and some anti-tumor activities at well-tolerated doses.

For a long time, it was considered that the primary mechanism by which TP53 suppresses tumor formation was the production of apoptotic cell death. Herein we show that the p53 status, a main determinant of anti-neoplastic drug efficacy, appears to impact also the cellular oxidative stress after CBD treatment. A CBD treatment induces complex events in p53wt CRC cells, including autophagy, activation of the chaperone system (Hsp70 induction) and stimulation of the keap1-Nrf2 signaling pathway. Inhibition of Hsp70 was shown to shift the CBD-induced autophagy towards caspase-8/9 mediated apoptosis. Taken together a combined treatment consisting of CBD and Hsp70 inhibition may enable an

improved programmed tumor cell death in p53wt CRC cells (Figure 10).

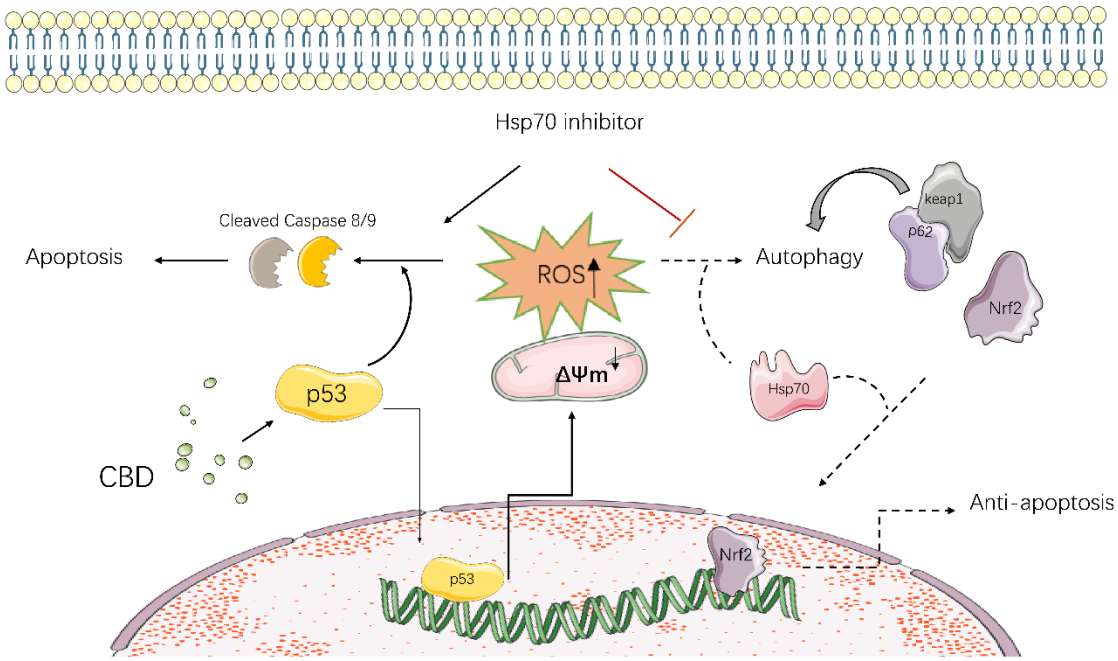

Figure 10. Potential mechanism of CBD in anti-tumor effect. Both the protective autophagy route and the programmed cell death pathway are activated in response to mitochondrial malfunction and ROS overproduction, which are caused by p53 nuclear translocation after CBD treatment. Hsp70-mediated autophagy degrades keap1, consequently, unbound Nrf2 is released for nuclear translocation and blocks p53-regulated apoptosis. (Cannabidiol-induced crosstalk of apoptosis and macroautophagy in colorectal cancer cells involves p53 and Hsp70, Fei Wang, et al. Cell Death Discov. 2023 Aug 5;9(1):286. doi: 10.1038/s41420-023-01578-9)

7. Supplementary Figures

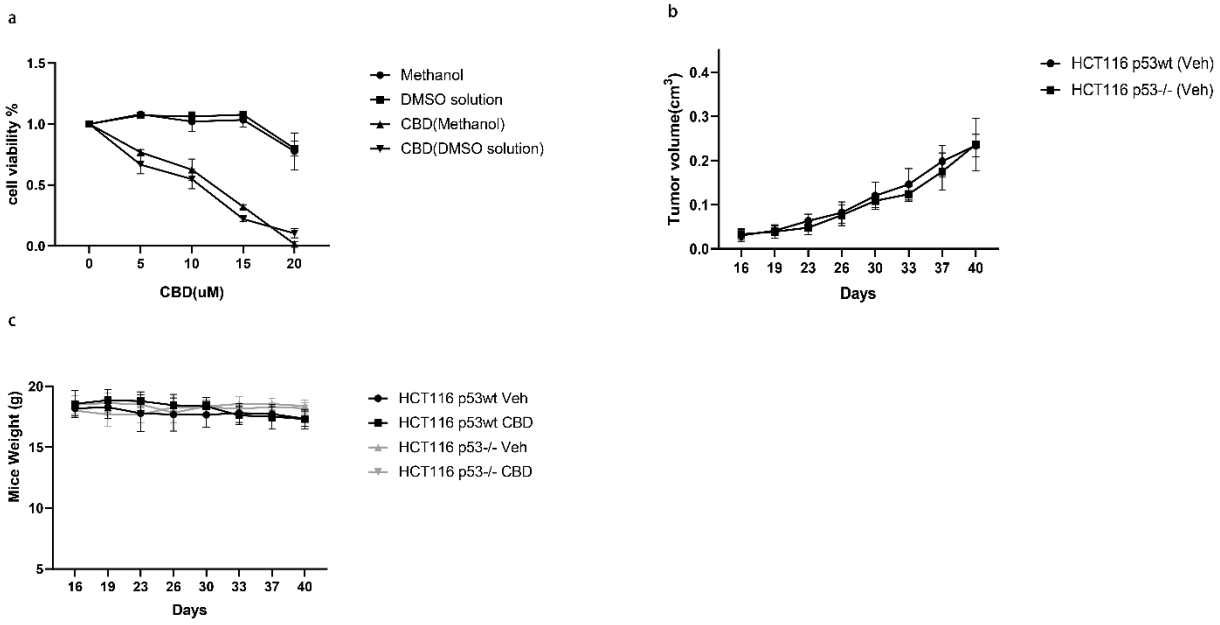

Supplementary Figure 1. (a) To determine the cytotoxicity of methanol and DMSO as well as the efficacy of CBD dissolved in these two different solvents, cell viability of HCT116 p53wt cells was determined by CCK8 assay in vitro.(b) The comparison of the tumor size between wide-type and knock-out with vehicle treatment. (c) Animal weights were measured twice per week. (Cannabidiol-induced crosstalk of apoptosis and macroautophagy in colorectal cancer cells involves p53 and Hsp70, Fei Wang, et al. Cell Death Discov. 2023 Aug 5;9(1):286. doi: 10.1038/s41420-023-01578-9)

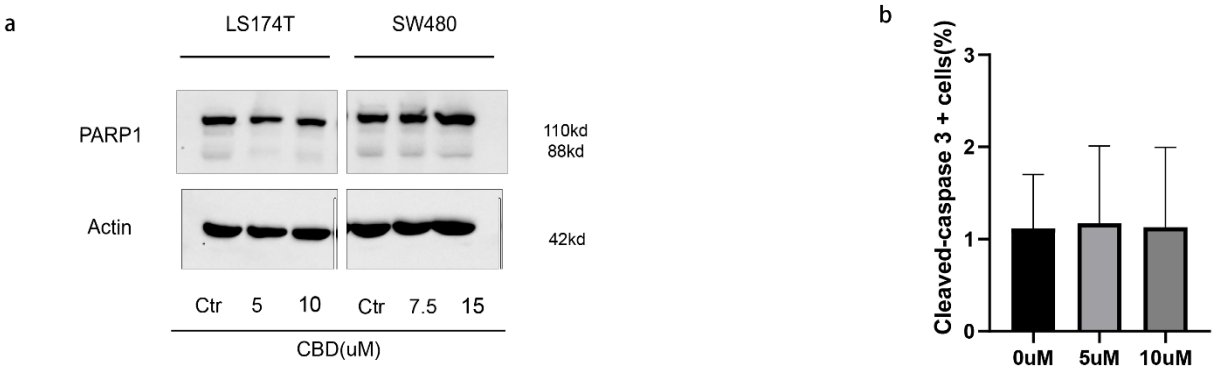

Supplementary Figure 2. (a) Immunoblot analysis of cytosolic PARP1 and cleaved-PARP1 expression in LS174T and SW480 cells after 24h CBD treatment. (b) Cleaved-caspase 3 assay has been performed to detect apoptotic cells after CBD treatment. One-way ANOVA was used. Statistical differences of each group were evaluated by compared to the control (* $p \leq 0.05$, ** $p \leq 0.01$ and *** $p \leq 0.001$) All data are expressed as the mean ± SD of three independent experiments. (Cannabidiol-induced crosstalk of apoptosis and macroautophagy in colorectal cancer cells involves p53 and Hsp70, Fei Wang, et al. Cell Death Discov. 2023 Aug 5;9(1):286. doi: 10.1038/s41420-023-01578-9)

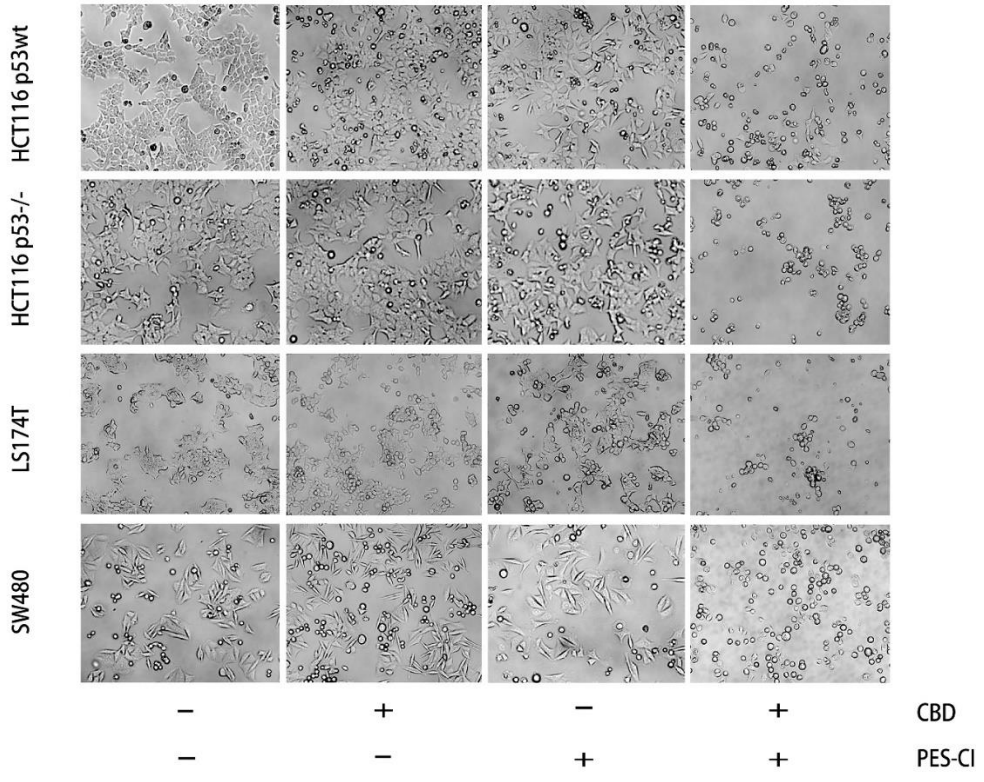

Supplementary Figure 3. Morphological changes of CRC cells upon treatment with CBD, PES-CI as well as combination. The concentration of CBD and PES-CI were determined according to the IC50 values respectively (100× magnification). (Cannabidiol-induced crosstalk of apoptosis and macroautophagy in colorectal cancer cells involves p53 and Hsp70, Fei Wang, et al. Cell Death Discov. 2023 Aug 5;9(1):286. doi: 10.1038/s41420-023-01578-9)

6. References

1. Bonini SA, Premoli M, Tambaro S, Kumar A, Maccarinelli G, Memo M, Mastinu A: **Cannabis sativa: A comprehensive ethnopharmacological review of a medicinal plant with a long history**. *Journal of ethnopharmacology* 2018, **227**:300-315.
2. Järvinen T, Pate DW, Laine K: **Cannabinoids in the treatment of glaucoma**. *Pharmacology & therapeutics* 2002, **95**(2):203-220.
3. Slatkin NE: **Cannabinoids in the treatment of chemotherapy-induced nausea and vomiting: beyond prevention of acute emesis**. *The journal of supportive oncology* 2007, **5**(5 Suppl 3):1-9.
4. Chadwick VL, Rohleder C, Koethe D, Leweke FM: **Cannabinoids and the endocannabinoid system in anxiety, depression, and dysregulation of emotion in humans**. *Current opinion in psychiatry* 2020, **33**(1):20-42.
5. Liang YC, Huang CC, Hsu KS: **Therapeutic potential of cannabinoids in trigeminal neuralgia**. *Current drug targets CNS and neurological disorders* 2004, **3**(6):507-514.
6. Abrams DI, Jay CA, Shade SB, Vizoso H, Reda H, Press S, Kelly ME, Rowbotham MC, Petersen KL: **Cannabis in painful HIV-associated sensory neuropathy: a randomized placebo-controlled trial**. *Neurology* 2007, **68**(7):515-521.
7. Pryce G, Baker D: **Emerging properties of cannabinoid medicines in management of multiple sclerosis**. *Trends in neurosciences* 2005, **28**(5):272-276.
8. ElSohly MA, Radwan MM, Gul W, Chandra S, Galal A: **Phytochemistry of Cannabis sativa L**. *Progress in the chemistry of organic natural products* 2017, **103**:1-36.

9. Zuardi AW: History of cannabis as a medicine: a review. *Revista brasileira de psiquiatria (Sao Paulo, Brazil : 1999)* 2006, 28(2):153-157.
10. Klumpers LE, Thacker DL: A Brief Background on Cannabis: From Plant to Medical Indications. *Journal of AOAC International* 2019, 102(2):412-420.
11. Pisanti S, Bifulco M: Modern History of Medical Cannabis: From Widespread Use to Prohibitionism and Back. *Trends in pharmacological sciences* 2017, 38(3):195-198.
12. Baron EP: Comprehensive Review of Medicinal Marijuana, Cannabinoids, and Therapeutic Implications in Medicine and Headache: What a Long Strange Trip It's Been …. *Headache* 2015, 55(6):885-916.
13. Kis B, Ifrim FC, Buda V, Avram S, Pavel IZ, Antal D, Paunescu V, Dehelean CA, Ardelean F, Diaconeasa Z *et al*: Cannabidiol-from Plant to Human Body: A Promising Bioactive Molecule with Multi-Target Effects in Cancer. *International journal of molecular sciences* 2019, 20(23).
14. Kumar A, Premoli M, Aria F, Bonini SA, Maccarinelli G, Gianoncelli A, Memo M, Mastinu A: Cannabimimetic plants: are they new cannabinoidergic modulators? *Planta* 2019, 249(6):1681-1694.
15. Morales P, Reggio PH, Jagerovic N: An Overview on Medicinal Chemistry of Synthetic and Natural Derivatives of Cannabidiol. *Frontiers in pharmacology* 2017, 8:422.
16. Pellati F, Borgonetti V, Brighenti V, Biagi M, Benvenuti S, Corsi L: Cannabis sativa L. and Nonpsychoactive Cannabinoids: Their Chemistry and Role against Oxidative Stress, Inflammation, and Cancer. *BioMed research international* 2018, 2018:1691428.
17. Appendino G, Chianese G, Taglialatela-Scafati O: Cannabinoids: occurrence and medicinal chemistry. *Current medicinal chemistry* 2011, 18(7):1085-1099.
18. Chandra S, Lata H, ElSohly MA, Walker LA, Potter D: Cannabis cultivation: Methodological issues for obtaining medical-grade product. *Epilepsy & behavior : E&B* 2017, 70(Pt B):302-312.
19. Andre CM, Hausman JF, Guerriero G: Cannabis sativa: The Plant of the Thousand and One Molecules. *Frontiers in plant science* 2016, 7:19.

20. Husni AS, McCurdy CR, Radwan MM, Ahmed SA, Slade D, Ross SA, ElSohly MA, Cutler SJ: **Evaluation of Phytocannabinoids from High Potency Cannabis sativa using In Vitro Bioassays to Determine Structure-Activity Relationships for Cannabinoid Receptor 1 and Cannabinoid Receptor 2**. *Medicinal chemistry research : an international journal for rapid communications on design and mechanisms of action of biologically active agents* 2014, **23**(9):4295-4300.
21. Rong C, Lee Y, Carmona NE, Cha DS, Ragguett RM, Rosenblat JD, Mansur RB, Ho RC, McIntyre RS: **Cannabidiol in medical marijuana: Research vistas and potential opportunities**. *Pharmacological research* 2017, **121**:213-218.
22. Boggs DL, Nguyen JD, Morgenson D, Taffe MA, Ranganathan M: **Clinical and Preclinical Evidence for Functional Interactions of Cannabidiol and Δ(9)-Tetrahydrocannabinol**. *Neuropsychopharmacology : official publication of the American College of Neuropsychopharmacology* 2018, **43**(1):142-154.
23. Baranauskaite J, Marksa M, Ivanauskas L, Vitkevicius K, Liaudanskas M, Skyrius V, Baranauskas A: **Development of extraction technique and GC/FID method for the analysis of cannabinoids in Cannabis sativa L. spp. santicha (hemp)**. *Phytochemical analysis : PCA* 2020, **31**(4):516-521.
24. Gul W, Gul SW, Radwan MM, Wanas AS, Mehmedic Z, Khan, II, Sharaf MH, ElSohly MA: **Determination of 11 Cannabinoids in Biomass and Extracts of Different Varieties of Cannabis Using High-Performance Liquid Chromatography**. *Journal of AOAC International* 2015, **98**(6):1523-1528.
25. Brighenti V, Pellati F, Steinbach M, Maran D, Benvenuti S: **Development of a new extraction technique and HPLC method for the analysis of non-psychoactive cannabinoids in fibre-type Cannabis sativa L. (hemp)**. *Journal of pharmaceutical and biomedical analysis* 2017, **143**:228-236.
26. Pertwee RG: **Cannabinoid pharmacology: the first 66 years**. *British journal of pharmacology* 2006, **147 Suppl 1**(Suppl 1):S163-171.
27. Elsohly MA, Slade D: **Chemical constituents of marijuana: the complex mixture of natural cannabinoids**. *Life sciences* 2005, **78**(5):539-548.

28. Jones P, Falvello L, Kennard O, Sheldrick G, Mechoulam R: Cannabidiol. *Acta Crystallographica Section B Structural Crystallography and Crystal Chemistry* 1977, **33**:3211-3214.
29. Agurell S, Halldin M, Lindgren JE, Ohlsson A, Widman M, Gillespie H, Hollister L: Pharmacokinetics and metabolism of delta 1-tetrahydrocannabinol and other cannabinoids with emphasis on man. *Pharmacological reviews* 1986, **38**(1):21-43.
30. Wilson RI, Nicoll RA: Endocannabinoid signaling in the brain. *Science (New York, NY)* 2002, **296**(5568):678-682.
31. Klein TW: Cannabinoid-based drugs as anti-inflammatory therapeutics. *Nature reviews Immunology* 2005, **5**(5):400-411.
32. Munro S, Thomas KL, Abu-Shaar M: Molecular characterization of a peripheral receptor for cannabinoids. *Nature* 1993, **365**(6441):61-65.
33. Griffin G, Atkinson PJ, Showalter VM, Martin BR, Abood ME: Evaluation of cannabinoid receptor agonists and antagonists using the guanosine-5'-O-(3-[35S]thio)-triphosphate binding assay in rat cerebellar membranes. *The Journal of pharmacology and experimental therapeutics* 1998, **285**(2):553-560.
34. Breivogel CS, Selley DE, Childers SR: Cannabinoid receptor agonist efficacy for stimulating [35S]GTPgammaS binding to rat cerebellar membranes correlates with agonist-induced decreases in GDP affinity. *The Journal of biological chemistry* 1998, **273**(27):16865-16873.
35. Howlett AC, Barth F, Bonner TI, Cabral G, Casellas P, Devane WA, Felder CC, Herkenham M, Mackie K, Martin BR *et al*: International Union of Pharmacology. XXVII. Classification of cannabinoid receptors. *Pharmacological reviews* 2002, **54**(2):161-202.
36. Fernández-Ruiz J, Romero J, Velasco G, Tolón RM, Ramos JA, Guzmán M: Cannabinoid CB2 receptor: a new target for controlling neural cell survival? *Trends in pharmacological sciences* 2007, **28**(1):39-45.
37. Pertwee RG: Pharmacology of cannabinoid receptor ligands. *Current medicinal chemistry* 1999, **6**(8):635-664.
38. Bayewitch M, Rhee MH, Avidor-Reiss T, Breuer A, Mechoulam R, Vogel Z: (-)-Delta9-tetrahydrocannabinol antagonizes the peripheral cannabinoid receptor-mediated inhibition of adenylyl

cyclase. *The Journal of biological chemistry* 1996, **271**(17):9902-9905.
39. Pertwee RG: **The diverse CB1 and CB2 receptor pharmacology of three plant cannabinoids: delta9-tetrahydrocannabinol, cannabidiol and delta9-tetrahydrocannabivarin**. *British journal of pharmacology* 2008, **153**(2):199-215.
40. Pertwee RG, Ross RA: **Cannabinoid receptors and their ligands**. *Prostaglandins, leukotrienes, and essential fatty acids* 2002, **66**(2-3):101-121.
41. Bisogno T, Hanus L, De Petrocellis L, Tchilibon S, Ponde DE, Brandi I, Moriello AS, Davis JB, Mechoulam R, Di Marzo V: **Molecular targets for cannabidiol and its synthetic analogues: effect on vanilloid VR1 receptors and on the cellular uptake and enzymatic hydrolysis of anandamide**. *British journal of pharmacology* 2001, **134**(4):845-852.
42. Thomas A, Baillie GL, Phillips AM, Razdan RK, Ross RA, Pertwee RG: **Cannabidiol displays unexpectedly high potency as an antagonist of CB1 and CB2 receptor agonists in vitro**. *British journal of pharmacology* 2007, **150**(5):613-623.
43. Laprairie RB, Bagher AM, Kelly ME, Denovan-Wright EM: **Cannabidiol is a negative allosteric modulator of the cannabinoid CB1 receptor**. *British journal of pharmacology* 2015, **172**(20):4790-4805.
44. Martínez-Pinilla E, Varani K, Reyes-Resina I, Angelats E, Vincenzi F, Ferreiro-Vera C, Oyarzabal J, Canela EI, Lanciego JL, Nadal X *et al*: **Binding and Signaling Studies Disclose a Potential Allosteric Site for Cannabidiol in Cannabinoid CB(2) Receptors**. *Frontiers in pharmacology* 2017, **8**:744.
45. De Petrocellis L, Ligresti A, Moriello AS, Allarà M, Bisogno T, Petrosino S, Stott CG, Di Marzo V: **Effects of cannabinoids and cannabinoid-enriched Cannabis extracts on TRP channels and endocannabinoid metabolic enzymes**. *British journal of pharmacology* 2011, **163**(7):1479-1494.
46. De Petrocellis L, Nabissi M, Santoni G, Ligresti A: **Actions and Regulation of Ionotropic Cannabinoid Receptors**. *Advances in pharmacology (San Diego, Calif)* 2017, **80**:249-289.
47. Vandewauw I, De Clercq K, Mulier M, Held K, Pinto S, Van Ranst N, Segal A, Voet T, Vennekens R, Zimmermann K *et al*: **A TRP**

channel trio mediates acute noxious heat sensing. *Nature* 2018, **555**(7698):662-666.
48. Hill TD, Cascio MG, Romano B, Duncan M, Pertwee RG, Williams CM, Whalley BJ, Hill AJ: **Cannabidivarin-rich cannabis extracts are anticonvulsant in mouse and rat via a CB1 receptor-independent mechanism**. *British journal of pharmacology* 2013, **170**(3):679-692.
49. Nilius B, Szallasi A: **Transient receptor potential channels as drug targets: from the science of basic research to the art of medicine**. *Pharmacological reviews* 2014, **66**(3):676-814.
50. Soethoudt M, Grether U, Fingerle J, Grim TW, Fezza F, de Petrocellis L, Ullmer C, Rothenhäusler B, Perret C, van Gils N *et al*: **Cannabinoid CB(2) receptor ligand profiling reveals biased signalling and off-target activity**. *Nature communications* 2017, **8**:13958.
51. Qin N, Neeper MP, Liu Y, Hutchinson TL, Lubin ML, Flores CM: **TRPV2 is activated by cannabidiol and mediates CGRP release in cultured rat dorsal root ganglion neurons**. *The Journal of neuroscience : the official journal of the Society for Neuroscience* 2008, **28**(24):6231-6238.
52. Muller C, Reggio PH: **An Analysis of the Putative CBD Binding Site in the Ionotropic Cannabinoid Receptors**. *Frontiers in cellular neuroscience* 2020, **14**:615811.
53. De Petrocellis L, Vellani V, Schiano-Moriello A, Marini P, Magherini PC, Orlando P, Di Marzo V: **Plant-derived cannabinoids modulate the activity of transient receptor potential channels of ankyrin type-1 and melastatin type-8**. *The Journal of pharmacology and experimental therapeutics* 2008, **325**(3):1007-1015.
54. Elmes MW, Kaczocha M, Berger WT, Leung K, Ralph BP, Wang L, Sweeney JM, Miyauchi JT, Tsirka SE, Ojima I *et al*: **Fatty acid-binding proteins (FABPs) are intracellular carriers for Δ9-tetrahydrocannabinol (THC) and cannabidiol (CBD)**. *The Journal of biological chemistry* 2015, **290**(14):8711-8721.
55. Di Marzo V: **Targeting the endocannabinoid system: to enhance or reduce?** *Nature reviews Drug discovery* 2008, **7**(5):438-455.

56. Oesch S, Gertsch J: Cannabinoid receptor ligands as potential anticancer agents--high hopes for new therapies? *The Journal of pharmacy and pharmacology* 2009, **61**(7):839-853.
57. Ohlsson A, Lindgren JE, Andersson S, Agurell S, Gillespie H, Hollister LE: Single-dose kinetics of deuterium-labelled cannabidiol in man after smoking and intravenous administration. *Biomedical & environmental mass spectrometry* 1986, **13**(2):77-83.
58. Fernández-Ruiz J, Sagredo O, Pazos MR, García C, Pertwee R, Mechoulam R, Martínez-Orgado J: Cannabidiol for neurodegenerative disorders: important new clinical applications for this phytocannabinoid? *British journal of clinical pharmacology* 2013, **75**(2):323-333.
59. De Petrocellis L, Di Marzo V: Non-CB1, non-CB2 receptors for endocannabinoids, plant cannabinoids, and synthetic cannabimimetics: focus on G-protein-coupled receptors and transient receptor potential channels. *Journal of neuroimmune pharmacology : the official journal of the Society on NeuroImmune Pharmacology* 2010, **5**(1):103-121.
60. Ross RA: The enigmatic pharmacology of GPR55. *Trends in pharmacological sciences* 2009, **30**(3):156-163.
61. Russo EB, Burnett A, Hall B, Parker KK: Agonistic properties of cannabidiol at 5-HT1a receptors. *Neurochemical research* 2005, **30**(8):1037-1043.
62. O'Sullivan SE, Sun Y, Bennett AJ, Randall MD, Kendall DA: Time-dependent vascular actions of cannabidiol in the rat aorta. *European journal of pharmacology* 2009, **612**(1-3):61-68.
63. Spelman K, Iiams-Hauser K, Cech NB, Taylor EW, Smirnoff N, Wenner CA: Role for PPARgamma in IL-2 inhibition in T cells by Echinacea-derived undeca-2E-ene-8,10-diynoic acid isobutylamide. *International immunopharmacology* 2009, **9**(11):1260-1264.
64. Ahrens J, Demir R, Leuwer M, de la Roche J, Krampfl K, Foadi N, Karst M, Haeseler G: The nonpsychotropic cannabinoid cannabidiol modulates and directly activates alpha-1 and alpha-1-Beta glycine receptor function. *Pharmacology* 2009, **83**(4):217-222.

65. Izzo AA, Borrelli F, Capasso R, Di Marzo V, Mechoulam R: Non-psychotropic plant cannabinoids: new therapeutic opportunities from an ancient herb. *Trends in pharmacological sciences* 2009, 30(10):515-527.
66. Ross HR, Napier I, Connor M: Inhibition of recombinant human T-type calcium channels by Delta9-tetrahydrocannabinol and cannabidiol. *The Journal of biological chemistry* 2008, 283(23):16124-16134.
67. Siegel RL, Miller KD, Jemal A: Cancer statistics, 2020. *CA: a cancer journal for clinicians* 2020, 70(1):7-30.
68. Cabral GA, Jamerson M: Marijuana use and brain immune mechanisms. *International review of neurobiology* 2014, 118:199-230.
69. Zhornitsky S, Potvin S: Cannabidiol in humans-the quest for therapeutic targets. *Pharmaceuticals (Basel, Switzerland)* 2012, 5(5):529-552.
70. Dumitru CA, Sandalcioglu IE, Karsak M: Cannabinoids in Glioblastoma Therapy: New Applications for Old Drugs. *Frontiers in molecular neuroscience* 2018, 11:159.
71. Zhang X, Qin Y, Pan Z, Li M, Liu X, Chen X, Qu G, Zhou L, Xu M, Zheng Q *et al*: Cannabidiol Induces Cell Cycle Arrest and Cell Apoptosis in Human Gastric Cancer SGC-7901 Cells. *Biomolecules* 2019, 9(8).
72. Massi P, Vaccani A, Bianchessi S, Costa B, Macchi P, Parolaro D: The non-psychoactive cannabidiol triggers caspase activation and oxidative stress in human glioma cells. *Cellular and molecular life sciences : CMLS* 2006, 63(17):2057-2066.
73. Massi P, Vaccani A, Ceruti S, Colombo A, Abbracchio MP, Parolaro D: Antitumor effects of cannabidiol, a nonpsychoactive cannabinoid, on human glioma cell lines. *The Journal of pharmacology and experimental therapeutics* 2004, 308(3):838-845.
74. Olivas-Aguirre M, Torres-López L, Valle-Reyes JS, Hernández-Cruz A, Pottosin I, Dobrovinskaya O: Cannabidiol directly targets mitochondria and disturbs calcium homeostasis in acute lymphoblastic leukemia. *Cell Death & Disease* 2019, 10(10):779.
75. McKallip RJ, Jia W, Schlomer J, Warren JW, Nagarkatti PS, Nagarkatti M: Cannabidiol-induced apoptosis in human leukemia

cells: A novel role of cannabidiol in the regulation of p22phox and Nox4 expression. *Molecular pharmacology* 2006, **70**(3):897-908.

76. Ramer R, Rohde A, Merkord J, Rohde H, Hinz B: **Decrease of plasminogen activator inhibitor-1 may contribute to the anti-invasive action of cannabidiol on human lung cancer cells**. *Pharmaceutical research* 2010, **27**(10):2162-2174.
77. Ramer R, Heinemann K, Merkord J, Rohde H, Salamon A, Linnebacher M, Hinz B: **COX-2 and PPAR-γ confer cannabidiol-induced apoptosis of human lung cancer cells**. *Molecular cancer therapeutics* 2013, **12**(1):69-82.
78. Casanova ML, Blázquez C, Martínez-Palacio J, Villanueva C, Fernández-Aceñero MJ, Huffman JW, Jorcano JL, Guzmán M: **Inhibition of skin tumor growth and angiogenesis in vivo by activation of cannabinoid receptors**. *The Journal of clinical investigation* 2003, **111**(1):43-50.
79. Vaccani A, Massi P, Colombo A, Rubino T, Parolaro D: **Cannabidiol inhibits human glioma cell migration through a cannabinoid receptor-independent mechanism**. *British journal of pharmacology* 2005, **144**(8):1032-1036.
80. Nabissi M, Morelli MB, Santoni M, Santoni G: **Triggering of the TRPV2 channel by cannabidiol sensitizes glioblastoma cells to cytotoxic chemotherapeutic agents**. *Carcinogenesis* 2013, **34**(1):48-57.
81. Neumann-Raizel H, Shilo A, Lev S, Mogilevsky M, Katz B, Shneor D, Shaul YD, Leffler A, Gabizon A, Karni R *et al*: **2-APB and CBD-Mediated Targeting of Charged Cytotoxic Compounds Into Tumor Cells Suggests the Involvement of TRPV2 Channels**. *Frontiers in pharmacology* 2019, **10**:1198.
82. Elbaz M, Ahirwar D, Xiaoli Z, Zhou X, Lustberg M, Nasser MW, Shilo K, Ganju RK: **TRPV2 is a novel biomarker and therapeutic target in triple negative breast cancer**. *Oncotarget* 2018, **9**(71):33459-33470.
83. Li X, Zhang Q, Fan K, Li B, Li H, Qi H, Guo J, Cao Y, Sun H: **Overexpression of TRPV3 Correlates with Tumor Progression in Non-Small Cell Lung Cancer**. *International journal of molecular sciences* 2016, **17**(4):437.

84. Shrivastava A, Kuzontkoski PM, Groopman JE, Prasad A: Cannabidiol induces programmed cell death in breast cancer cells by coordinating the cross-talk between apoptosis and autophagy. *Molecular cancer therapeutics* 2011, **10**(7):1161-1172.
85. Torres S, Lorente M, Rodríguez-Fornés F, Hernández-Tiedra S, Salazar M, García-Taboada E, Barcia J, Guzmán M, Velasco G: A combined preclinical therapy of cannabinoids and temozolomide against glioma. *Molecular cancer therapeutics* 2011, **10**(1):90-103.
86. Marcu JP, Christian RT, Lau D, Zielinski AJ, Horowitz MP, Lee J, Pakdel A, Allison J, Limbad C, Moore DH *et al*: Cannabidiol enhances the inhibitory effects of delta9-tetrahydrocannabinol on human glioblastoma cell proliferation and survival. *Molecular cancer therapeutics* 2010, **9**(1):180-189.
87. Ligresti A, Moriello AS, Starowicz K, Matias I, Pisanti S, De Petrocellis L, Laezza C, Portella G, Bifulco M, Di Marzo V: Antitumor activity of plant cannabinoids with emphasis on the effect of cannabidiol on human breast carcinoma. *The Journal of pharmacology and experimental therapeutics* 2006, **318**(3):1375-1387.
88. Elbaz M, Nasser MW, Ravi J, Wani NA, Ahirwar DK, Zhao H, Oghumu S, Satoskar AR, Shilo K, Carson WE, 3rd *et al*: Modulation of the tumor microenvironment and inhibition of EGF/EGFR pathway: novel anti-tumor mechanisms of Cannabidiol in breast cancer. *Molecular oncology* 2015, **9**(4):906-919.
89. Holland ML, Panetta JA, Hoskins JM, Bebawy M, Roufogalis BD, Allen JD, Arnold JC: The effects of cannabinoids on P-glycoprotein transport and expression in multidrug resistant cells. *Biochemical pharmacology* 2006, **71**(8):1146-1154.
90. Holland ML, Allen JD, Arnold JC: Interaction of plant cannabinoids with the multidrug transporter ABCC1 (MRP1). *European journal of pharmacology* 2008, **591**(1-3):128-131.
91. Feinshtein V, Erez O, Ben-Zvi Z, Erez N, Eshkoli T, Sheizaf B, Sheiner E, Huleihel M, Holcberg G: Cannabidiol changes P-gp and BCRP expression in trophoblast cell lines. *PeerJ* 2013, **1**:e153.

92. Piñeiro R, Maffucci T, Falasca M: **The putative cannabinoid receptor GPR55 defines a novel autocrine loop in cancer cell proliferation**. *Oncogene* 2011, **30**(2):142-152.
93. Ford LA, Roelofs AJ, Anavi-Goffer S, Mowat L, Simpson DG, Irving AJ, Rogers MJ, Rajnicek AM, Ross RA: **A role for L-alpha-lysophosphatidylinositol and GPR55 in the modulation of migration, orientation and polarization of human breast cancer cells**. *British journal of pharmacology* 2010, **160**(3):762-771.
94. Soroceanu L, Murase R, Limbad C, Singer E, Allison J, Adrados I, Kawamura R, Pakdel A, Fukuyo Y, Nguyen D *et al*: **Id-1 is a key transcriptional regulator of glioblastoma aggressiveness and a novel therapeutic target**. *Cancer research* 2013, **73**(5):1559-1569.
95. Swarbrick A, Roy E, Allen T, Bishop JM: **Id1 cooperates with oncogenic Ras to induce metastatic mammary carcinoma by subversion of the cellular senescence response**. *Proceedings of the National Academy of Sciences of the United States of America* 2008, **105**(14):5402-5407.
96. Ramer R, Bublitz K, Freimuth N, Merkord J, Rohde H, Haustein M, Borchert P, Schmuhl E, Linnebacher M, Hinz B: **Cannabidiol inhibits lung cancer cell invasion and metastasis via intercellular adhesion molecule-1**. *FASEB journal : official publication of the Federation of American Societies for Experimental Biology* 2012, **26**(4):1535-1548.
97. Cheng CJ, Tietjen GT, Saucier-Sawyer JK, Saltzman WM: **A holistic approach to targeting disease with polymeric nanoparticles**. *Nature reviews Drug discovery* 2015, **14**(4):239-247.
98. Deng Y, Yang F, Cocco E, Song E, Zhang J, Cui J, Mohideen M, Bellone S, Santin AD, Saltzman WM: **Improved i.p. drug delivery with bioadhesive nanoparticles**. *Proceedings of the National Academy of Sciences of the United States of America* 2016, **113**(41):11453-11458.
99. Fraguas-Sánchez AI, Fernández-Carballido A, Simancas-Herbada R, Martin-Sabroso C, Torres-Suárez AI: **CBD loaded microparticles as a potential formulation to improve paclitaxel and doxorubicin-based chemotherapy in breast cancer**. *International journal of pharmaceutics* 2020, **574**:118916.

100. Viudez-Martínez A, García-Gutiérrez MS, Navarrón CM, Morales-Calero MI, Navarrete F, Torres-Suárez AI, Manzanares J: Cannabidiol reduces ethanol consumption, motivation and relapse in mice. *Addiction biology* 2018, 23(1):154-164.
101. Fraguas-Sánchez AI, Torres-Suárez AI, Cohen M, Delie F, Bastida-Ruiz D, Yart L, Martin-Sabroso C, Fernández-Carballido A: PLGA Nanoparticles for the Intraperitoneal Administration of CBD in the Treatment of Ovarian Cancer: In Vitro and In Ovo Assessment. *Pharmaceutics* 2020, 12(5).
102. Aparicio-Blanco J, Romero IA, Male DK, Slowing K, García-García L, Torres-Suárez AI: Cannabidiol Enhances the Passage of Lipid Nanocapsules across the Blood-Brain Barrier Both in Vitro and in Vivo. *Molecular pharmaceutics* 2019, 16(5):1999-2010.
103. Fleming M, Ravula S, Tatishchev SF, Wang HL: Colorectal carcinoma: Pathologic aspects. *Journal of gastrointestinal oncology* 2012, 3(3):153-173.
104. Siegel R, Desantis C, Jemal A: Colorectal cancer statistics, 2014. *CA: a cancer journal for clinicians* 2014, 64(2):104-117.
105. Grady WM, Markowitz S: Genomic instability and colorectal cancer. *Current opinion in gastroenterology* 2000, 16(1):62-67.
106. Markowitz SD, Bertagnolli MM: Molecular origins of cancer: Molecular basis of colorectal cancer. *The New England journal of medicine* 2009, 361(25):2449-2460.
107. Lane D, Levine A: p53 Research: the past thirty years and the next thirty years. *Cold Spring Harbor perspectives in biology* 2010, 2(12):a000893.
108. Greenblatt MS, Bennett WP, Hollstein M, Harris CC: Mutations in the p53 tumor suppressor gene: clues to cancer etiology and molecular pathogenesis. *Cancer research* 1994, 54(18):4855-4878.
109. Sidransky D, Hollstein M: Clinical implications of the p53 gene. *Annual review of medicine* 1996, 47:285-301.
110. Wood LD, Parsons DW, Jones S, Lin J, Sjöblom T, Leary RJ, Shen D, Boca SM, Barber T, Ptak J *et al*: The genomic landscapes of human breast and colorectal cancers. *Science (New York, NY)* 2007, 318(5853):1108-1113.
111. Wishart DS, Feunang YD, Guo AC, Lo EJ, Marcu A, Grant JR, Sajed T, Johnson D, Li C, Sayeeda Z *et al*: DrugBank 5.0: a major update

to the DrugBank database for 2018. *Nucleic acids research* 2018, 46(D1):D1074-d1082.
112. Daina A, Michielin O, Zoete V: SwissTargetPrediction: updated data and new features for efficient prediction of protein targets of small molecules. *Nucleic acids research* 2019, 47(W1):W357-w364.
113. Nickel J, Gohlke BO, Erehman J, Banerjee P, Rong WW, Goede A, Dunkel M, Preissner R: SuperPred: update on drug classification and target prediction. *Nucleic acids research* 2014, 42(Web Server issue):W26-31.
114. Fishilevich S, Nudel R, Rappaport N, Hadar R, Plaschkes I, Iny Stein T, Rosen N, Kohn A, Twik M, Safran M *et al*: GeneHancer: genome-wide integration of enhancers and target genes in GeneCards. *Database : the journal of biological databases and curation* 2017, 2017.
115. Zhou Y, Zhou B, Pache L, Chang M, Khodabakhshi AH, Tanaseichuk O, Benner C, Chanda SK: Metascape provides a biologist-oriented resource for the analysis of systems-level datasets. *Nature communications* 2019, 10(1):1523.
116. Kim S, Thiessen PA, Bolton EE, Chen J, Fu G, Gindulyte A, Han L, He J, He S, Shoemaker BA *et al*: PubChem Substance and Compound databases. *Nucleic acids research* 2016, 44(D1):D1202-1213.
117. Han H, Shim H, Shin D, Shim JE, Ko Y, Shin J, Kim H, Cho A, Kim E, Lee T *et al*: TRRUST: a reference database of human transcriptional regulatory interactions. *Scientific reports* 2015, 5:11432.
118. Rochette PJ, Bastien N, Lavoie J, Guérin SL, Drouin R: SW480, a p53 double-mutant cell line retains proficiency for some p53 functions. *Journal of molecular biology* 2005, 352(1):44-57.
119. Guadagno TM, Newport JW: Cdk2 kinase is required for entry into mitosis as a positive regulator of Cdc2-cyclin B kinase activity. *Cell* 1996, 84(1):73-82.
120. Maillet A, Pervaiz S: Redox regulation of p53, redox effectors regulated by p53: a subtle balance. *Antioxidants & redox signaling* 2012, 16(11):1285-1294.
121. Jäättelä M: Escaping cell death: survival proteins in cancer. *Experimental cell research* 1999, 248(1):30-43.

122. Beere HM, Wolf BB, Cain K, Mosser DD, Mahboubi A, Kuwana T, Tailor P, Morimoto RI, Cohen GM, Green DR: **Heat-shock protein 70 inhibits apoptosis by preventing recruitment of procaspase-9 to the Apaf-1 apoptosome**. *Nature cell biology* 2000, **2**(8):469-475.
123. Balaburski GM, Leu JI, Beeharry N, Hayik S, Andrake MD, Zhang G, Herlyn M, Villanueva J, Dunbrack RL, Jr., Yen T *et al*: **A modified HSP70 inhibitor shows broad activity as an anticancer agent**. *Molecular cancer research : MCR* 2013, **11**(3):219-229.
124. Leu JI, Pimkina J, Frank A, Murphy ME, George DL: **A small molecule inhibitor of inducible heat shock protein 70**. *Molecular cell* 2009, **36**(1):15-27.
125. Rubinsztein DC, Shpilka T, Elazar Z: **Mechanisms of autophagosome biogenesis**. *Current biology : CB* 2012, **22**(1):R29-34.
126. Pankiv S, Clausen TH, Lamark T, Brech A, Bruun JA, Outzen H, Øvervatn A, Bjørkøy G, Johansen T: **p62/SQSTM1 binds directly to Atg8/LC3 to facilitate degradation of ubiquitinated protein aggregates by autophagy**. *The Journal of biological chemistry* 2007, **282**(33):24131-24145.
127. Budina-Kolomets A, Balaburski GM, Bondar A, Beeharry N, Yen T, Murphy ME: **Comparison of the activity of three different HSP70 inhibitors on apoptosis, cell cycle arrest, autophagy inhibition, and HSP90 inhibition**. *Cancer biology & therapy* 2014, **15**(2):194-199.
128. Yamamoto A, Tagawa Y, Yoshimori T, Moriyama Y, Masaki R, Tashiro Y: **Bafilomycin A1 prevents maturation of autophagic vacuoles by inhibiting fusion between autophagosomes and lysosomes in rat hepatoma cell line, H-4-II-E cells**. *Cell structure and function* 1998, **23**(1):33-42.
129. Tasdemir E, Maiuri MC, Orhon I, Kepp O, Morselli E, Criollo A, Kroemer G: **p53 represses autophagy in a cell cycle-dependent fashion**. *Cell cycle (Georgetown, Tex)* 2008, **7**(19):3006-3011.
130. Katsuragi Y, Ichimura Y, Komatsu M: **Regulation of the Keap1–Nrf2 pathway by p62/SQSTM1**. *Current Opinion in Toxicology* 2016, **1**:54-61.
131. Ni HM, Woolbright BL, Williams J, Copple B, Cui W, Luyendyk JP, Jaeschke H, Ding WX: **Nrf2 promotes the development of fibrosis**

and tumorigenesis in mice with defective hepatic autophagy. *Journal of hepatology* 2014, **61**(3):617-625.
132. Jain A, Lamark T, Sjøttem E, Larsen KB, Awuh JA, Øvervatn A, McMahon M, Hayes JD, Johansen T: **p62/SQSTM1 is a target gene for transcription factor NRF2 and creates a positive feedback loop by inducing antioxidant response element-driven gene transcription**. *The Journal of biological chemistry* 2010, **285**(29):22576-22591.
133. Dinkova-Kostova AT, Holtzclaw WD, Cole RN, Itoh K, Wakabayashi N, Katoh Y, Yamamoto M, Talalay P: **Direct evidence that sulfhydryl groups of Keap1 are the sensors regulating induction of phase 2 enzymes that protect against carcinogens and oxidants**. *Proceedings of the National Academy of Sciences of the United States of America* 2002, **99**(18):11908-11913.
134. Vousden KH, Lu X: **Live or let die: the cell's response to p53**. *Nature reviews Cancer* 2002, **2**(8):594-604.
135. Engeland K: **Cell cycle regulation: p53-p21-RB signaling**. *Cell Death & Differentiation* 2022, **29**(5):946-960.
136. Muller PA, Vousden KH: **Mutant p53 in cancer: new functions and therapeutic opportunities**. *Cancer cell* 2014, **25**(3):304-317.
137. Liu G, Chen X: **Regulation of the p53 transcriptional activity**. *Journal of cellular biochemistry* 2006, **97**(3):448-458.
138. Lim YP, Lim TT, Chan YL, Song AC, Yeo BH, Vojtesek B, Coomber D, Rajagopal G, Lane D: **The p53 knowledgebase: an integrated information resource for p53 research**. *Oncogene* 2007, **26**(11):1517-1521.
139. Drane P, Bravard A, Bouvard V, May E: **Reciprocal down-regulation of p53 and SOD2 gene expression-implication in p53 mediated apoptosis**. *Oncogene* 2001, **20**(4):430-439.
140. Polyak K, Xia Y, Zweier JL, Kinzler KW, Vogelstein B: **A model for p53-induced apoptosis**. *Nature* 1997, **389**(6648):300-305.
141. Rivera A, Maxwell SA: **The p53-induced gene-6 (proline oxidase) mediates apoptosis through a calcineurin-dependent pathway**. *The Journal of biological chemistry* 2005, **280**(32):29346-29354.
142. Thomas AF, Kelly GL, Strasser A: **Of the many cellular responses activated by TP53, which ones are critical for tumour suppression?** *Cell death and differentiation* 2022, **29**(5):961-971.

143. Mosser DD, Caron AW, Bourget L, Denis-Larose C, Massie B: **Role of the human heat shock protein hsp70 in protection against stress-induced apoptosis**. *Molecular and cellular biology* 1997, **17**(9):5317-5327.
144. Schreiber M, Kolbus A, Piu F, Szabowski A, Möhle-Steinlein U, Tian J, Karin M, Angel P, Wagner EF: **Control of cell cycle progression by c-Jun is p53 dependent**. *Genes & development* 1999, **13**(5):607-619.
145. Eferl R, Ricci R, Kenner L, Zenz R, David JP, Rath M, Wagner EF: **Liver tumor development. c-Jun antagonizes the proapoptotic activity of p53**. *Cell* 2003, **112**(2):181-192.
146. Tournier C, Hess P, Yang DD, Xu J, Turner TK, Nimnual A, Bar-Sagi D, Jones SN, Flavell RA, Davis RJ: **Requirement of JNK for stress-induced activation of the cytochrome c-mediated death pathway**. *Science (New York, NY)* 2000, **288**(5467):870-874.
147. Gao Y, Han C, Huang H, Xin Y, Xu Y, Luo L, Yin Z: **Heat shock protein 70 together with its co-chaperone CHIP inhibits TNF-alpha induced apoptosis by promoting proteasomal degradation of apoptosis signal-regulating kinase1**. *Apoptosis : an international journal on programmed cell death* 2010, **15**(7):822-833.
148. Dhanasekaran DN, Reddy EP: **JNK signaling in apoptosis**. *Oncogene* 2008, **27**(48):6245-6251.
149. Brentnall M, Rodriguez-Menocal L, De Guevara RL, Cepero E, Boise LH: **Caspase-9, caspase-3 and caspase-7 have distinct roles during intrinsic apoptosis**. *BMC Cell Biology* 2013, **14**(1):32.
150. Wu MH, Jin Xk Fau - Yu A-Q, Yu Aq Fau - Zhu Y-T, Zhu Yt Fau - Li D, Li D Fau - Li W-W, Li Ww Fau - Wang Q, Wang Q: **Caspase-mediated apoptosis in crustaceans: cloning and functional characterization of EsCaspase-3-like protein from Eriocheir**. (1095-9947 (Electronic)).
151. Rodríguez-Vargas JM, Ruiz-Magaña MJ, Ruiz-Ruiz C, Majuelos-Melguizo J, Peralta-Leal A, Rodríguez MI, Muñoz-Gámez JA, de Almodóvar MR, Siles E, Rivas AL *et al*: **ROS-induced DNA damage and PARP-1 are required for optimal induction of starvation-induced autophagy**. *Cell research* 2012, **22**(7):1181-1198.

152. Maiuri MC, Zalckvar E, Kimchi A, Kroemer G: Self-eating and self-killing: crosstalk between autophagy and apoptosis. *Nature reviews Molecular cell biology* 2007, 8(9):741-752.
153. Leu JI, Pimkina J, Pandey P, Murphy ME, George DL: HSP70 inhibition by the small-molecule 2-phenylethynesulfonamide impairs protein clearance pathways in tumor cells. *Molecular cancer research : MCR* 2011, 9(7):936-947.
154. Chiang HL, Terlecky SR, Plant CP, Dice JF: A role for a 70-kilodalton heat shock protein in lysosomal degradation of intracellular proteins. *Science (New York, NY)* 1989, 246(4928):382-385.
155. Zhao X, Liu HQ, Wang LN, Yang L, Liu XL: Current and emerging molecular and epigenetic disease entities in acute myeloid leukemia and a critical assessment of their therapeutic modalities. *Seminars in cancer biology* 2022, 83:121-135.
156. Nollen EA, Salomons FA, Brunsting JF, van der Want JJ, Sibon OC, Kampinga HH: Dynamic changes in the localization of thermally unfolded nuclear proteins associated with chaperone-dependent protection. *Proceedings of the National Academy of Sciences of the United States of America* 2001, 98(21):12038-12043.

The work has been published on :

1.Cell death & discovery: Cannabidiol-induced crosstalk of apoptosis and macroautophagy in colorectal cancer cells involves p53 and Hsp70, Fei Wang, et al. Cell Death Discov. 2023 Aug 5;9(1):286. doi: 10.1038/s41420-023-01578-9.

2.Biomolecules: Repurposing Cannabidiol as a Potential Drug Candidate for Anti-Tumor Therapies,Fei Wang, Gabriele Multhoff, Biomolecules. 2021 Apr 15;11(4):582. doi: 10.3390/biom11040582.

8. Acknowledgements

I would like to express my deep and sincere gratitude to my research supervisor, Prof. Gabriele Multhoff, and mentor Prof. Agnes Görlach. Their guidance and valuable advice carried me through all the stages of my project. His dynamism, vision, sincerity and motivation have deeply inspired me. My supervisor has taught me the methodology to carry out the research and to present the research works as clearly as possible. It was a great privilege and honor to work and study under her guidance. I am extremely grateful for what she has offered me. I would also like to thank for her friendship, empathy, and great sense of humor. I would also like to thank my members for letting my daily work be an enjoyable moment, and for your brilliant comments and suggestions, thanks to you.

I am extremely grateful to my parents for their love, prayers, caring and sacrifices for educating and preparing me for my future. I am very much thankful to my fiancé Fei Tang for his love, understanding, prayers and continuing support to complete this research work. Your prayer for me was what sustained me this far.

Finally, my thanks go to all the people who have supported me to complete the research work directly or indirectly.